AD NUMBER
AD479589
LIMITATION CHANGES

TO:

Approved for public release; distribution is unlimited. Document partially illegible.

FROM:

Distribution authorized to U.S. Gov't. agencies and their contractors; Administrative/Operational Use; 1962. Other requests shall be referred to U.S. Naval Postgraduate School, Monterey, CA 93943.

AUTHORITY
USNPS ltr, 27 Sep 1971

DITHER SELF ADAPTIVE SYSTEM PERFORMANCE AND CLOSED LOOP RESPONSE CRITERION

ALFRED P. AMORUSO

31 August 1962

62-AN/CD-3920

Professor G. R. Luckett
Director of Libraries
U. S. Naval Postgraduate School
Monterey, California

Subject: Release of Information

Reference: (a) Letter to Autonetics, Attn: Mr. L. K. Mattingly From
                G. R. Luckett, Professor, Director of Libraries,
                U.S. Naval Postgraduate School, Monterey
                Dated 13 July 1962, Same Subject

Dear Professor Luckett:

Autonetics is pleased to provide unconditional release of the material
included in the thesis "Dither Self Adaptive System Performance and
Closed Loop Response Criterion" by Lt. Alfred P. Amoruso, as noted on
the attached letter (Enclosure 1).

For your information and possible utilization, the reference on Page 19
to Figure 2.6 can be made more specific by further reference to a paper
entitled "A Self Adaptive Control System for a Space Booster of the
Saturn Class" by R. R. Smyth and J. C. Davis (both of Autonetics) pre-
sented 23 April 1962 before the Joint Automatic Control Conference at
New York University.

Lt. Amoruso and your organization are to be congratulated on a well
prepared publication.

                                    Very truly yours,

                                    AUTONETICS

                                    R. L. Doty
                                    Chief Engineer
                                    Computers and Data Systems

EAO:bll

 4145AN/CD
 Enclosure: (1) One Copy of Ref. (a) Letter Above (Uncl)
                 with Autonetics' release signatures
                 attached thereon

DITHER SELF ADAPTIVE SYSTEM PERFORMANCE

AND

CLOSED LOOP RESPONSE CRITERION

* * * * *

Alfred P. Amoruso

United States Naval Postgraduate School

Degree: Master of Science in
         Electrical Engineering

Classification:

         Thesis: Unclassified
         Abstract: Unclassified
         Title Of Thesis:
           Unclassified
         Contains proprietary informa-
         tion

DITHER SELF ADAPTIVE SYSTEM PERFORMANCE

AND

CLOSED LOOP RESPONSE CRITERION

* * * * *

Alfred P. Amoruso

DITHER SELF ADAPTIVE SYSTEM PERFORMANCE

AND

CLOSED LOOP RESPONSE CRITERION

by
Alfred P. Amoruso

Lieutenant, United States Navy

Submitted in partial fulfillment of
the requirements for the degree of

MASTER OF SCIENCE
IN
ELECTRICAL ENGINEERING

United States Naval Postgraduate School
Monterey, California

1 9 6 2

DITHER SELF ADAPTIVE SYSTEM PERFORMANCE

AND

CLOSED LOOP RESPONSE CRITERION

by

Alfred P. Amoruso

This work is accepted as fulfilling

the thesis requirements for the degree of

MASTER OF SCIENCE

IN

ELECTRICAL ENGINEERING

from the

United States Naval Postgraduate School

ABSTRACT

The use of a self adaptive technique to compensate for the varying
parameters of a flight control system is desirable for high performance
aircraft and space vehicles. The technique discussed in this study con-
sists of using a sinusoidal signal to measure the change in the parameters
and of compensating for the change by a gain adjustment. Analog and digital
computer methods are used to investigate the performance of the system and
the accuracy of the Amplitude Closed Loop Response Criterion for measuring
damping ratio. The effects of varying airframe flexibility, center of
gravity, frequency of the sinusoidal signal, and the Reference signal value
are included. The applicability of the self adaptive technique for a
particular vehicle depends on the dynamic characteristics of the airframe
and on the desired maximum variations of the performance characteristics.

The writer wishes to express his appreciation for the assistance and
encouragement given him by Dr. G. J. Thaler, Professor of Electrical
Engineering at the U. S. Naval Postgraduate School. The writer also
wishes to express appreciation to Mr. L. K. Mattingly who supervised the
study during a field trip at Autonetics in the summer of 1961.

LIST OF TABLES

iv

SYMBOLS

ϵ_{SA} $\triangleq$ Adaptive Loop Error

δ $\triangleq$ Damping Ratio

$\Delta\delta$ $\triangleq$ Maximum Damping Ratio Variation During a Flight

δ_c $\triangleq$ Command Error Signal in Degrees

δ_T $\triangleq$ Thrust Vector Signal in Degrees

$K\delta$ $\triangleq$ Adaptive Gain

K_{SA} $\triangleq$ Adaptive Servo Gain Setting

K_V $\triangleq$ Product of Adaptive Gain and Vehicle Dynamics Transfer Function Considering Small Perturbations

SAE $\triangleq$ Signal from Adaptive Loop Rectifier

M_δ $\triangleq$ Aerodynamic Gain

w_n $\triangleq$ Natural Frequency in Radians per Second

α $\triangleq$ Attack Angle in Degrees

Θ $\triangleq$ Reference Pitch Angle in Degrees

Θ_F $\triangleq$ Platform Pitch Angle in Degrees

d_1 $\triangleq$ First Bending Mode in Feet

d_2 $\triangleq$ Second Bending Mode in Feet

d_3 $\triangleq$ Third Bending Mode in Feet

ΔI $\triangleq$ First Ignition Fuel Slosh Mode in Feet

ΔLOX $\triangleq$ First Liquid Oxygen Slosh Mode in Feet

ΔLH $\triangleq$ First Liquid Hydrogen Slosh Mode in Feet

CHAPTER I

INTRODUCTION

The dynamic characteristics of an airframe vary when changes in speed, altitude, position of center or gravity, and dynamic pressure occur. The variation in the dynamic characteristics cause variations in the response of the airframe to commands from a pilot or program unless some method of compensation is used. Many autopilots employ some form of gain variation for compensation. For propeller and early jet aircraft the gain variation was accomplished by a schedule which was a function of some air data parameter such as dynamic pressure, altitude, or Mach number. In space vehicles and high-performance supersonic aircraft the gain scheduling becomes very complex or impossible for the following reasons:

1. The dynamic and static characteristics of the airframe change rapidly over wide ranges.

2. Air data measurements are not accurate or are not available at high speeds and altitudes.

3. The airframe dynamic characteristics are not known with sufficient certainty to permit scheduling.

To eliminate the requirement for scheduling and air data measurements, automatic control systems are being developed which include a self adaptive loop. The purpose of the self adaptive loop is to maintain optimum response of the airframe by compensating for the changes in the dynamic characteristics without the necessity for external measurements.

1

The Dither Self-Adaptive System is one method for obtaining optimum response by self compensation. A study of this system for pitch control was undertaken with the following objectives:

1. To determine the ability of the system to correct for the varying dynamic characteristics of a flexible airframe.

2. To determine the optimum variation of the damping ratio and natural frequency of the short period mode during a typical flight and how this variation is affected by airframe bending and by changes in the center of gravity of the airframe.

The first objective was investigated by the comparison of digital and analog computer results. The second objective was investigated primarily from an empirical approach although some analytical verification is included.

2

DITHER SELF ADAPTIVE CONTROL SYSTEM

2.1 Self Adaptive Systems

Any closed loop control system has in effect some self-adaptive ability. In the usual control system a desirable static output is obtained under varying input and open loop parameter conditions by proper design of the feedback loops. The name "self-adaptive" (1), however, is reserved for only those control systems which maintain optimum dynamic response under varying conditions instead of the static response that normal feedback optimalizes.

Self-adaptive systems can be classified according to the ability to automatically compensate for either changes in the system input or changes in the system parameters, such as environmental variations. The ideal self-adaptive system would compensate for both input and system parameter changes. Flight control systems are generally concerned with parameter changes and hence, are designed to compensate for only those changes. Since this investigation is concerned with a flight control system, only the ability of the system to optimalize the dynamic response under varying aerodynamic parameters will be considered.

There are three basic operations which an adaptive loop must perform:

1) A continuous measurement of system dynamic performance - The dynamic performance measuring method should have a negligible effect on the system response signal and, in like manner, the system response signal should have negligible effect on the measuring method.

3

2) A continuous evaluation of the dynamic performance on the
basis of some predetermined criterion - The selection of the
evaluation criterion depends on the physical capabilities of
the system. Factors, such as realizability, complexity, and
cost, may prevent incorporating into the system the ability to
maintain a constant dynamic response. Compromises would have
to be made so that the system would be physically capable of
maintaining optimum a characteristic of the response; as, the
relative stability - damping ratio - or the natural frequency.
A figure of merit - which is a number or a method of compari-
son - is then selected on the basis of accurately representing
the selected dynamic response characteristic to be maintained
constant.

3) A continuous readjustment, based on the measured performance
and evaluation, of system control parameters for optimum
operation -- The methods used to adjust the parameters to
obtain optimum operation can be listed under three headings:
High Gain Linear Feedback, Programmed Compensation, and Compen-
sation Using an Optimalizing Controller.

In the High Gain Linear Feedback Method of adjusting performance under
varying parameters the forward loop gain is maintained high by compensa-
tion or with a relay. The desired dynamic response characteristics are
contained in the feedback loop. The high gain with feedback makes the
varying parameters in the forward loop negligible while the feedback loop
determines the dynamic response of the system. This is not a new method and
is used in many electronic applications for stabilization.

4

The Programmed Compensation Method measures the varying parameter, or the conditions which vary the parameter, and adjusts the compensating parameters in a controller in the forward loop to counteract the system variation. The adjustment is accomplished through a program which requires a knowledge of the relationship between the system and compensation parameters.

The Compensation Using an Optimalizing Controller Method is a type of feedback control which adjusts parameters so that a characteristic of the system response is optimized; such as, the damping ratio. In the Controller Method an error signal using the output response level of the system can not be used as an error signal for the parameter adjustment as in a normal feedback method because the Controller is optimalizing a characteristic of the output and not necessarily the output level. The system may be used in conjunction with a model which gives the optimum characteristic in its output for a particular system input. The Controller samples the characteristic in the system output and compares the value with the optimum output of the model. The Controller then adjusts parameters until the model and system characteristic coincide.

2.2   Description of Pitch Control System to be Investigated.

The Dither Self-Adaptive System is capable of controlling a vehicle about its pitch, roll, and yaw axes. This investigation, however, will be concerned only with pitch control. The system which is to be investigated is shown in Figure 2.1. The position, rate and acceleration sensors that are required for the feedback loops are assumed to have a unity transfer function. The rectifier in the self adaptive loop is also assumed to have a unity transfer function.

5
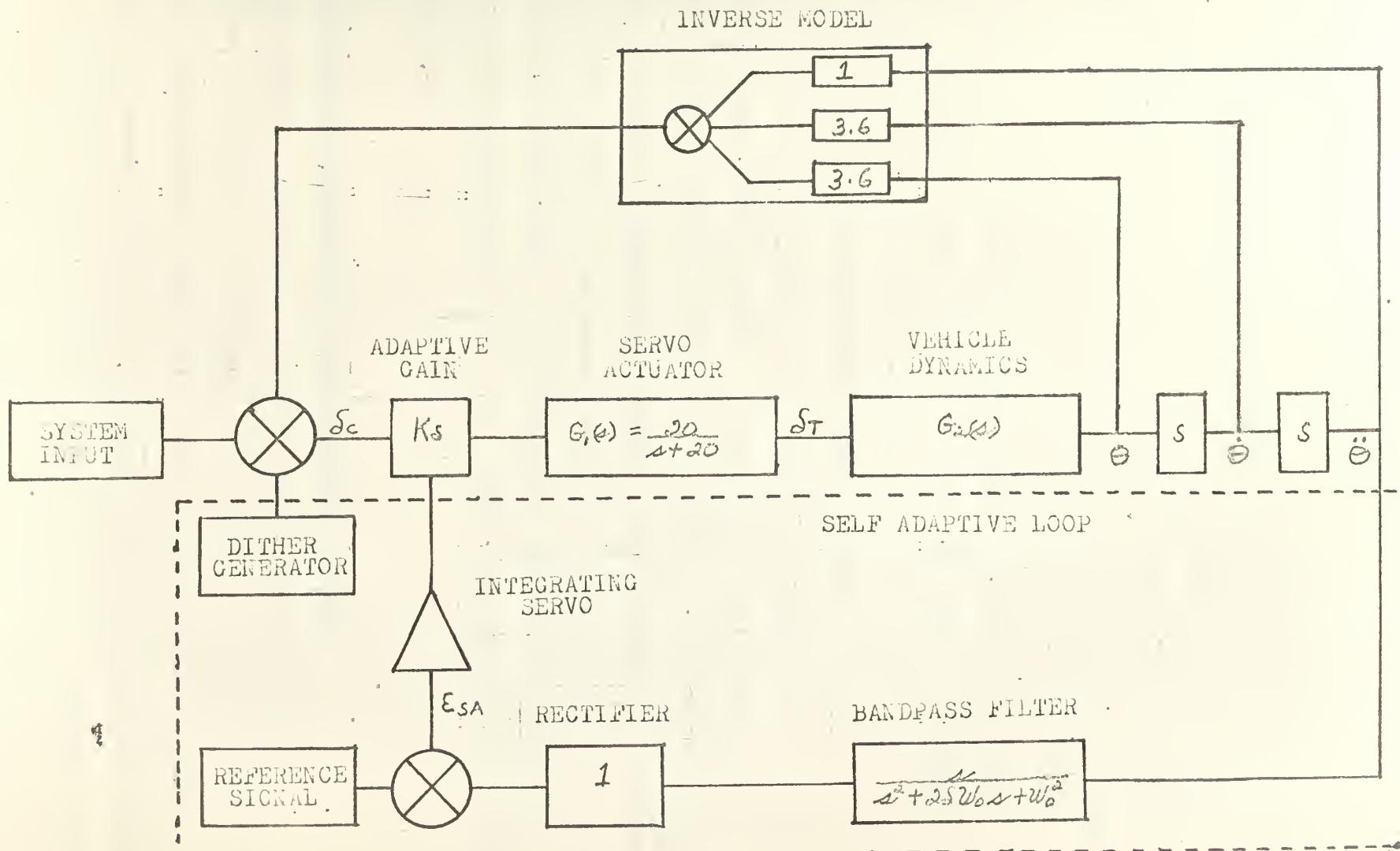
Figure 2.1. Dither System

In the conventional loop an error signal, δc, is formed by comparing the feedback signal to the command input signal. The error signal is amplified by the adaptive gain, k_δ, and the resulting signal operates the servo actuator. This investigation involves a missile which has gimbaled thrust chambers. The servo actuator controls the direction of the chamber axis which results in a thrust vector signal δt. The thrust vector signal affects the vehicle performance which is represented by the block labeled "Vehicle Dynamics". The reaction of the vehicle airframe to the change in direction of the thrust axis is detected by position, rate, and acceleration sensors and is fed back through the Inverse Model to the input. The function of the Inverse Model will be explained in Section 2.3.

For the self adaptive loop a dither signal is introduced at the input. This signal is then amplified by k_δ, operates the servo actuator, and excites the vehicle dynamics. The pitch acceleration, $\ddot{\theta}$, is passed through a bandpass filter where the dither frequency is separated from the command input signal frequencies. The dither frequency is then rectified and compared with a reference signal. The error, $\mathcal{E}_{SA}$, operates an integrating servo which varies the adaptive gain, k_δ, until the reference and rectified signals are equal.

2.3 Principles Used to Maintain Optimum Dynamic Response.

When a physical aerodynamic parameter changes, all the dynamic characteristic parameters of the system are affected. Typical physical aerodynamic parameters are Mach number and altitude, and typical dynamic characteristic parameters are natural frequencies and damping ratios. In terms of the system transfer function a change in a physical parameter could

7

shift the position of all the poles and zeros of the transfer function.
If constant dynamic response was desired for the system, the variation in
all the poles and zero would have to be counter-balanced. The complexity
of the situation can be visualized by placing a root locus plot alongside
a missile traveling many times the speed of sound. The physical parameters
of the missile are constantly changing, and each parameter would be varying
all the poles and zeros on the root locus. A typical root locus with vary-
ing poles and zeros is shown in Figure 2.2. A controller would have to be
built to sense each of the variations and then decide how to counter-
balance by compensation. In practice exact compensation is too complicated
to be useful and approximations are always made.

Simplicity is one of the main objectives of the dither adaptive loop.
The only components that have been added to the existing ptich control
system are a dither generator, filter, rectifier, and a comparison-integra-
tion network. No variable shaping networks are used, and all adjustable
compensation is accomplished by varying the gain of the system.

Aviators are primarily affected physically by the short period mode
of the pitch aerodynamic equations. Tests have indicated that pilots prefer
a damping ratio of 0.7 and a natural frequency of 3 radians per second for
this mode (2). Since the missile used in this investigation is designed
for manned flights, the damping ratio of 0.7 and frequency of 3 were de-
sired. Since the dither system does not use variable shaping networks, it is
physically impossible to maintain both the damping ratio and frequency con-
stant at the desired values. Therefore, a damping ratio of 0.7 with a
minimum natural frequency variation are defined as the optimum dynamic
characteristics of the short period mode during a flight.
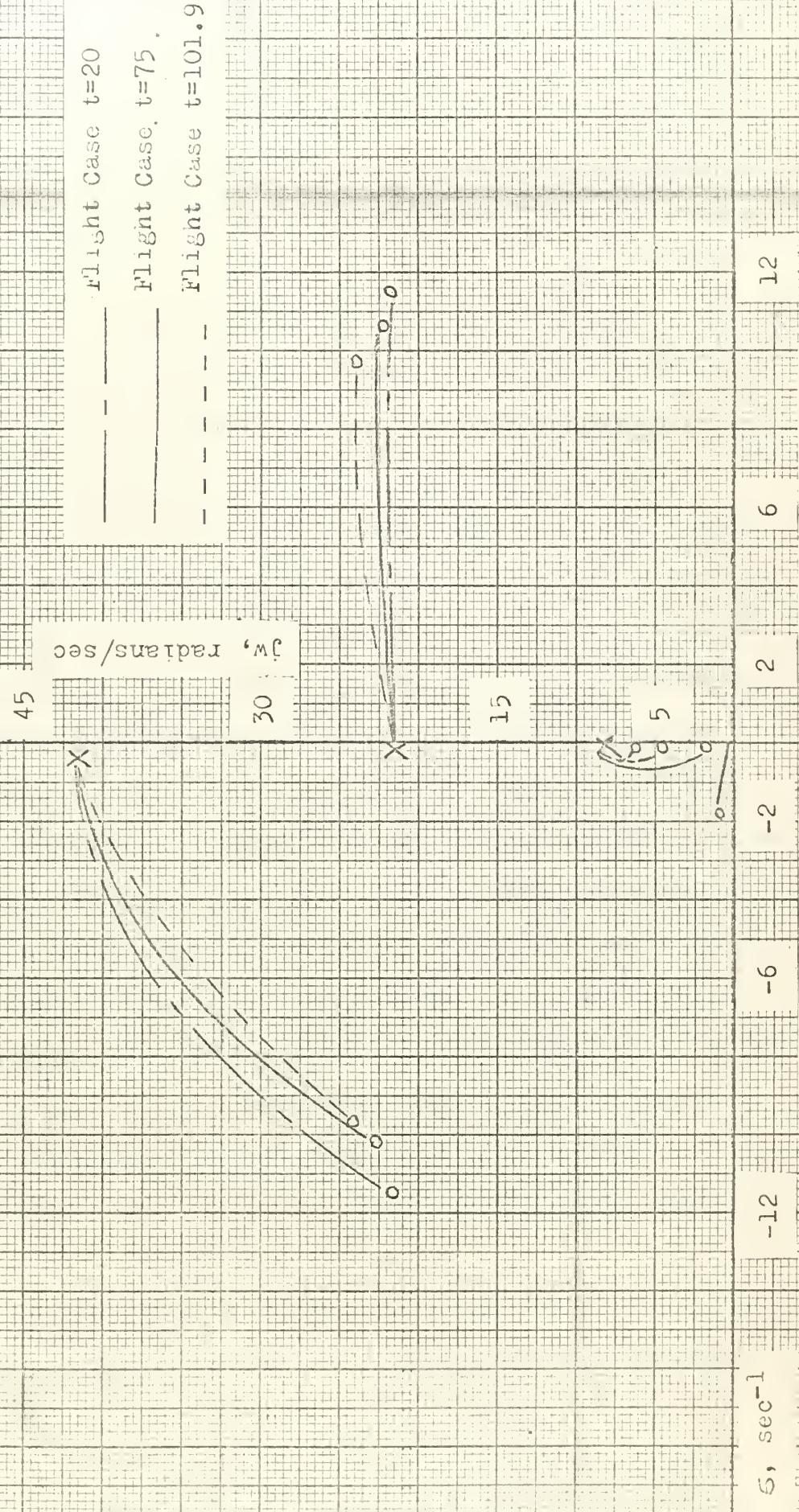
Figure 2.2. Root Locus Pole and Zero Variation

Flight Case t=20

Flight Case. t=75 .

Flight Case t=101.9

jw, radians/sec

45

30

15

5

2

6

12

-2

-6

-12

δ, sec⁻¹

There are actually two methods being employed in the overall system for varying the control parameter to obtain optimum performance. The control parameter of the system is the gain. The two methods, which are discussed in Section 2.1, are High Gain Linear Feedback and Programmed Compensation.

If the gain of the system could be maintained at a high value, the desired dynamic response characteristic could be inserted in a feedback loop and would determine the dynamic response of the overall system. This is the principle of the High Gain Linear Feedback Method shown in Figure 2.3. $H(s)$ is referred to as the "Inverse Model" since the inverse of its transfer function determines the dynamic response of the system. If a damping ratio of 0.7 and a natural frequency of 3 radians per second were desired, the Inverse Model would have a transfer function of $s^2+4.2s+9$. Unfortunately, the varying dynamic characteristics of the airframe, as represented by $G2(s)$, cannot be submerged by merely using high gain feedback loops (3). The required aerodynamic control moments and power required for high gains in flight control systems are not available due to limits imposed by vehicle design considerations unrelated to the automatic control system design. Even if high gains could be obtained, the gains could result in severe bending and slosh mode oscillations when considering flexible airframes. The values that the Inverse Model transfer function can assume and still affect the short period mode in the desired manner are also limited for flexible airframes. The limit on the values of the transfer function for this investigation is discussed in Section 2.5.

For flight control systems the limitation on high gains and on values of the Inverse Model prevents the use of a true High Gain Linear Feedback

10
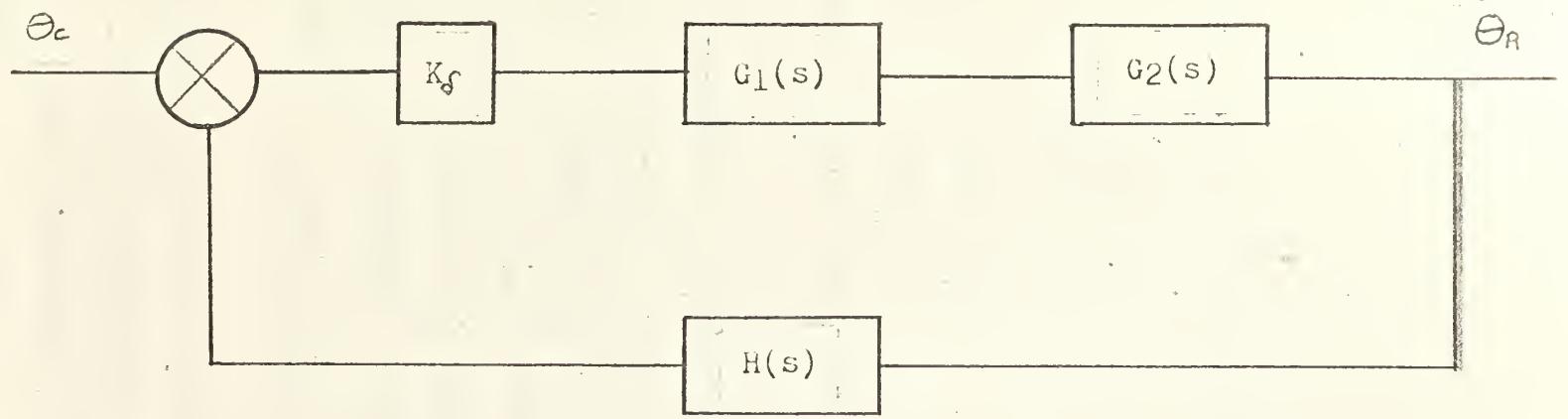
$G_2(s) = M_\delta G_2^*(s)$ where M_δ is the aerodynamic gain.

$$\frac{\Theta_R}{\Theta_c} = \frac{K_\delta G_1(s)G_2(s)}{1 + K_\delta H(s)G_1(s)G_2(s)} .$$

If K_δ is large and $K_\delta H(s)G_1(s)G_2(s) \gg 1$, then

$$\frac{\Theta_R}{\Theta_c} = \frac{1}{H(s)} .$$

Figure 2.3. General Feedback System.

self adaptive scheme, however, the Inverse Model can be used as a fixed

shaping network to improve the dynamic characteristics of the short period

mode and is employed as such in the system under investigation.

In view of restricting the Inverse Model to the idea of a fixed shaping

network, the self adaptive scheme used in the Dither System can be thought

of as a form of the Programmed Compensation Method. The three basic opera-

tions that an adaptive loop must perform are listed in Section 2.1. The

manner in which the Dither System performs these operations are listed below:

1. The dither signal is the means for the continuous measurement
    of the system dynamic response. In order to have a negligible
    effect on the system response signal, the dither frequency
    should be five or more times the short period mode frequency
    and the input level should be small so that the oscillations
    are not noticeable to the vehicle personnel. The reason for
    using pitch acceleration instead of pitch angle or rate as the
    pickoff for the adaptive loop is to enable smaller inputs for
    the same output. The upper limit for the dither frequency
    depends on the ability of the actuator to respond to the fre-
    quency and on the bandwidths of the rest of the system components.
    The upper limit is around 40 radians per second for available
    systems.

2. The continuous evaluation of the dynamic performance is per-
    formed by comparing the amplitude of the pitch acceleration to
    dither input level evaluated at the dither frequency to the
    Performance Criterion Reference. It remains to be discussed
    below and in Chapter 4 how accurately the dynamic performance
    is being evaluated. In this investigation the damping ratio

is being used as the measure of dynamic performance.

3. The continuous readjustment of the system control parameter, which is the gain, is accomplished by a servo driven by the error resulting from the evaluation procedure.

In the Programmed Compensation Method the parameter adjustment is accomplished through a program which requires a knowledge of the relationship between the system and compensation parameters. In the dither system the program consists of a single reference level which requires a knowledge of the variation of the system damping ration with the amplitude of the acceleration to dither input level ratio.

The degree of self adaptability of the dither system depends on the accuracy with which the damping ratio is measured by the acceleration to input level ratio. There are many figures of merit that can be used as a criterion for the dynamic performance of a system. Some of the figures of merit are $\int_0^\infty \varepsilon \, dt$, $\int_0^\infty \varepsilon^2 \, dt$, $\int_0^\infty |\varepsilon| \, dt$, $\int_0^\infty t\varepsilon \, dt$, $\int_0^\infty t|\varepsilon| \, dt$ where ε is an error signal. The applicability of these figures of merit for use in establishing a damping ratio of 0.7 has been determined for a second order system to be as follows: (4)

$\int_0^\infty \varepsilon \, dt$ selects zero damping ratio as optimum.

$\int_0^\infty \varepsilon^2 \, dt$ selects 0.5 damping ratio as optimum.

$\int_0^\infty |\varepsilon| \, dt$ selects 0.7 damping ratio as optimum.

$\int_0^\infty t\varepsilon \, dt$ selects zero damping ratio as optimum.

$\int_0^\infty t|\varepsilon| \, dt$ selects 0.7 damping ratio as optimum.

If the system was of second order, both $\int_0^\infty |\varepsilon| \, dt$ and $\int_0^\infty t|\varepsilon| \, dt$ would select 0.7 as the optimum damping ratio based on the figure of merit approaching a minimum value at a damping ratio of 0.7. The $\int_0^\infty t|\varepsilon| \, dt$ figure of merit has the sharpest minimum and would be the

13

preferred criterion. With a flexible airframe the system can not usually be approximated by a second order system with any accuracy, and the applicability of the above criterion for establishing optimum damping ratios of the short period mode under these conditions is not known. The components required to mechanize the $\int_0^\infty t\,|\epsilon|\,dt$ criterion into a system is certainly more complex than the Dither System, and the possibility of the criterion selecting a damping ratio of 0.7 for a non second order system is considered doubtful. A different figure of merit called the Impluse Response Area Ration (IRAR) will permit the selection of any desired damping ratio and have the error signal assume a zero value when the response is at the selected damping ratio (5). The method required for use of the IRAR criterion would be to pulse the system and then measure the area of the response. The area is a measure of the damping ratio. By comparing the area with a reference area corresponding to the desired damping ratio an error signal is developed which would vary the gain of the system until the error was zero. In a flexible airframe control system which does not use shaping networks, the poles and zeros of the vehicle transfer function are continually varying. For the reference area to indicate the true damping ratio it would also have to vary with the parameters and in effect would need a self adaptive loop to adjust its value. The system would be very complex if not impossible to mechanize.

The Dither System works on the principle of maintaining the gain of the system constant throughout the flight and assumes that a constant gain will maintain an optimum damping ratio. Referring to Figure 2.3 and substituting $\Theta_c = E_M \sin W_o t$ AND $\Theta_R = \ddot{\Theta}_R$ an adaptive loop is formed.

$$\frac{\ddot{\Theta}_R}{E_M}(j w_o) = \frac{K_\delta M_\delta\, G_1(j w_o)\, G_2^*(j w_o)}{1 + K_\delta M_\delta\, G_1(j w_o)\, G_2^*(j w_o)\, H(j w_o)} \; .$$

14

Since $K_\delta M_\delta \, G_1(j\omega_0) \, G_2^*(j\omega_0) \, H(j\omega_0)$ has a denominator of greater order than the numerator, $\frac{\ddot{\Theta}_R}{E_M}(j\omega_0) \cong K_\delta M_\delta \, G_1(j\omega_0) \, G_2^*(j\omega_0)$ when ω_0 is a large value. Therefore, $\frac{\ddot{\Theta}_R}{E_M}(j\omega_0)$ is a direct measure of the gain, $K_\delta M_\delta$, of the system. The self adaptive loop maintains the value of $K_\delta M_\delta$ equal to the reference value. If a constant value of $K_\delta M_\delta$ is an accurate measure of the damping ratio, δ, for a flight control system, then a plot of $K_\delta M_\delta$ versus δ should show a constant $K_\delta M_\delta$ for a particular δ for all flight cases. Using the M_δ's of the flight cases to be investigated a plot of $K_\delta M_\delta$ vs δ is shown in Figure 2.4 for aerodynamic equations with no bending modes included, the first bending mode included and the first and third bending modes included. The aerodynamic equations and conditions are discussed in Section 2.4. As is observed from the Figure, $K_\delta M_\delta$ is an accurate criterion for a constant δ for no bending, but as bending modes are included and the order of the system increases $K_\delta M_\delta$ becomes a less accurate figure of merit. The investigation of the variation of the damping ratio for the various aerodynamic conditions and the determination of the optimum Performance Criterion Reference and the optimum dither frequency is contained in Chapter 4.

Figure 2.4. $K_\delta M_\delta$ vs δ

16

2.4 Aerodynamic Equations and Modifications.

The airframe used in this investigation is the two staged Saturn
Booster. Perturbated aerodynamic equations with coefficients for four
flight cases are included in Appendix A. The flight cases are identified
by the time in seconds after launch. The flight cases are t = 20, t = 75,
t = 101.9, and t = 200. The t = 200 case is for the second stage only,
as the first stage separates before t = 200 seconds. The reference for
the equations is the nose of the second stage. For flight cases t = 20, t =
75, and t = 101.9 the acceleration, rate, and position sensors are located
on the same platform in the first stage. The variation in performance for
various platform positions will not be covered in this investigation. The
platform position used had been selected for maximum system stability
immediately after launch and for airframe considerations. The platform
position for case t = 200 is in the nose of the second stage. The transfer
functions which were determined from the equations using digital computers
are included in Appendix A.

The aerodynamic equations contain three bending modes and one fuel
slosh mode. A typical root locus is shown in Figure 2.5. It will be
observed from the Figure that the open loop system is unstable. Case t =
20, which is the first case considered after launch and where the missile
is still verticle, is the only flight case with a stable open loop. An
unstable aerodynamic condition occurs when the center of pressure is for-
ward of the center of gravity. A missile of conventional shape will be
unstable unless stabilizing fins are attached because the center of
pressure of the fuselage alone is close to the shoulder whereas the center
of gravity is close to the geometric center (6). For large missiles, such
as the Saturn, the trend is towards stabilization through a control system

17
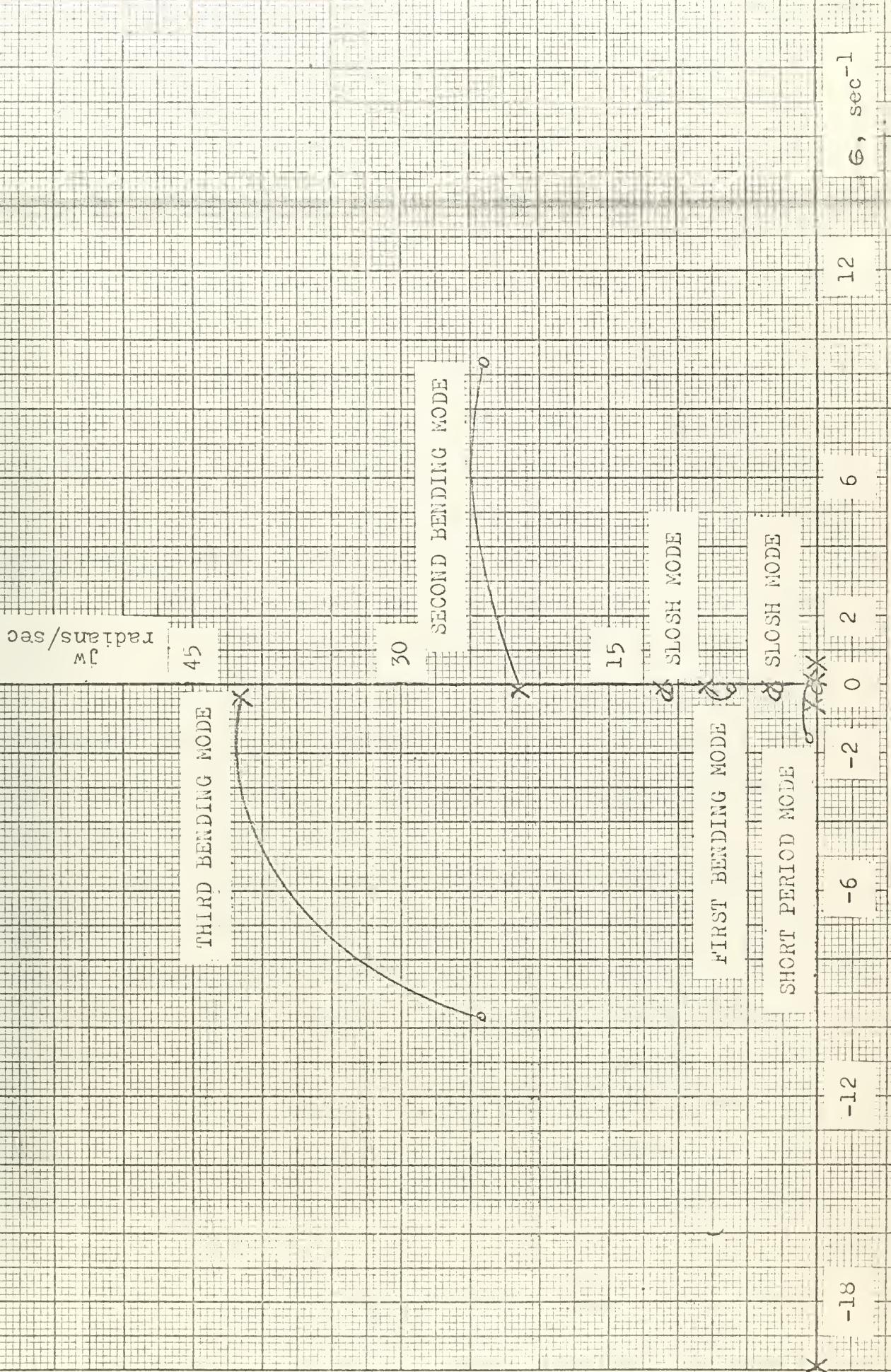
Figure 2.5. Typical Root Locus

rather than providing for a stable airframe because of the weight required
for the stabilizing fins. The control torques required for the control
system are provided for in the Saturn by gimbaled thrust chambers. It
will also be observed from the Figure that the Slosh Mode has a negligible
effect on the system stability. Multitank design with slosh suppressors
are used in the Saturn to obtain this condition. The different slosh mode
frequencies correspond to different tanks.

The second bending mode becomes unstable for an adaptive variable gain
of approximately 0.1 for the t = 20, 75, and 101.9 cases. In order to
eliminate the possibility of obscuring the actual dither system performance
by the complexity of adding bending mode cancellation schemes, the unstable
second bending mode was handled in one of two ways:

1. The second bending mode was eliminated from the aerodynamic
equations assuming that a bending cancellation method was in use.

2. The second bending mode was eliminated by assuming that a
compensation method was in use, such as a frequency tracker and notch
filter scheme, which placed a pole and zero over the open loop zero and
pole respectively of the bending mode.

A bending cancellation method which could be used for procedure 1
above is shown in Figure 2.6. This is one of many cancellation methods
proposed by the Autonetics Division of North American Aviation. The purpose
of the system is to form a signal of equal magnitude and opposite phase to
the bending mode signal. The signal formed is then added to the control
signal and effectively cancels the bending mode from the system response
signal. Bandpass filters land 2 are variable tuned filters with center
frequencies of w_0 . If filter 1 is not tuned to the bending frequency,

See
19
letters in front of thein
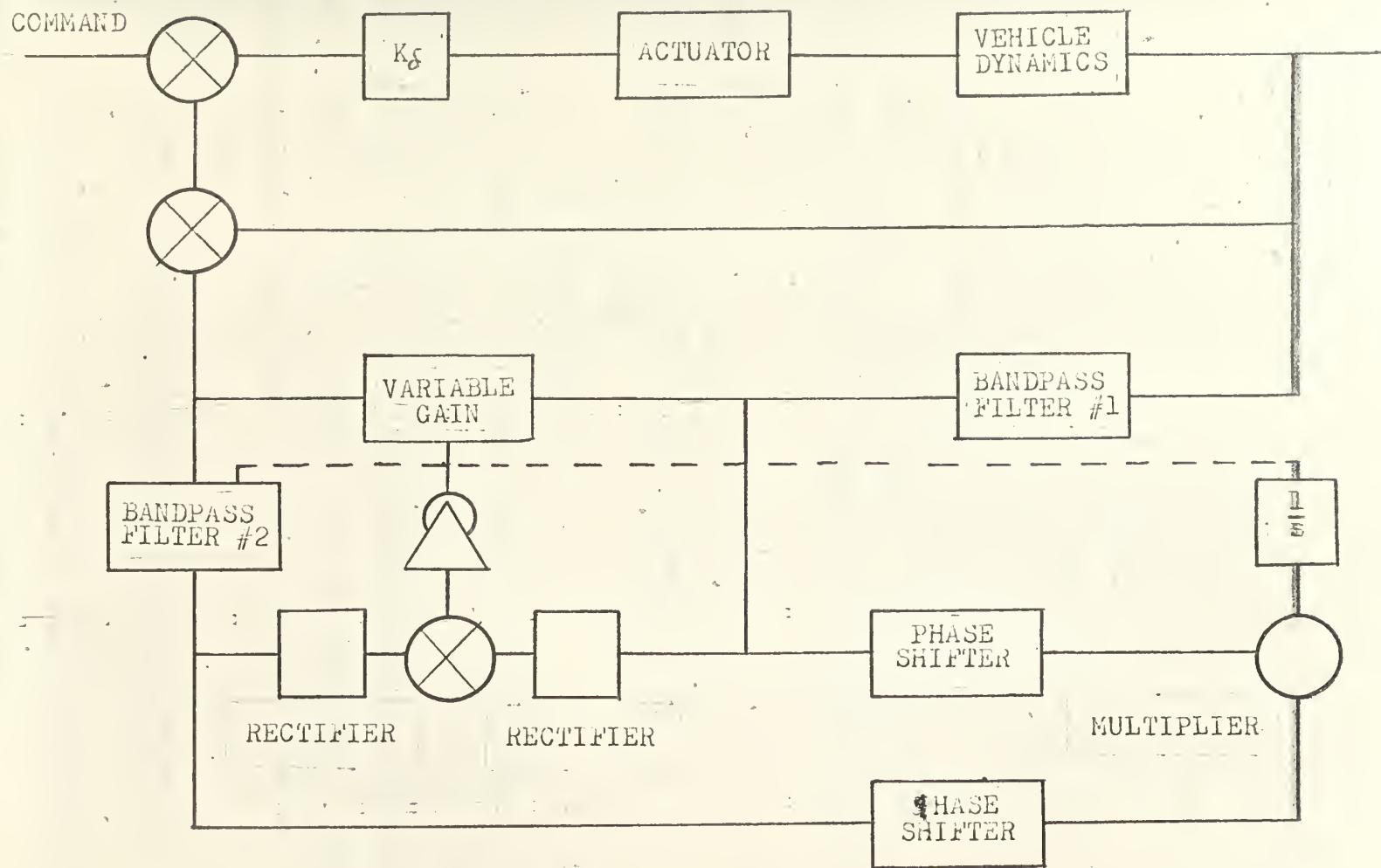
Figure 2.6. Bending Cancellation Method

the bending frequency signal component is phase shifted by an amount ϕ and the output signal from filter 1 is $\sin(\omega_0 t + \phi)$. The bending signal is again phase shifted by an amount ϕ by filter 2 with output signal being $\sin(\omega_0 t + 2\phi)$. The outputs from the two filters pass through phase shifters which produce a 90 degree phase shift between the signals. The shifted signals are then multiplied, and the resulting signal drives an integrator which varies the center frequencies of the filters until the output from the multiplier is zero. As is shown below, the output of the multiplier is zero when the filters are tuned to the bending frequency.

Output of multiplier $= \sin(\omega_0 t + \phi) \quad \cos(\omega_0 t + \phi)$

$= (\sin \omega_0 t \cos \phi + \cos \omega_0 t \sin \phi)(\cos \omega_0 t \cos 2\phi - \sin \omega_0 t \sin 2\phi)$.

The integrator is not sensitive to frequencies much greater than the bending frequency.

Therefore,

Effective Output $= 1/2 \cos 2\phi \sin \phi - 1/2 \cos \phi \sin 2\phi$

$= 1/2 \sin \phi$

$= 0$ when ϕ is zero.

With the filters tuned to the bending frequency, the 180 degree phase shift is accomplished by subtraction from the feedback signal. The amplitude of the bending signal is adjusted by the rectifier-integrator comparison loop using the outputs of filters 1 and 2, for the comparison. Another bending mode cancellation method using a rejection filter philosophy is contained in Reference 7.

The different aerodynamic conditions that are investigated are listed below:

1. No bending and no slosh modes included in the equations. The resulting equations are the rigid body equations.

21

2.   The first bending mode added to the rigid body equations.

3.   The first and third bending modes added to the rigid body equations. The second bending mode is assumed removed by a bending mode cancellation method.

4.   The first and third bending and first slosh modes added to the rigid body equations. The second bending mode is assumed removed by a frequency tracker and notch filter method.·

In Chapter 3 the analog computer investigation was conducted using aerodynamic conditions 1, 2, and 3 and flight cases t = 20, 75, 101.9 and 200. The second bending mode was included in condition 3 for flight case t = 200 because the mode is not unstable for this case.

In Chapter 4, the empirical investigation was conducted using aerodynamic conditions 1,2,3, and 4 and flight cases t = 20, 75, and 101.9.

2.5   Limitations on Inverse Model by Flexible Airframe.

The system under investigation is unstable unless a shaping network is employed. From a root locus viewpoint if a complex pair of zeros were provided in the left half plane, the unstable short period mode would be shaped into the left half plane and the system would be stabilized. The Inverse Model provides these shaping zeros.

If a damping ratio of 0.7 and a natural frequency of 3 radian per second were the desired dynamic characteristics of the short period mode, the Inverse Model should ideally provide a pair of zeros at $s = -2.1 \pm j2.18$ on the root locus. A high system gain would then establish a complex pair of roots of the system characteristic equation at values $s = -2.1 \pm j\ 2.18$. The roots would fix the dynamic characteristics of the short period mode at a damping ratio of 0.7 and a frequency of 3. As was discussed in Section

2.3, high gain capabilities are not available in flight control systems.

The desired dynamic characteristics could still be obtained even though high gains are not available by increasing the real and imaginary coordinates of the Inverse Model zeros. The zeros could shape the short period dynamic characteristic curve in such a manner that for lower values of gain the desired characteristics are available. Increasing the coordinates of the Inverse Model zeros is possible in a rigid airframe with negligible center of gravity movement. For flexible airframes the bending modes must be considered in establishing the position of the Inverse Model zeros.

If the coordinates of the zeros are increased beyond certain values with a flexible airframe system, the zeros shape primarily a different mode than the short period mode. While the short period mode would be stabilized, its maximum damping ratio and natural frequency values would be less and its coupling with the shaped mode would be greater than when the zeros shape primarily the short period mode. A digital computer investigation of the optimum position of the zeros was conducted.

The preliminary investigation showed that flight case $t = 75$ was the critical flight case and that the two bending modes plus slosh mode condition was the critical condition. Flight case $t = 75$ was further investigated as to the benefit of using rate and position feedback which would give one real axis zero or of using acceleration, rate, and position feedback which would give the complex pair of zeros. The complex zero arrangement provided for more shaping of the short period mode and less possible coupling between the first bending mode and short period mode. The coordinates of the complex zeros were then varied to obtain optimum values.

23

Typical root loci are shown in Figure 2.7. For Inverse Model position 3, the zeros shape primarily the first bending mode. While the short period mode is stabilized, it is not being shaped in an optimum manner and has the disadvantages of decreasing in damping ratio as gain increases beyond a certain value and of being coupled with the bending mode. The short period mode could never obtain a 0.7 damping ratio. For Inverse Model positions 1 and 2, the short period mode is being primarily shaped. The bending mode is also shaped further into the left half plane increasing its stability while producing a negligible increase in coupling. Position 2, with the zeros at $s = 1.8 \pm j.6$, appears to be the optimum position. The maximum natural frequency of the short period mode at a damping ratio of 0.7 occurs at this position. As is observed, the natural frequency will never reach 3 radians per second. A more complicated shaping network could be used to increase the natural frequency, but since one of the principal advantages of the Dither System is simplicity, a compromise has been made on the desired dynamic characteristics. As was defined in Section 2.3, the optimum dynamic characteristics of the short period mode for the investigation are a damping ratio of 0.7 with a minimum natural frequency variation.

The optimum Inverse Model transfer function for the severest flight case and condition will remain fixed at $s^2 + 3.6s + 3.6$ for all flight cases and for all aerodynamic conditions.
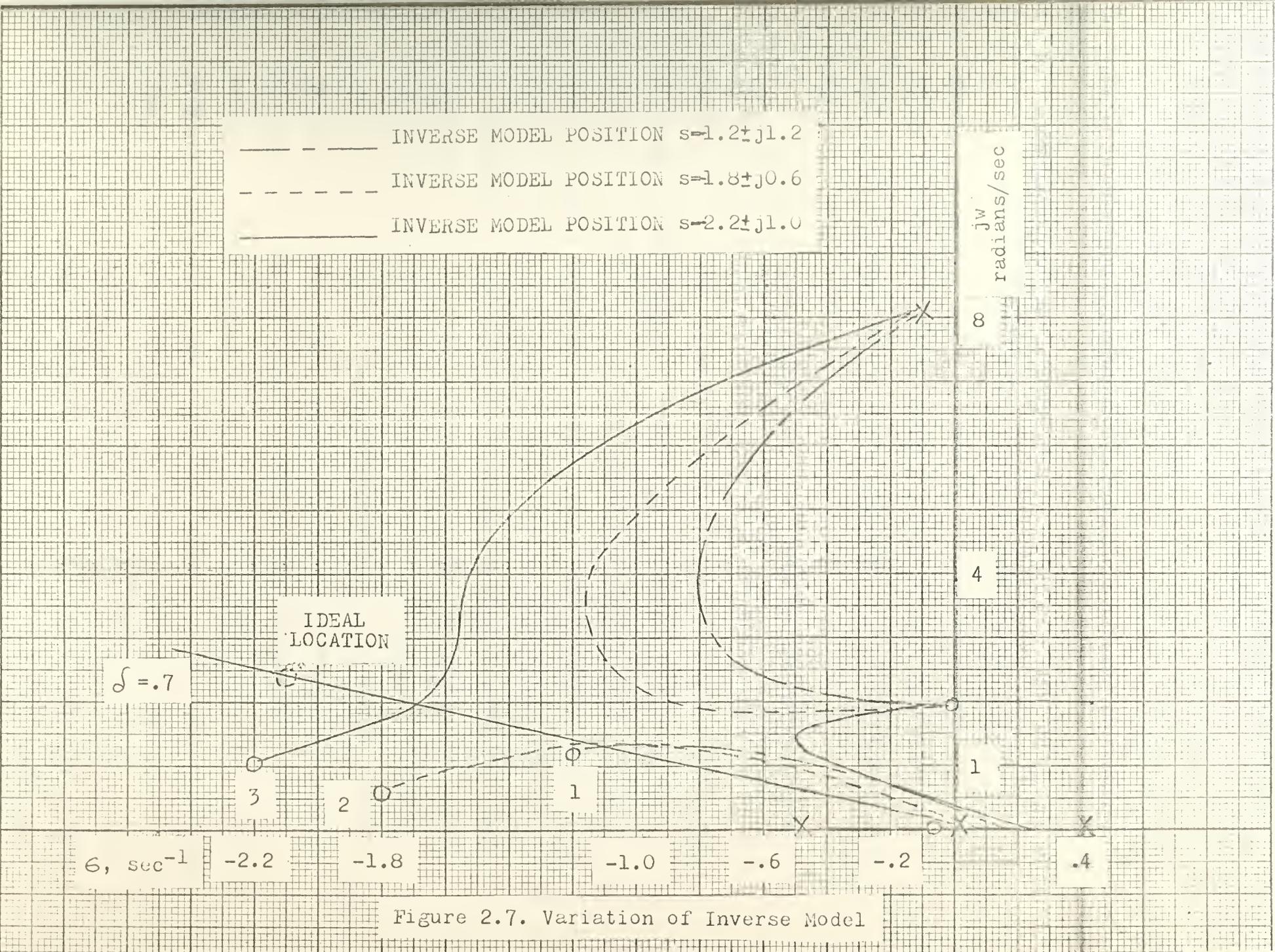
Figure 2.7. Variation of Inverse Model

CHAPTER 3

COMPUTER SIMULATION

3.1 Introduction.

The object of this Chapter is to investigate the ability of the
Dither Self Adaptive System to correct for the varying dynamic character-
istics of a flexible airframe during a typical flight. The correction is
made by the adjustment of the control parameter which is the adaptive gain,
k_δ .

An analog computer simulation was conducted for the primary purpose
of determining the values of the adaptive gain which the system selected
for the various flight cases and for the various aerodynamic conditions.
The values of gain which were selected in the computer simulation are
compared with the values of gain determined by digital computer methods.
Digital computer techniques are employed in the investigation in Chapter 4,
and the comparison with analog computer results in this Chapter is used as
an indication of the accuracy of the results of Chapter 4 when the transi-
tion is made from numerical to electrical simulation. The damping ratios
of the short period modes which are associated with the gains selected by
the analog simulation for the various aerodynamic conditions are determined
from root loci using digital computer techniques and are compared to show
the effect of a flexible airframe on the ability of the dither system to
maintain a constant damping ratio. The damping ratios of the short period
mode resulting from the use of the dither system are also compared with the
damping ratios resulting from the use of a constant K_δ system.

The dither frequency and reference level which would maintain through
the flight an average damping ratio of the short period mode of 0.7 with a
minimum variation of the damping ratio and natural frequency were not used

26

in the computer simulation. The results of the computer simulation indicated the necessity of determining optimum frequencies and reference levels. The investigation of this area is contained in Chapter 4.

The secondary purpose of the analog computer simulation was to determine for the various flight cases and aerodynamic conditions the rate at which the adaptive gain was adjusted and the reaction of the self adaptive loop to wind gusts, actuator movements, and loss of the dither signal. A complete analysis of the self adaptive loop was not conducted in the investigation; and therefore, the values of the loop gain and filter bandwidth for optimum dynamic response of the loop were not determined. The investigation was conducted using different loop gains for the various flight cases. A qualitative discussion of the adaptive loop is contained in Section 3.5.

3.2 Analog Computer Setup.

The analog investigation was conducted using aerodynamic conditions 1,2, and 3 as described in Section 2.4. For Flight Case t = 200 the second bending mode was included because the mode is not unstable for this case. The system was simulated in two, forty amplifier, Pace Computers by Electronic Association Inc. The voltmeter used to determine the K_δ values and the integrating servo and rectifier used in the adaptive loop were inherent components of the computers. Two six channel Sanborn recorders were used. A Hewlett-Packard, Low Frequency, Function Generator was used as the source of the dither signal.

The computer simulation diagram is shown in Figure B-1. The reference values of pitch acceleration, $\ddot{\theta}$, pitch rate $\dot{\theta}$, and pitch angle, θ, which are measured at the nose of the second stage are converted to the platform values, $\ddot{\theta}_F$, $\dot{\theta}_F$, and θ_F, for flight cases t = 20, 75, and 101.9, because the sensors for these cases are on the same platform which is located

27

in the first stage. The reference values are the platform values for Flight Case t = 200, because the platform for this case is in the nose of the second stage.

The first flight case simulated was t = 75 for aerodynamic condition 3. Static and dynamic checks were conducted. The procedure used for the dynamic checks was to excite the bending and short period modes by voltage steps introduced into the amplifiers of the various mode simulations and to compare the resulting frequencies and damping ratios with the frequencies and damping ratios determined by digital computer techniques. The transfer function resulting from the removal of the poles and zeros associated with the second bending mode from the vehicle dynamic transfer function, which was derived from the aerodynamic equations with three bending modes and one slosh mode, was considered a good approximation for determining the first and third bending mode frequencies for condition 3. A comparison with the analog results of the dynamic checks indicated that new transfer functions based on the applicable aerodynamic equations were required. The transfer function for flight case t = 75 for aerodynamic condition 3 indicated that the only poles and zeros of the transfer function, which was derived from the aerodynamic equations with three bending modes and one slosh mode, that were appreciably moved were the zeros associated with the third bending mode. The value of the zeros were changed from $s = -11.56 \pm j21.63$ to $s = -.17 \pm j24.3$. The effect of the bending and slosh mode parameters on the vehicle dynamic characteristics can be determined by observing the movement of the poles and zeros of the transfer functions, which are contained in Appendix A, for the various aerodynamic conditions. The static checks agreed to within one half of a per cent with analytical values. The mode

frequencies of the analog computer agreed to within two per cent of the
frequencies determined by digital methods, and the damping ratios agreed
to within five per cent.

The procedure used to simulate the self adaptive loop was as follows:

1. The filter was simulated and the bandwidth was varied until
a sharp peaked frequency response was obtained with the peak at the dither
frequency of 30 radians per second. A bandwidth of 3 radians per second
produced a sharp peak.

2. Two diodes which were inherent components of the computer
were used to form a rectifier. The outputs from the two diodes were of
different values; and therefore, gain pots were included with each of the
diodes so that equal outputs could be obtained.

3. The adaptive gain, k_δ , was simulated by using a linear
gain pot driven by an integrating servo. The servo and pot were inherent
components of the computer. One volt into the servo resulted in a gain
change of 0.2. A linear pot was used because it was readily available.
A shaped gain pot should be used in reality to obtain a small gain to servo
input ratio for low values of gain and a large ratio for large values of
gain. A small gain to servo input ratio is desired at low values of gain
so that a wind gust or other disturbance would not reduce the gain apprec-
ably with the possibility of the system going unstable. As the gain in-
creases the dynamics of the short period mode improve so that while a
disturbance at high gains would vary the gain more than at low gains the
response time is improved and stability considerations are not as critical.
Compromises must be made in the shaping of the gain pot between the large
ratio of gain to servo input desired for fast adaptive response, the small
ratio desired when disturbances are experienced, and the ratio required for

29

constant dynamic characteristics of the adaptive loop itself during a flight. The discussion of maintaining the adaptive loop gain appreciably constant during a flight is contained in Section 3.5.

4. A gain pot was inserted before the integrating servo to provide for varying the ratio of K_δ to servo input and the adaptive loop gain. The adaptive loop gain was adjusted by varying the gain pot, K_A , until the gain adjustment response, K_δ , ceased to oscillate and was critically damped with a suitable rate of change of the value of K_δ . The Reference DC signal was then adjusted to provide for a value of K_δ of 1. The adjustment of the adaptive loop gain to give a suitable rate of change of K_δ and the setting of the Reference level so that K_δ had a value of 1 was performed for each aerodynamic condition of Flight Case t = 75 in order to obtain reference values. The reference values that were obtained eliminated the necessity for a complete evaluation of the analog simulated loop and were used in the other flight cases to form the basis for the comparison of the values of K_δ that the system selected.

When the system was energized, the servo chattered because it was following the half cycle sinusoidal like waveform at its input. A smoothing network would be required at the rectifier output to produce a flatter output and eliminate the servo chatter. In order to maintain the adaptive loop as simple as possible and also to investigate the effect of bending interference the bandwidth of the filter was increased to 5 radians. The third bending mode frequency which was now at the limits of the bandwidth was passing through the loop because the waveform from the rectifier flattened out so that the servo stopped chattering. Since a dither frequency of 30 radians per second excited the third bending mode for aerodynamic condition 3, the computer results would indicate the performance of the

30

dither system when bending or noise signals were contained in the filtered frequency of the self adaptive loop. In order to determine the performance of the system with no bending and minimum noise signals in the self adaptive loop, reference values were also recorded for Flight Case $t = 75$ for aerodynamic condition 3 with a dither frequency of 20 radians per second. The filter was adjusted for a center frequency of 20 and a bandwidth of 3. The lower frequency did not cause the servo to chatter.

The general procedure used in the simulation for Cases $t = 20$, 101.9, and 200 was as follows:

1. The computer was set up for condition 3 of the particular flight case.

2. Static and dynamic checks were conducted.

3. The Reference level and Ks_A were set at the values used for the corresponding aerodynamic condition and dither frequency of Flight Case $t = 75$.

4. The values of K_δ as read from the computer voltmeter were recorded for aerodynamic conditions 1, 2, and 3 with a dither frequency of 30 radians per second and for condition 3 with a dither frequency of 20 radians per second.

5. The value of Ks_A was adjusted to give a suitable rate of change of K_δ for the particular aerodynamic condition and flight case. The Reference level was then adjusted to give the corresponding value of K_δ as determined in Step 4 with a dither frequency of 30.

6. Recordings were made at the dither frequency of 30 for aerodynamic conditions 1 and 3. During the run for each condition, K_δ was offset by a step voltage put into the integrating servo amplifier; an actuator signal, δ_T, was put into the system by a step voltage into the

simulation for the actuator; a wind gust was simulated by a step voltage into the attack angle, α , amplifier; and a dither signal failure was simulated by turning off the signal generator.

Step 6 was also conducted for Case t = 75.

3.3 Comparison of System Selected Gains.

The values of the adaptive gain, K_δ , which were recorded by the procedures described in Section 3.2 during the analog computer simulation are compared in this Section with values of gain determined from digital methods to establish a correspondnece between the two procedures. A Recomp II Computer was used for the digital calculations. The damping ratios of the short period modes corresponding to the recorded adaptive gains are compared to establish the relative adaptibility of the system under vary- ing aerodynamic conditions and dither frequencies and are compared with the damping ratios corresponding to a fixed gain system to establish the benefit of the adaptive system for the airframe being used for the investi- gation. The analog computer simulation was conducted for aerodynamic conditions 1, 2, and 3 as described in Section 2.4. The digital investiga- tion included aerodynamic condition 4, and the damping ratios associated with the gains for a particular Dither Reference level for this aerodynamic condition are included in the comparison of the damping ratios of the ana- log computer.

The determination by digital methods of the values of K_δ which the system would select was accomplished by computing the amplitudes of the closed loop response for various gains and for frequencies of 20 and 30 radians per second. Plots of the amplitudes of the closed loop response versus K_δ for a dither frequency of 30 were made of the flight cases for

each aerodynamic condition. For aerodynamic condition 3 plots were made

for dither frequencies of 30 and 20. The plots are shown on Figures B-2

(a) through B-2(f). An adaptive gain of 1 was set on the analog computer

for each aerodynamic condition of Flight Case t = 75 and was used as the

standard for determining the values of Reference level and adaptive loop

gain pot settings which were maintained constant in recording the adaptive

gains of the remaining flight cases. The adaptive gain value of 1 for Case

t = 75 was also used as the standard for the digital method. The reference

amplitude of the system was determined on the plots by the intersection of

the K_δ equal to 1 line with the Flight Case t = 75 curve. The reference

amplitude eliminated the necessity of evaluating the components of the

adaptive loop to determine a Reference Signal level and was used to deter-

mine the values of gain which the system would select for the other flight

cases by the intersection of the reference amplitude and the particular

flight case curve.

The comparison of the adaptive gains determined by analog and digital

methods is shown in Table I and II for aerodynamic conditions 1and 2

respectively at a dither frequency of 30. The reference amplitude deter-

mined for aerodynamic condition 3 at a dither frequency of 30 was too large

for use with Flight Cases t = 101.9 & 200 as shown on Figures B-2(c). The

dither frequency was varied in the digital method for each flight case

until a reference amplitude was determined which resulted in the gains which

were selected by the analog computer. The dither frequencies required to

obtain the gains are shown in Table III. The plots of closed loop response

amplitude versus K_δ for the different dither frequencies required are shown

in Figure B-2(d). The third bending mode was excited at a dither frequency

of 30 radians per second and the filter bandwidth allowed the bending signal

TABLE I

Gain Comparison for Aerodynamic Condition 1 at Dither Frequency of 30

Flight Case	Gain Selected by Analog Computer	Gain Determined by Digital Procedure
t = 20	1.73	1.69
t = 75	1.0	1.0
t = 101.9	0.54	0.535
t = 200	1.15	1.17

TABLE II

Gain Comparison for Aerodynamic Condition 2 at Dither Frequency of 30

Flight Case	Gain Selected by Analog Computer	Gain Determined by Digital Procedure
t = 20	1.35	1.3
t = 75	1.0	1.0
t = 101.9	0.8	0.72
t = 200	3.4	3.42

34

to pass through the adaptive loop as was discussed in Section 3.2. The dither signal source could not be accurately set to within 0.628 radians per second; and since two dither frequencies were used for each flight case, the signal source had to be adjusted for each case. The variation in the digital frequencies required to obtain the analog gains is approximately within the accuracy of the signal source settings. The necessity for very accurate determination and setting of the dither frequency and Reference Signal level when bending modes are excited close to the dither frequency is illustrated by the difficulty in obtaining a comparison of the gains for the digital and analog methods. When bending or noise signals pass through the adaptive loop, there is a possibility of the system having a choice of selecting either of two adaptive gains which are relatively close in magnitude. The selection of the wrong gain might cause the system to be unstable. As is shown in Figure B-2(d), the reference amplitude intersects the flight cases at two relatively close values of K_δ. The comparison of the gains determined for aerodynamic condition 3 at a dither frequency of 20 is shown in Table IV. The difficulties experienced with a dither frequency of 30 were not experienced at a frequency of 20 where bending modes are not excited. The plots of closed loop response versus K_δ for a dither frequency of 20 are shown in Figure B-2(e).

Root loci were determined for the various flight cases and aerodynamic conditions using a Recomp II digital computer. The damping ratios of the short period modes corresponding to the gains selected by the analog computer with a dither frequency of 30 and to the gains selected by digital techniques for aerodynamic condition 4 with a dither frequency of 30 were determined from the root loci and are compared in Table V.

TABLE III

Frequencies Required by Digital Method for Gains Determined by Analog
Method for Aerodynamic Condition 3 at Dither Frequency of 30

Flight Case	Gain Selected by Analog Computer	Frequency Required by Digital Method in Radians per Second
t = 20	1.0	28.5
t = 75	1.0	28.5
t = 101.9	2.1	30.0
t = 200	5.0	28.17

TABLE IV

Gain Comparison for Aerodynamic Condition 3 at Dither Frequency of 20

Flight Case	Gain Selected by Analog Computer	Gain Determined by Digital Procedure
= 20	1.35	1.42
t = 75	1.0	1.0
t = 101.9	0.6	0.6
t = 200	1.5	1.5

TABLE V

Damping Ratio Comparison for Flights Under Various Aerodynamic Conditions

Flight Case	Damping Ratios for Aerodynamic Condition 1	Damping Ratios for Aerodynamic Condition 2	Damping Ratios for Aerodynamic Condition 3	Damping Ratios for Aerodynamic Condition 4
t = 20	.82	.78	.725	.685
t = 75	.794	.838	.843	.72
t = 101.9	.838	.87	.912	.875
t = 200	.89	.924	.93	.89
Total Variation in Damping Ratio	.1	.14	.21	.21
Average Damping Ratio for Flight	.836	.853	.852	.792
Variation from t = 75 Reference	+.09ː -.0	+.086 -.058	+.087 -.118	+.17 -.035

Flight Case t = 75 was used as the reference for both the analog and digital procedures; and therefore, the maximum variations of the damping ratios of a particular flight from the damping ratio of cases t = 75 is probably the best criterion to show the effect of bending modes on the adaptibility of the system. The results of the comparison of the first three aerodynamic conditions shows adaptibility decreasing as bending is included, but the comparison is valid only for a dither frequency of 30 and must be checked for other dither frequencies. The investigation as to the effect on the results of a comparison when the dither frequency is varied is contained in Chapter 4. A different method was used in aero-dynamic condition 4 than in condition 3 to remove the second bending mode. The different methods resulted in a large variation of the position of the zeros associated with the third bending mode as is noted by examining the transfer functions in Appendix A. The comparison of the two conditions in Table V indicates that for a dither frequency of 30 the frequency track-ing and notch filter scheme for removing the second bending mode results in a more adaptive system than the bending cancellation scheme. The total varia-tion of the damping ratios of the two conditions is the same but condition 4 includes a slosh mode, has the larger value of variation from the reference value of the t = 75 case towards greater damping, and has an average damping ratio during the flight less than condition 3. For a larger average damping ratio during a flight, a smaller variation in the damping ratios would be expected because a larger average damping ratio means larger gains are used and large gains force the damping ratios towards the constant damping ratio determined by the position of the Inverse Model.

The damping ratios as determined from the root loci for the gains select-ed by the analog computer for aerodynamic condition 3 with dither frequencies

38

of 30 and 20 are compared in Table VI with the damping ratios of a fixed gain system with the gain set at a value of 1. The gain of a value of 1 was selected for the fixed gain system in order to establish the same reference for Case t = 75 that was used for the Dither System. The results of the comparison show that the fixed gain system is more adaptive than the dither system at a frequency of 30 radians per second but is less adaptive than the dither system at a frequency of 20. The great difference in the performance of the dither system as the dither frequency was varied led to the investigation of obtaining the optimum dither frequencies for the different aerodynamic conditions. This investigation is contained in Chapter 4.

3.4 Reaction of the System to Disturbances.

Aerodynamic conditions 1 and 3 were used in the investigation of the rate at which the adaptive gain was adjusted and the reaction of the adaptive loop to wind gusts, actuator movements, and loss of dither signal. The investigation was conducted with a dither frequency of 30 radians per second so that the evaulation of the adaptive loop for aerodynamic condition 3 would be performed under the unfavorable conditions of having bending signals included with the filtered dither signal in the adaptive loop. Since a complete analysis of the adaptive loop was not performed, the adaptive loop gain was adjusted for each flight case with the following considerations:

1. To produce a suitable rate of change of the adaptive gain, K_δ.

2. To show the variation in the loop performance for different flight cases with the same setting of the servo gain pot, K_{SA}.

3. To use several values of K_{SA} for the flight cases with one value producing an overshoot in the K_δ response.

TABLE VI

Damping Ratio Comparison of Dither System and Fixed Gain System

Flight Case	Damping Ratios for Dither Frequency of 30	Damping Ratios for Dither Frequency of 20	Damping Ratios for Fixed Gain System
$t = 20$	.725	.78	.725
$t = 75$	.843	.838	.843
$t = 101.9$	.912	.844	.88
$t = 200$	.93	.9	.882
Total Variation in Damping Ratio	.21	.12	.16
Average Damping Ratio for Flight	.852	.84	.832
Variation from $t = 75$ Reference	+.09 -.118	+.06 -.06	+.039 -.118

The same K_{SA} setting was used for corresponding flight cases under the different aerodynamic conditions to show the effect of bending on the loop performance.

Recordings were made of the reaction of the system to various disturbances for the different flight cases and aerodynamic conditions. The traces for the flight cases for aerodynamic condition 3 showing the actuator command signal, δ_{T}; the attack angle, α ; the adaptive gain response, K_δ ; the signal from the adaptive loop rectifier, SAE; and the first bending mode, d_1, are contained in Figures B-3(a) through B-3(d). The procedure used in obtaining the traces is contained in Steps 5 and 6 of the procedure used to simulate Cases t = 20, 101.9, and 200 in Section 3.2.

The comparison of the rates of change of K_δ when K_δ is offset above and below the undisturbed magnitudes selected by the system for the various cases and conditions is shown in Table VII. Cases t = 20 and 75 have the same K_{SA} setting, or K_δ to servo input ratio, but the response times vary considerably. The variation illustrates the fact that the K_δ to servo input ratio must also be programmed for the flight if constant dynamic conditions are to exist in the system. There must be an optimum Reference Level, Dither Frequency, and Adaptive Loop Gain for optimum operation of the dither system. The program required to maintain the optimum value of the K_δ to servo input ratio can be placed into the loop in the form of a shaped gain curve for pot K_{SA} as is explained in Section 3.5. The adaptive loop gain for Case t = 101.9 resulted in an overshoot in the K_δ response as is shown on Figure B-3(c) The response time for this case is the fastest as would be expected since the K_δ responses for the other cases are over damped. As bending was added the response time increased except for Case t = 101.9 where the response time remained constant. In order to form some basis

TABLE VII

Comparison of Rates of Change of the Adaptive Gain for Various Loop Gains
and Aerodynamic Conditions

Flight Case	Undisturbed Values of K_δ	Time (Seconds) per Unity Change in K_δ		Gain Setting in Adaptive Loop K_{SA}	K_{SA}
Aerodynamic Condition		1	3	1	3
t = 20 offset above	.0	3.4	22.0	.025	.025
offset below		3.8	4.5	.025	.025
offset above	1.0	5.0	14.0	.025	.025
t = 75 offset below		5.0	15.0	.025	.025
offset above	2.1	2.6	2.6	0.2	0.2
t = 101.9 offset below		4.0	4.0	0.2	0.2
offset above	5.0	6.6	11.0	0.0	0.1
t = 200 offset below		4.4	7.2	0.0	0.1

for establishing if the times listed in Table VII are sufficiently fast for the system to function properly, the time intervals between flight cases are divided by the gain changes required between flight cases to establish figures of merit. The figures of merit are based on the assumption that K_δ is changing linearly with the time between flight cases and are listed below:

t = 20 to 75 ∞ seconds per unity change in K_δ

t = 75 to 101.9   24.6 seconds per unity change in K_δ

t = 101.9 to 200   33.8 seconds per unity change in K_δ

Even though the loop was not optimized the times listed in Table VII are well within the values established as figures of merit.

The comparison of the reaction of the adaptive loop to actuator signals for the various flight cases and aerodynamic conditions is shown in Table VIII. The magnitude of K_δ was changed in all cases and conditions when an actuator signal was introduced into the system, but the adaptive loop returned K_δ, while the signal was still being applied, to the original magnitudes for all cases and conditions in relatively small time intervals. The ideal system would result in no change in K_δ when an actuator signal was experienced. Excessive per cent changes in K_δ occurred for Flight Case t = 20 for aerodynamic conditions 1 and 3 and for Flight Case t = 101.9 for aerodynamic condition 3. If the adaptive loop had an optimized gain with a properly shaped K_δ gain pot instead of the linear pot used in the simulation, these large changes in K_δ would be greatly reduced. One of the considerations that must be used in arriving at the proper shape for the gain curve of the pot is to have a small ratio of K_δ to servo input for small values of K_δ. The undisturbed magnitudes of K_δ for Case t = 20 was 1 and for t = 101.9 was 2.1 so that the shaped pot would aid these cases

43

TABLE VIII

Comparison of the Reaction of the Adaptive Loop to
Actuator Signals

Flight Case Aerodynamic Condition 3	δ_c Step Input in Degrees	Change in Angle of Attack, α, in Degrees	Change in K_δ	Per Cent Change in K_δ	Time (Seconds) to return to Undisturbed Value of K_δ	Gain Setting in Adaptive Loop K_{SA}
t = 20	-0.6	1.0	-0.2	20.0	4.6	.025
	+0.6	1.0	-0.2	20.0	4.8	.025
t = 75	-0.4	0.6	-0.08	8.0	5.0	.025
	+0.4	0.6	+0.16	16.0	20.1	.025
t = 101.9	-0.15	0.6	+0.8	33.0	4.8	0.2
	+0.15	0.6	-0.8	33.0	3.0	0.2
t = 200	-0.62	0.5	-0.4	7.1	9.0	0.1
	+0.62	0.5	+0.4	7.1	8.5	0.1
Flight Case Aerodynamic Condition 1						
t = 20	-0.85	1.1	-0.2	20.0	3.0	.025
	+0.85	1.1	+0.2	20.0	3.0	.025
t = 75	-0.7	0.7	-0.11	10.0	3.6	.025
	+0.7	0.7	+0.11	10.0	3.8	.025
t = 101.9	-0.2	1.0	+0.16	7.2	3.0	0.2
	+0.2	1.0	-0.08	3.6	2.0	0.2
t = 200	-0.5	0.45	-0.2	3.8	8.0	0.1
	+0.5	0.45	+0.2	3.8	7.8	0.1

in preventing large changes in k_δ when disturbances were experienced. The same magnitude actuator signals for the bending aerodynamic condition produced approximately the same change in the angle of attack as for the no bending aerodynamic condition, but the bending condition resulted in greater changes in K_δ and longer time intervals to return to conditions that existed before the disturbance than the no bending condition.

The comparison of the reaction of the adaptive loop to wind gusts for the various flight cases and aerodynamic conditions is shown in Table IX. A one degree change in the angle of attack corresponds to wind velocities greater than would be expected by the missile during the flight. The per cent change in K_δ for all flight cases and conditions is small, within 11 per cent. The values of K_δ are returned to the undisturbed magnitudes while the gust is still being experienced for all flight cases and conditions in small intervals of time. The per cent change in K_δ and the time interval to return to conditions that existed before the disturbance increase as the airframe becomes more flexible.

The Reference signal is set so that if the dither signal source fails the value of K_δ is increased to insure that the system will not become unstable. The comparison of the rates of change of K_δ for the various flight cases and aerodynamic conditions when a dither failure occurs is shown in Table X. The rate of increase of K_δ decreases as the airframe becomes more flexible.

The results of the investigation contained in this Chapter show that for the computer simulation of the dither system the performance of the adaptive loop deteriorated when the airframe became flexible. The adaptive gain is varied by actuator signals and wind gusts while the ideal system would have no variation of gain when experiencing disturbances. The

45

TABLE IX

Comparison of the Reaction of the Adaptive Loop to Wind Gusts

Flight Case Aerodynamic Condition 3	Magnitude of Change in Angle of Attack in Degrees	Change in K_δ	Per Cent Change in K_δ	Time (seconds) to Return to Original K_δ	Gain Setting in Adaptive Loop
t = 20	-4.0	0.0	0.0	0	.025
	+4.0	0.0	0.0	0	.025
t = 75	-1.0	+0.04	4.0	6.4	.025
	+1.0	-0.1	10.0	6.4	.025
t = 101.9	-1.0	-0.4	1.7	2.4	0.2
	+1.0	-0.4	1.7	2.4	0.2
t = 200	-3.0	-0.6	10.7	11.0	0.1
	+3.0	-0.6	10.7	14.6	0.1
Flight Case Aerodynamic Condition 1					
t = 20	-1.0	0.0	0.0	0	.025
	+1.0	0.0	0.0	0	.025
t = 75	-1.0	+0.02	1.8	4.0	.025
	+1.0	-0.09	8.2	4.4	.025
t = 101.9	-1.0	0.0	0.0	0	0.2
	+1.0	+0.1	4.5	1.2	0.2
t = 200	-3.0	0.0	0.0	0	0.1
	+3.0	0.0	0.0	0	0.1

TABLE X

Comparison of Rates of Change of the Adaptive Gain for Dither Failures

Flight Case Aerodynamic Condition 3	K_δ Increase Per Second
t = 20	1.2
t = 75	1.12
t = 101.9	5.6
t = 200	1.8
Flight Case Aerodynamic Condition 1	
t = 20	1.2
t = 75	3.8
t = 101.9	6.2
t = 200	3.2

variations of gain for wind gusts were small and were corrected during the gusts in a relatively short period of time. The variations of gain for actuator signals were large for two flight cases and small for the remaining flight cases. The variations of gain were corrected during the signal in relatively short periods of time. The rates of change of adaptive gain were satisfactorily based on the criterion of a constant rate of change of gain required between flight cases. By optimizing the gain of the self adaptive loop and properly shaping the adaptive gain pot the rates of change of gain could be increased, the variation in the adaptive gain due to actuator and wind gusts could be greatly reduced, and the time required to correct for disturbances could be reduced.

3.5 Self Adaptive Loop.

The importance of optimizing the gain of the adaptive loop was shown in Section 3.4. For small perturbations the loop is linearized in order that a qualitative investigation may be conducted (8). The linearized loop with the Reference value as the input is shown in Figure 3.1. The Reference value is compared with the rectified filtered dither signal, and an error signal is formed. The error signal drives the integrating servo with the output shaft position indicated by ϕ. The adaptive gain pot has a transfer function of $\frac{d K_\delta}{d \phi}$ which is the slope of the curve of K_δ versus servo shaft position. The gain, K_δ, is then multiplied by the vehicle dynamics transfer function, $\frac{d \ddot{\theta}}{d K_\delta}$, which is the slope of the Closed Loop Response Amplitude versus K_δ curve at the Reference value for the particular flight under consideration. The resulting signal, $\ddot{\theta}$, is then fed back through the filter. The characteristic equation of the

48
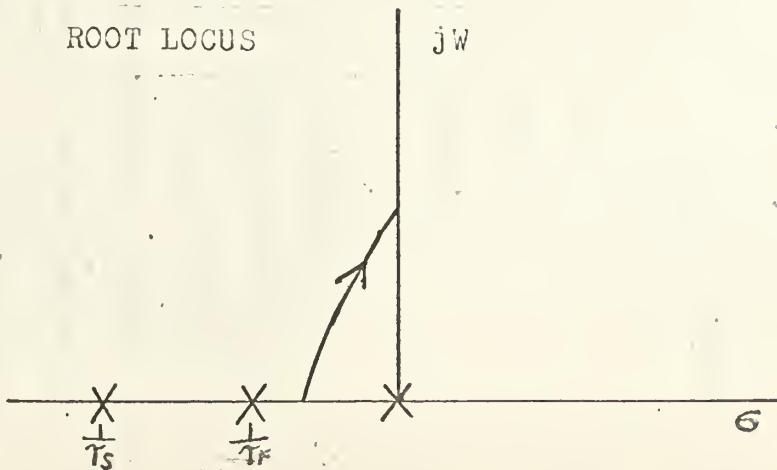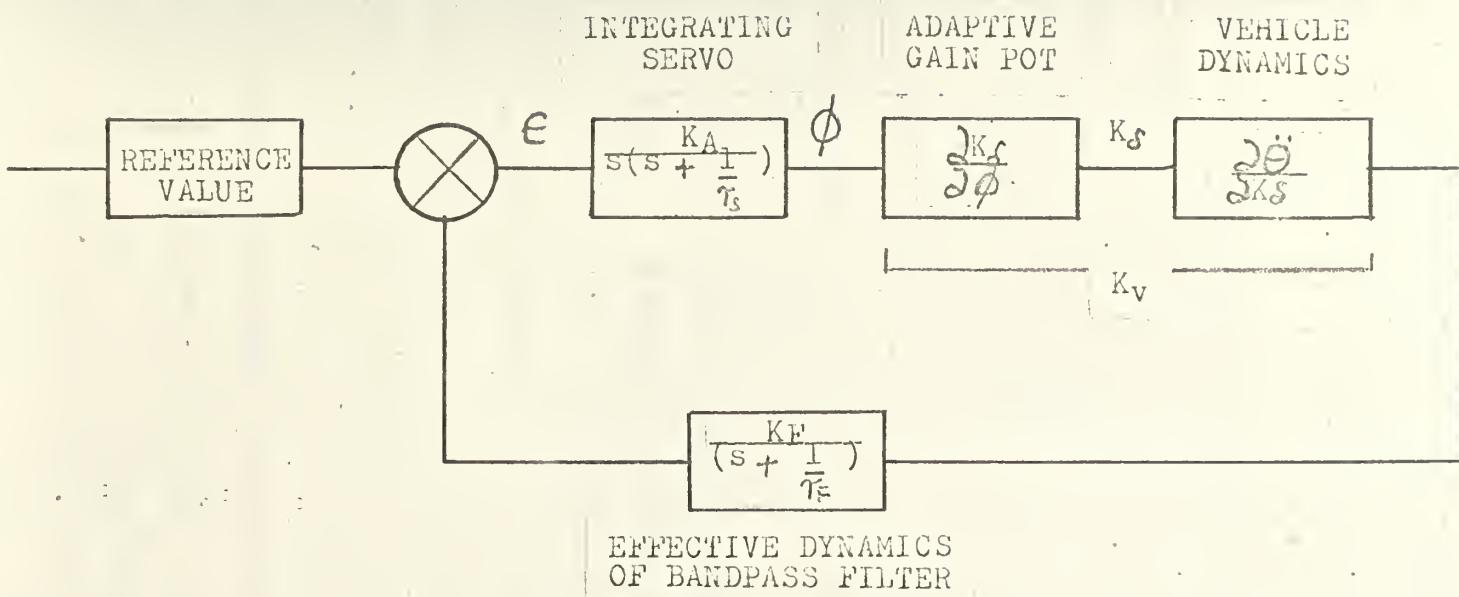
Figure 3.1. Linearized Self Adaptive Loop.

loop is $\dfrac{K_A K_F K_V}{s(s + \frac{1}{T_V})(s + \frac{1}{T_F})} = -1$. The root locus is shown in Figure 3.1.
As the loop gain increases, the response oscillates. It was found dur-
ing the analog computer study that if the gain of the adaptive loop was
increased beyond a certain value for a particular flight case that the
K_δ response would oscillate and as the gain was reduced the K_δ response
became over damped. The observations of the study agree with the root
locus.

In order to maintain the adaptive loop gain constant at the optimum
value that is determined, the product of the Adaptive Gain Pot transfer
function and the Vehicle Dynamic transfer function must be a constant. If
the pot is shaped so that $\dfrac{dK_\delta}{d\phi}$ is the reciprocal of $\dfrac{d\ddot\theta}{dK_\delta}$ at the value
of K_δ that the system selects for the particular flight case, the value
of Kv will be a constant equal to 1. The shape of the gain curve for the
pot for aerodynamic condition 3 with a dither frequency of 30 radians per
second is shown in Figure 3.2.

In an actual design a fixed loop gain could be established by varying
K_A and K_F until a desirable time response was obtained for the servo out-
put shaft, and the gain of the K_δ pot could be shaped as explained above.
If the performance of the loop was not satisfactory as to the rate of gain
change, the change in gain caused by disturbances, or the time required to
correct the gain after a disturbance, compromises would have to be made.
The slope of the gain curve could be varied to improve the performance.
In varying the slope, however, Kv would vary and the adaptive loop gain would
no longer be a constant for a flight. A varying Kv would vary the time
response of the servo shaft, and the performance of the loop would be af-
fected. A different dither frequency with its corresponding Reference
value could vary the shape of the gain curve resulting in the satisfactory
performance of the loop. Optimum setting of the loop gains and shape of the

50
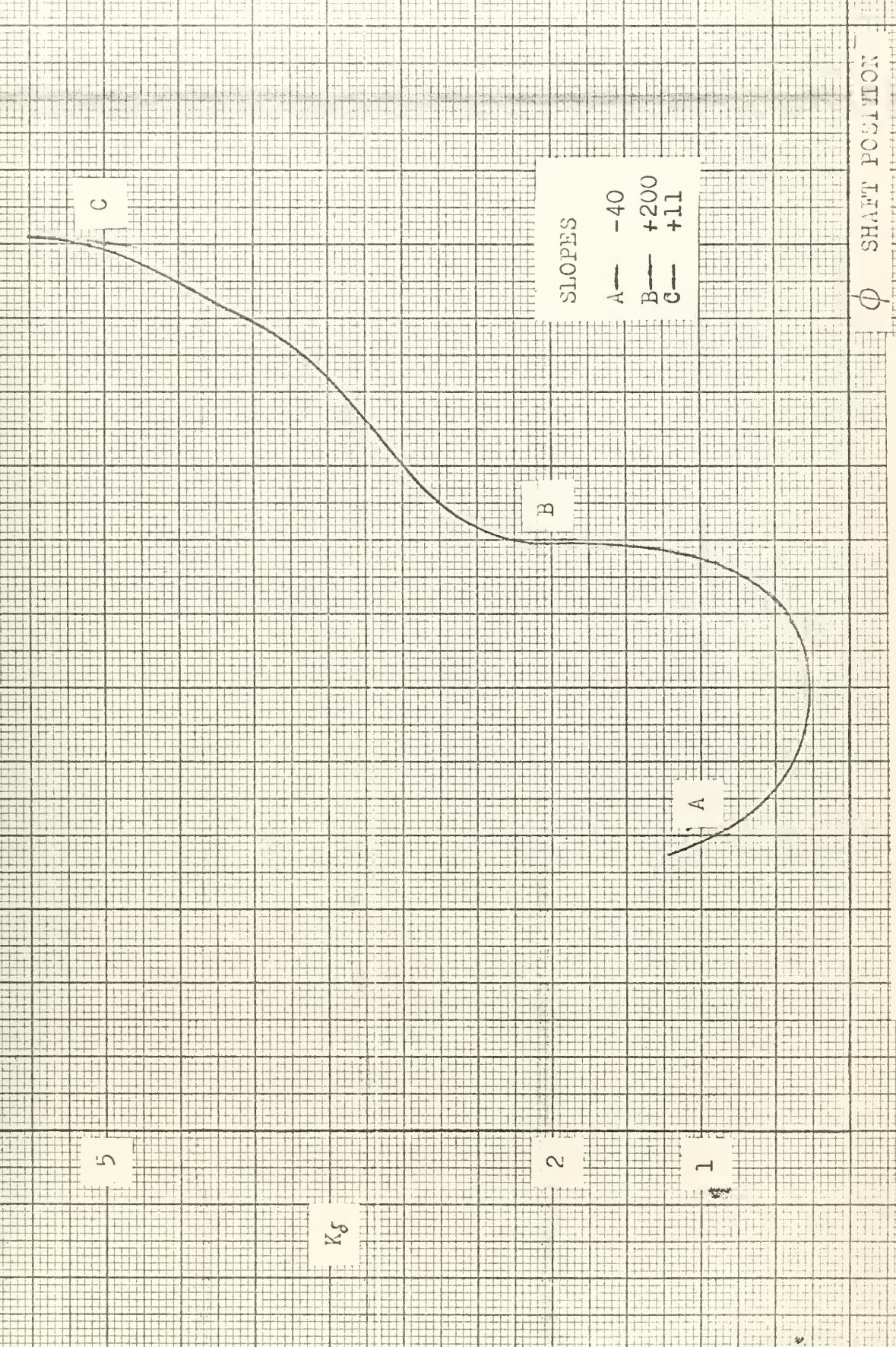
Figure 3.2. Gain Curve for Adaptive Gain Pot.

gain curve for the K_S pot could be determined by a trial and error procedure.

CLOSED LOOP RESPONSE AMPLITUDE AS A CRITERION FOR CONSTANT DYNAMIC RESPONSE

4.1 Introduction.

The object of this Chapter is to determine for the dither system the accuracy of evaluating the dynamic performance of a variable parameter control system - a flight control system - by the amplitude of the closed loop response. A dither signal is used as an input to the system and is varied by the dynamic characteristics of the system. The dynamic characteristics are then evaluated by the comparison of the amplitude of the dither signal with a fixed level Reference signal which represents the desired dynamic characteristics. The optimum dynamic performance of the system under investigation was defined in Section 2.3 as a damping ratio of the short period mode of 0.7 with a minimum variation of the natural frequency. Therefore, the accuracy of evaluating the dynamic performance by the amplitude of the closed loop response is based primarily on the accuracy of evaluating the damping ratio of 0.7.

The Reference signal values for dither frequencies of 20 and 30 radians per second were not determined for an average damping ratio of 0.7 for the flight for the computer simulation discussed in Chapter 3. The Reference values used, however, resulted in approximately equal average damping ratios for the flights, but the maximum variation of the damping ratios was twice as large for the dither frequency of 30 as for the frequency of 20. The maximum variation of the damping ratios of a flight also differed with the flexibility of the airframe and with the consideration of variable fuel load. The effect of varying the dither frequency, of increasing the flexibility of the airframe, and of varying the center of gravity on the accuracy of the performance evaluation will be determined in this Chapter. The results of the investigation will permit the selection of the Reference

signal value and the dither frequency, or frequencies, which result in the optimum variation of the damping ratio and natural frequency of the short period mode from the desired system dynamic performance.

The investigation was conducted principally from an empirical viewpoint although some analytical verification is included in Appendix C. Aerodynamic Conditions 1, 2, 3, and 4 and Flight Cases t = 20, 75, and 101.9, which are described in Section 2.4, are included in the investigation. Flight Case t = 200 was not included because the sensors are located in a different location than the sensors for the other cases. The performance of flights evaluated from cases that are measuring the reactions of the system at different positions in the airframe was not considered a true indication of the capabilities of the dither system. Therefore, the performance of flights are evaluated in this investigation with only flight cases that are measuring reactions at the same airframe position. Application of the results to a general variable parameter system is discussed in Section 4.4.

4.2 Procedure.

The investigation of the effect of varying the dither frequency on the accuracy of the closed loop response amplitude in determining the damping ratio of 0.7 was conducted using Cases t = 20, 75, and 101.9 as representative of a typical flight. The dither frequency was varied in the range from 0 to 40 radians per second. The upper limit of 40 radians was selected because available actuators will not respond to higher frequencies. For various frequencies in the dither range of each of the four aerodynamic conditions Reference signal values were determined which resulted in an average damping ratio during the flight of 0.7. At the Reference value for a particular aerodynamic condition and dither frequency the maximum variation of the damping ratios during the flight was determined. Plots of the

54

maximum damping ratio variation, $\Delta\delta$, versus the dither frequency, $\mathcal{W}$,
were then made for the four aerodynamic conditions. The procedure employ-
ed in determining the Reference value and the maximum damping ratio varia-
tion will be described by the use of a typical example. A dither frequency
of 22 radians per second and aerodynamic condition 3 will be used for the
example.

Root loci for the three flight cases were determined for aerodynamic
condition 3 using a Recomp II digital computer. The damping ratios, δ ,
of the short period modes associated with the adaptive gains, K_δ , were
determined from the root loci, and plots of δ versus K_δ were made for the
flight cases as shown in Figure 4.1. The amplitudes of the condition 3
closed loop transfer functions were evaluated at the dither frequency of
22 radians per second for various values of adaptive gain. The plots of
closed loop response amplitude versus adaptive gain for the flight cases
are shown in Figure 4.2. A graph of the damping ratio versus flight case
was constructed as shown in Figure 4.3. The procedure used in establishing
the closed loop response amplitude which would result in an average damping
ratio during the flight of 0.7 was as follows:

1. An amplitude for the closed loop response was selected, and
the values of K_δ corresponding to the amplitude were determined for the
three flight cases from the Amplitude versus K_δ plots.

2. The values of the damping ratios corresponding to the values
of K_δ , which resulted from the selected amplitude, were determined from
the δ versus K_δ plots.

3. The values of damping ratios were plotted on the damping ratio
versus flight case graph.

4. If the average of the three damping ratios corresponding to
the same closed loop response amplitude was not 0.7, a different response
amplitude was selected. Steps 1 through 4 were repeated until the average

55

Figure 4.1. Damping Ratio vs Adaptive Gain for Aerodynamic Condition 3

Figure 4.2. Closed Loop Response Amplitude vs Adaptive Gain for Dither Frequency of 22 and Aerodynamic Condition 3
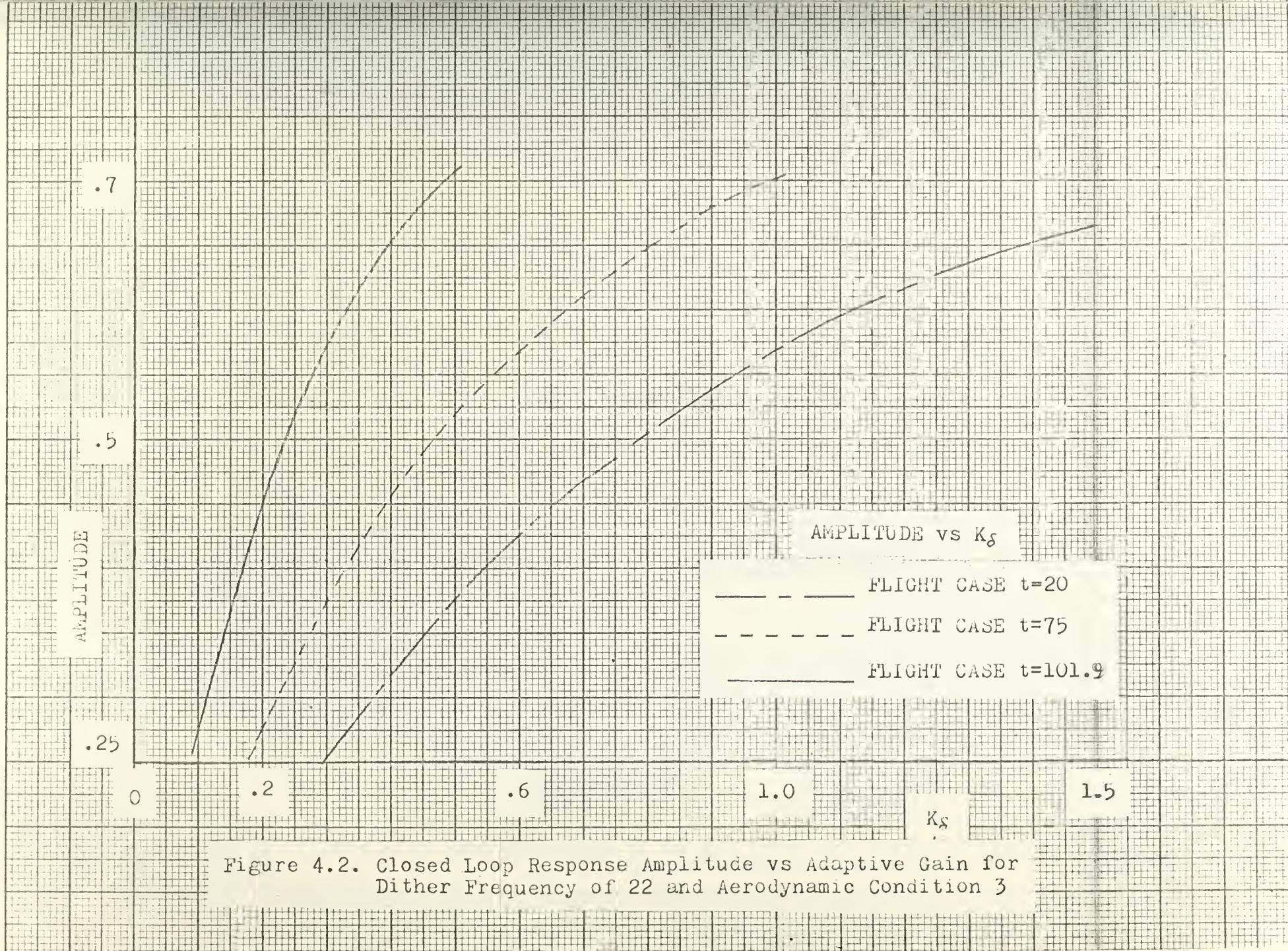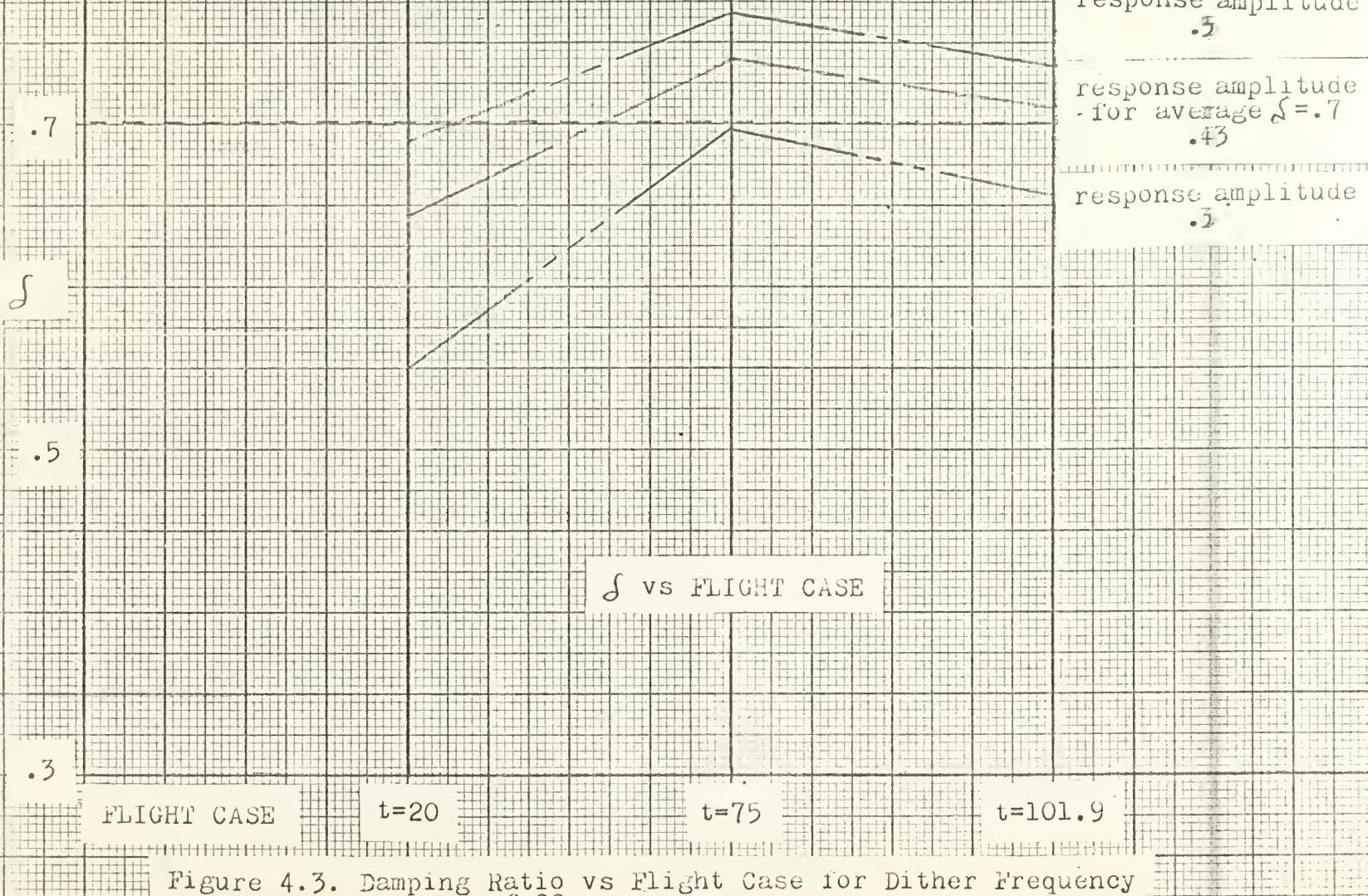
Figure 4.3. Damping Ratio vs Flight Case for Dither Frequency of 22 and Aerodynamic Condition 3

damping ratio was 0.7.

When the closed loop response amplitude which resulted in an average damping ratio of 0.7 was determined, the difference between the maximum and minimum values of the damping ratios for the three flight cases was taken as the maximum variation of the damping ratio, $\Delta\zeta$, during the flight for a dither frequency of 22 radians per second. The maximum variation and dither frequency were plotted on the $\Delta\zeta$ versus w graph, shown in Figure 4.4, for aerodynamic condition 3. The procedure was repeated for various frequencies for the various aerodynamic conditions to construct the $\Delta\zeta$ versus w plots for the dither frequency range.

The optimum dynamic performance was defined as a damping ratio of 0.7 with a minimum variation of the natural frequency. The procedure that has been described determined the variation of the damping ratios with varying dither frequencies while maintaining an average ratio of 0.7 during a flight. The procedure that will be described determined the variation of the natural frequencies of the short period modes with varying dither frequencies while maintaining the same average damping ratio as that used in determining the damping ratio variation. The reference for determining the damping ratio variation was the defined optimum performance ratio of 0.7. The reference for determining the natural frequency variation was selected as the average natural frequency of the short period modes of the three flight cases at the damping ratio of 0.7. The procedure employed in determining the natural frequency variation will be described by the use of the same example that was used for the damping ratio variation: namely, a dither frequency of 22 radians per second and aerodynamic condition 3.

The natural frequencies of the short period modes at a damping ratio of 0.7 were determined from the root loci for the three flight cases.
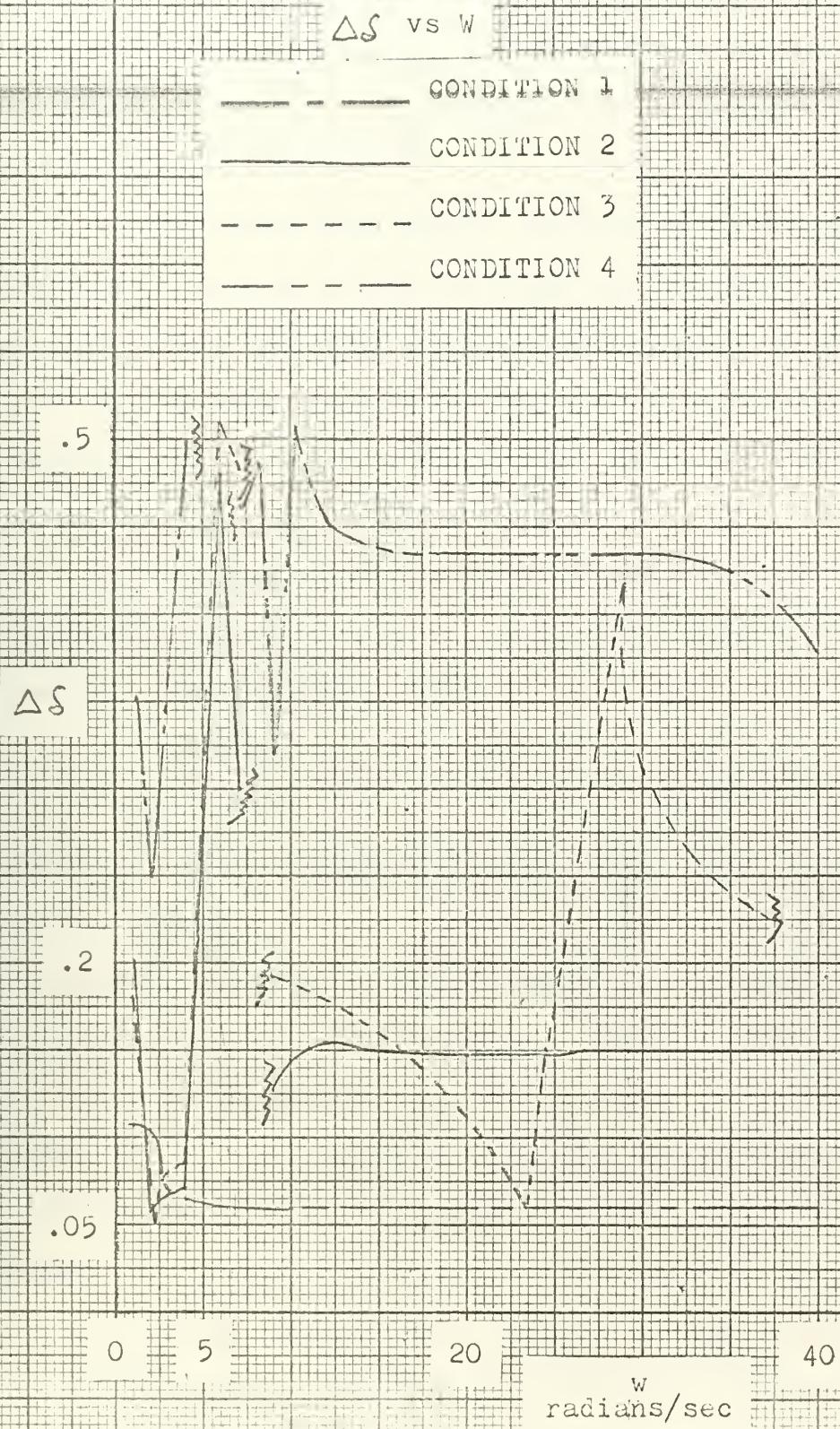
Figure 4.4. Damping Ratio Variation vs Dither Frequency
for Aerodynamic Condition 1, 2, 3, and 4.

The three frequencies were averaged to determine the reference natural

frequency for condition 3. The associated adaptive gains, K_δ , and

natural frequencies, W_n, of the short period modes were determined from

the root loci, and plots of W_n versus K_δ were made for the flight cases

as are shown in Figure 4.5. The procedure used to determine the frequency

variation was as follows:

1. The closed loop response amplitude which resulted in an

average damping ratio of 0.7 for the flight was determined from the damping

ratio versus flight case graph for the dither frequency of 22.

2. The adaptive gains for the flight cases which correspond to

the amplitude which resulted in the average damping ratio of 0.7 were deter-

mined from the Amplitude versus K_δ plots.

3. The adaptive gains determined from the Amplitude versus K_δ

plots were used to enter the W_n versus K_δ plots to determine the natural

frequencies of the three flight cases.

4. The three natural frequencies were averaged. The reference

natural frequency was then subtracted from the averaged frequency to

determine the natural frequency variation for the dither frequency of 22

radians per second.

The natural frequency variation, ΔW_n , was plotted on the ΔW_n

versus W graph which is shown in Figure 4-6 for aerodynamic condition 3.

The procedure was repeated for various frequencies of the various aerodynamic

conditions to construct the ΔW_n versus W plots for the dither frequency range.

The plots of $\Delta \delta$ versus W and ΔW_n versus W for the four aerodynamic

conditions will be used in Section 4.3 to determine the accuracy of the

closed loop response amplitude as a criterion for constant dynamic response

and the effect on the accuracy of varying the dither frequencies, increasing

the flexibility of the airframe, and varying the center of gravity.

61
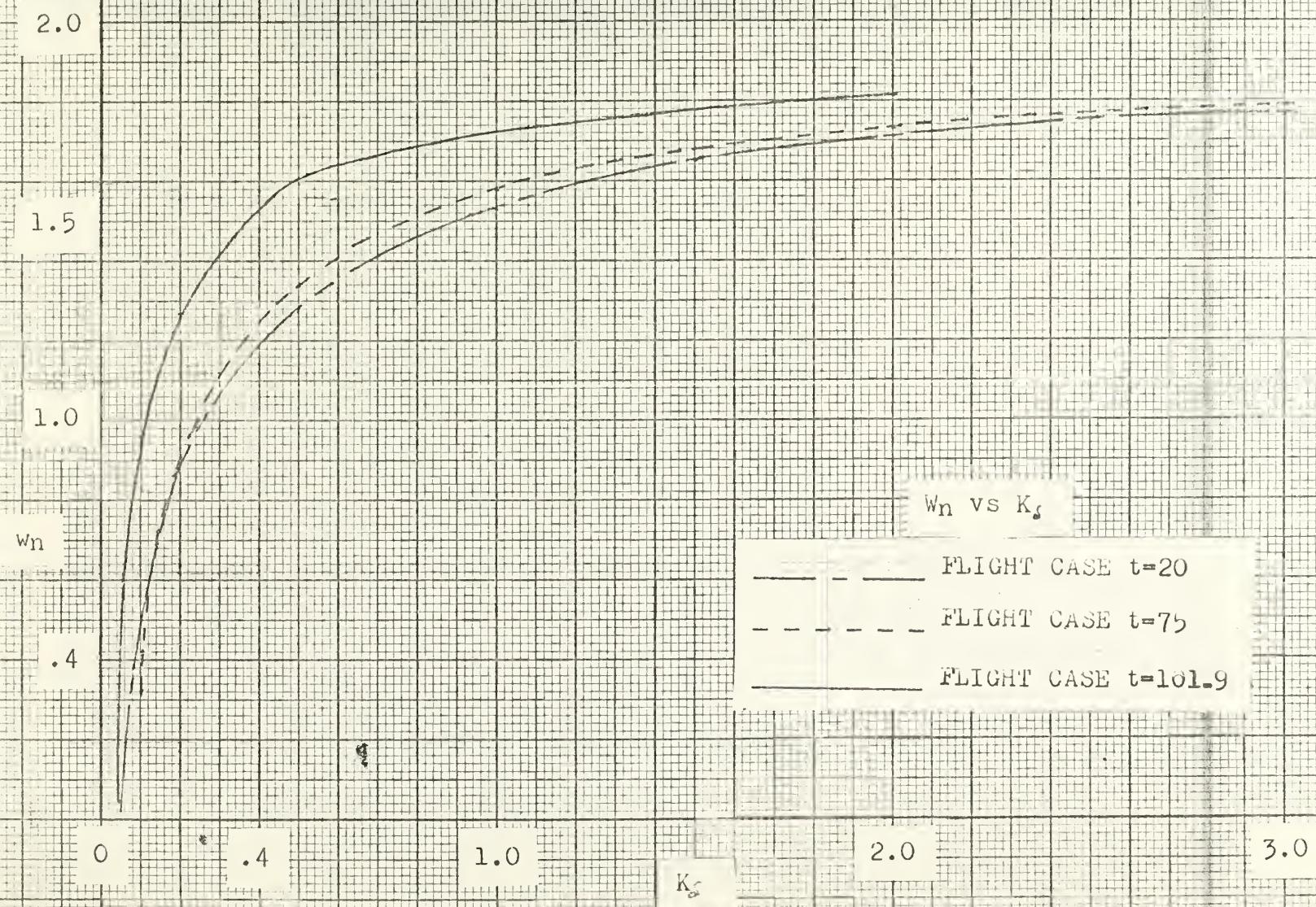
Figure 4.5. Natural Frequency vs Adaptive Gain for Aerodynamic Condition 3
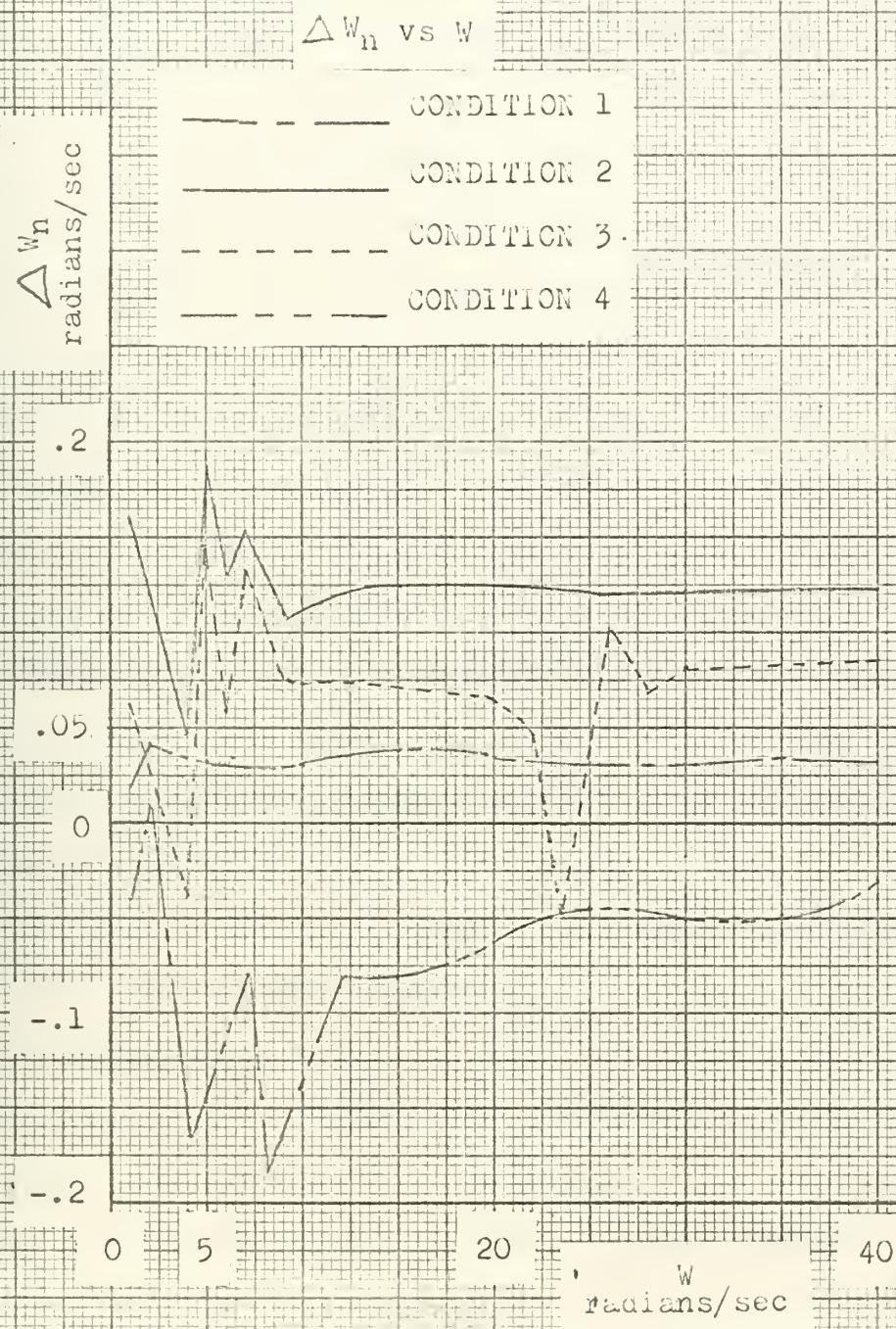
Figure 4.6. Natural Frequency Variation vs. Dither Frequency for Aerodynamic Conditions 1, 2, 3, and 4.

4.3 Results of the Empirical Investigation.

One of the basic operations, which are discussed in Section 2.1, of an adaptive loop is the continuous measurement of the system dynamic performance. The measuring method must have a negligible effect on the system response signal. In the dither self adaptive flight control system the measuring method involves a dither signal, and the important system response signal is the short period mode response. The possible frequencies of the short period mode response are never greater than 1.5 radians per second for the cases and aerodynamic conditions considered. To insure that the dither signal does not interfere with the short period mode response the lower limit for the dither frequency range was set at 10 radians per second. The upper limit was previously set at 40 radians per second to conform to the characteristics of available actuators.

The effect of varying the dither frequency, increasing the flexibility of the airframe, and varying the center of gravity on the accuracy of evaluating the specified damping ratio is shown in Figure 4.4. The $\Delta \delta$ versus w plots are based on the requirement that an average damping ratio of 0.7 is maintained for the flight. The accuracy with which the damping ratio is evaluated for aerodynamic conditions 1 and 2 is independent of the dither frequency in the range from 10 to 40 radians per second. The damping ratio for aerodynamic condition 1, which is the rigid airframe condition, is very accurately evaluated with a variation of 0.06 between the high and low values of the damping ratios during the flight. As the airframe becomes flexible by including the first bending mode, aerodynamic condition 2, the accuracy decreases. The variation of the damping ratios for condition 2 is approximately 0.15. As the flexibility of the airframe increases by including bending modes 1, 2, and 3 but eliminating mode 2 by a bending mode cancellation

64

method, aerodynamic condition 3, the accuracy of evaluation the damping

ratio depends on the dither frequency. A difference in the variation of

the damping ratios for dither frequencies of 20 and 30 radians per second

was determined in the computer simulation, discussed in Chapter 3, for

this aerodynamic condition. The average variation of the damping ratios

for the dither frequency range is approximately 0.24 with a minimum varia-

tion at a dither frequency of 23 radians per second of approximately the

same magnitude as that for a rigid airframe: namely, 0.06. If bending

modes 1, 2, and 3 with bending mode 2 eliminated by a frequency tracking

and notch filter method and a varying center of gravity in the form of a

slosh mode are included in the airframe equations, the accuracy of evalua-

ting the damping ratio is independent of the dither frequency from 12 to

35 radians per second. The variation of the damping ratios for aerodynamic

condition 4 in the 12 to 35 frequency range is approximately 0.435. For

dither frequencies greater than 35 the variation decreases and is 0.375 at

a frequency of 40 radians per second. The different methods used in eliminat-

ing the second bending mode in aerodynamic conditions 3 and 4 resulted in

large differences in the values of the real parts of the zeros associated

with the third bending mode of the airframe transfer function as is discussed

in Section 3.2. The zero for the third bending mode for condition 3 is close

to the imaginary axis while the zero for condition 4 is not.

In summary, the frequency in the dither range has no appreciable affect

on the accuracy of evaluating the damping ratio for aerodynamic conditions

1, 2, and 4. The accuracy depends greatly on the choice of the dither fre-

quency for condition 3 with the magnitude of the variation varying from the

small values obtained in condition 1 to the large values obtained in condi-

tion 4. The accuracy decreases as the airframe becomes flexible and as a

varying center of gravity is included. The large variations of condition 4 could be reduced by using an average damping ratio of greater than 0.7 for the flight because for large damping ratios the amount of change of gain per unit change in damping ratio is greater than for small damping ratios as is shown in Figure 4.1.

The effect of varying the dither frequency, increasing the flexibility of the airframe, and varying the center of gravity on the natural frequency variation is shown in Figure 4.6. The variation of the natural frequencies for aerodynamic conditions 1 and 2 is independent of the dither frequency in the range from 10 to 40 radians per second. The variation for condition 1 is approximately 0.034 radians per second and for condition 2 is approximately 0.123. The reference natural frequency for condition 1 was 1.355 radians per second and for condition 2 was 1.185. The variation of the natural frequency depends on the dither frequency for aerodynamic conditions 3 and 4. The average variation of the natural frequency for condition 3 for dither frequencies in the dither range is approximately 0.068 radians per second. At dither frequencies of approximately 23 and 24 radians per second there are no variations. The average variation of the natural frequency for condition 4 is approximately 0.06 radians per second with a minimum variation of 0.028 at a dither frequency of 40 radians per second. The reference natural frequency for condition 3 was 1.225 radians per second and for condition 4 was 1.51.

In summary, the variation of the natural frequency does not depend on the dither frequency for aerodynamic conditions 1 and 2 but does depend on the dither frequency for conditions 3 and 4. The variations were small for all conditions with 10 per cent of the corresponding reference value being the maximum variation determined. The effect of the flexibility of the

66

airframe and of a varying center of gravity on the variations of the natural frequency is not clearly indicated. The magnitudes of the average variations of the natural frequencies for the aerodynamic conditions varied from large to small in the following order: condition 2, 3, 4, and 1.

The investigation of the variations of the damping ratios and natural frequencies was conducted with the amplitude of the closed loop response selected to result in an average damping ratio during the flight of 0.7. Since the defined optimum performance of the system was a damping ratio of 0.7 with a minimum variation of the natural frequency, the optimum dither frequency, or frequencies, for each of the aerodynamic conditions was determined on the basis of minimizing the variation in damping ratio and natural frequency. The error criterion used to determine the minimization of the variation in damping ratio and natural frequency was $\sqrt{\Delta\delta^2 + \Delta W_n^2}$. Plots of $\Delta\delta$ versus ΔW_n are shown in Figures 4.7 through 4.10 for four aerodynamic conditions. The optimum dither frequencies selected for the aerodynamic conditions are shown in Table XI with the corresponding error criterion value, the variation in the damping ratio, the variation in the natural frequency, and the Reference signal value. Two dither frequencies with different error criterion values are listed for condition 4. The dither frequency of 40 has the lower criterion value, but the Amplitude versus K_δ curve for that frequency has a very small slope at the Reference value which would require a very accurate setting of the Reference signal. The dither frequency of 36 has a larger slope and would be the preferred frequency if the system was actually mechanized.

The Reference signal values listed in Table XI are equal to the closed loop response amplitudes required for an average damping ratio of 0.7 for
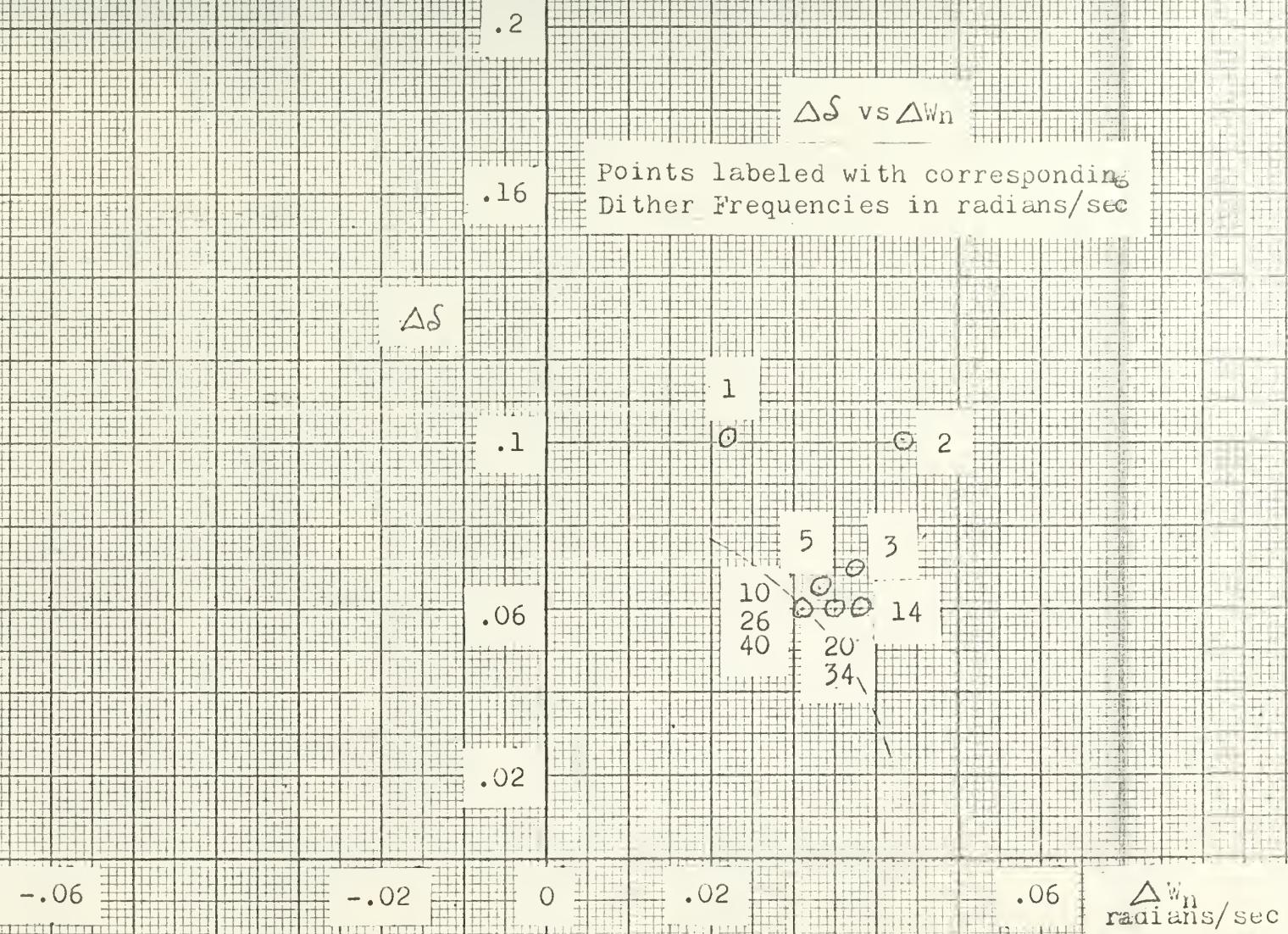
Figure 4.7. Variation in Damping Ratio vs Variation in Natural Frequency for Aerodynamic Condition 1.

Figure 4.8. Variation in Damping Ratio vs Variation in Natural Frequency for Aerodynamic Condition 2.
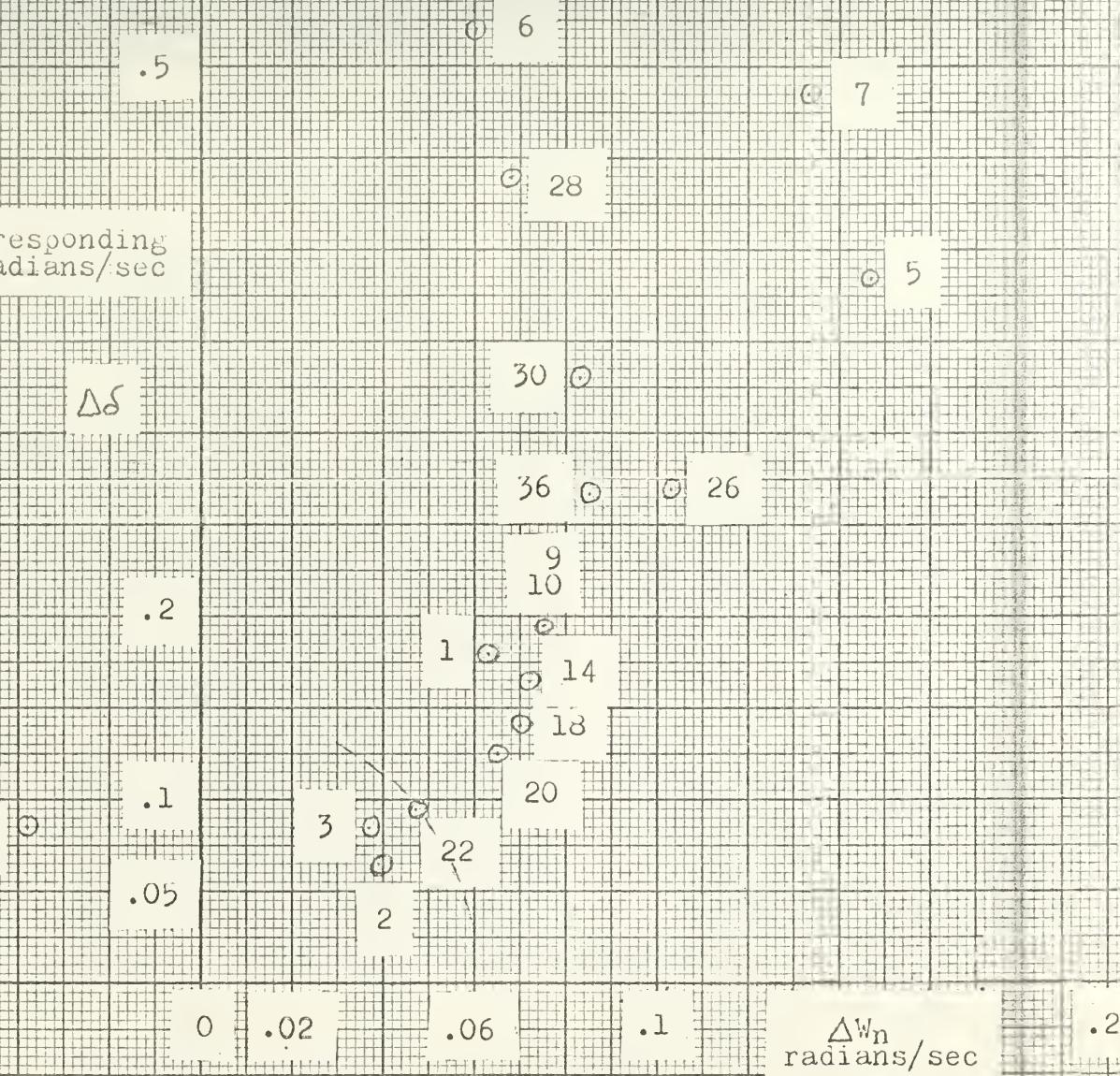
Figure 4.9. Variation in Damping Ratio vs Variation in Natural Frequency for Aerodynamic Condition 3.
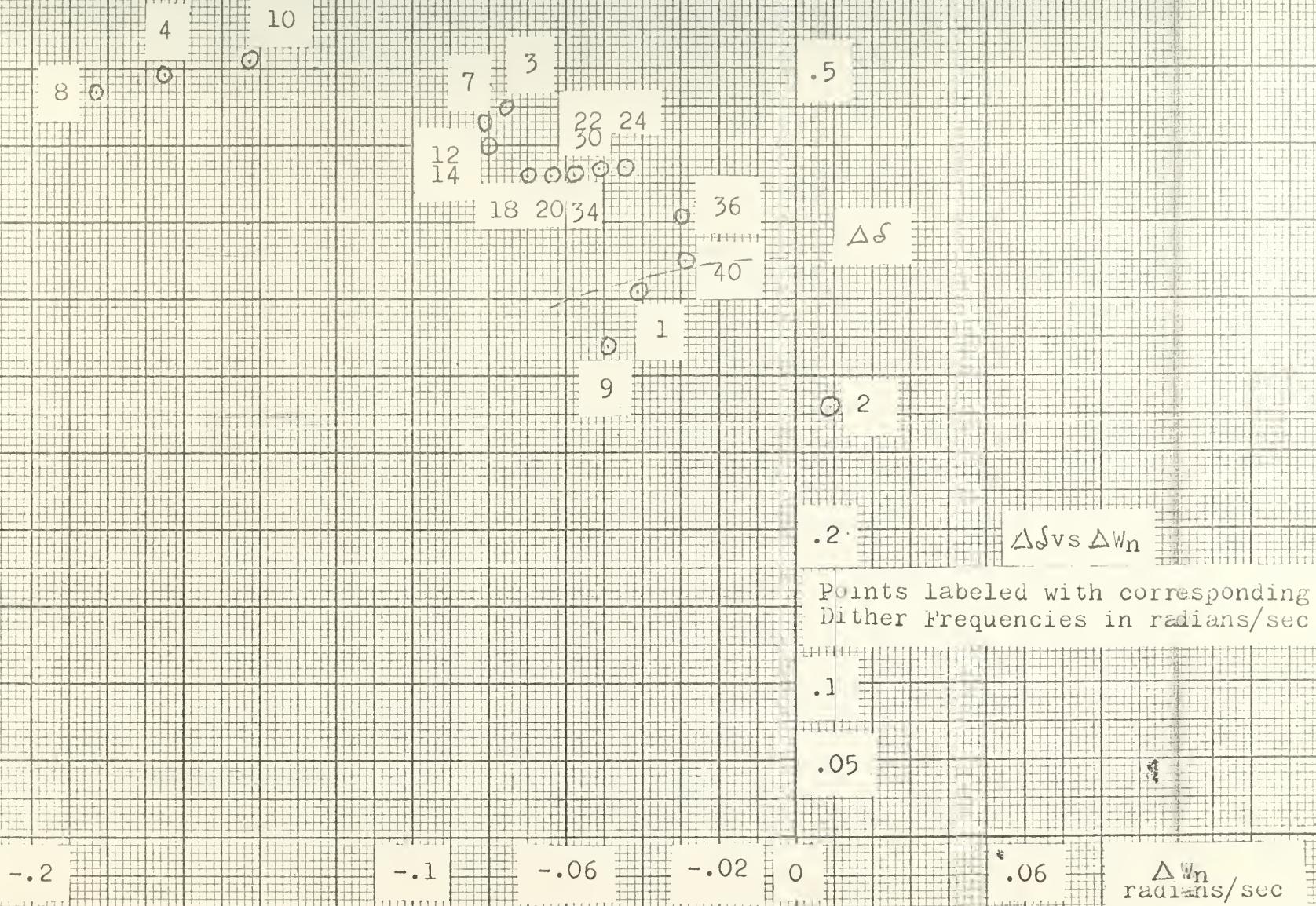
Figure 4.10. Variation in Damping Ratio vs Variation in Natural Frequency for Aerodynamic Condition 4.

TABLE XI

Optimum Dither Frequencies and Reference Values

Aerodynamic Condition	Optimum Dither Frequency or Frequencies (Rad/Sec.)	Error Criterion Value	Variation in Damping Ratio	Variation in Natural Frequency (Rad/Sec.)	Reference Signal Value
Condition 1	10 26 40	0.068	0.06	0.032	0.56 0.485 0.42
Condition 2	10 12 26	0.19	0.15	0.118	0.835 0.79 0.7
Condition 3	22	0.105	0.095	0.047	0.43
Condition 4	40 36	0.375 0.405	0.375 0.405	0.027 0.028	0.993 0.975

the flight. The equality is correct if the average half cycle value of
the dither input signal and the gains of the filter and rectifier in the
adaptive loop are equal to unity. If the values are not unity, the
Reference value listed must be corrected by being multiplied by the pro-
duct of the half cycle average of the filter, and the gain of the rectifier.

4.4 Application of the Results to a General Case.

The object of this section is to formulate a procedure from the empiri-
cal results discussed in Section 4.3 and from the analytical verification
contained in Appendix C to facilitate the rapid selection of the optimum
dither frequency. The selection will be based on minimizing the damping
ratio variation. Once the dither frequency or area of frequencies is
selected, the procedures of Section 4.2 can be used for the frequency to
determine the Reference value and the magnitude of the damping ratio varia-
tion for the average damping ratio desired for the flight.

The dither range is established by selecting the lower frequency limit
five or more multiples greater than the maximum short period frequency to
eliminate coupling. The maximum frequency of the short period mode can be
approximated by the square root of the square of the real and imaginary
parts of the zeros of the Inverse Model. The upper limit of the range is
fixed by the actuator requirements at 40 radians per second.

The assumption is made that the control system will be investigated by
a point study of the flight trajectory. From the root loci shown in Figure
4.11, it is noted that the open loop poles associated with the bending modes
remain relatively stationary during a flight but that the open loop zeros
associated with bending modes move during the flight from smaller to larger
values. If slosh modes are temporarily ignored, the effect that the varying
values of the bending zeros have on the short period mode is to vary the
shape of the short period characteristic. The bending zeros must be in the

73
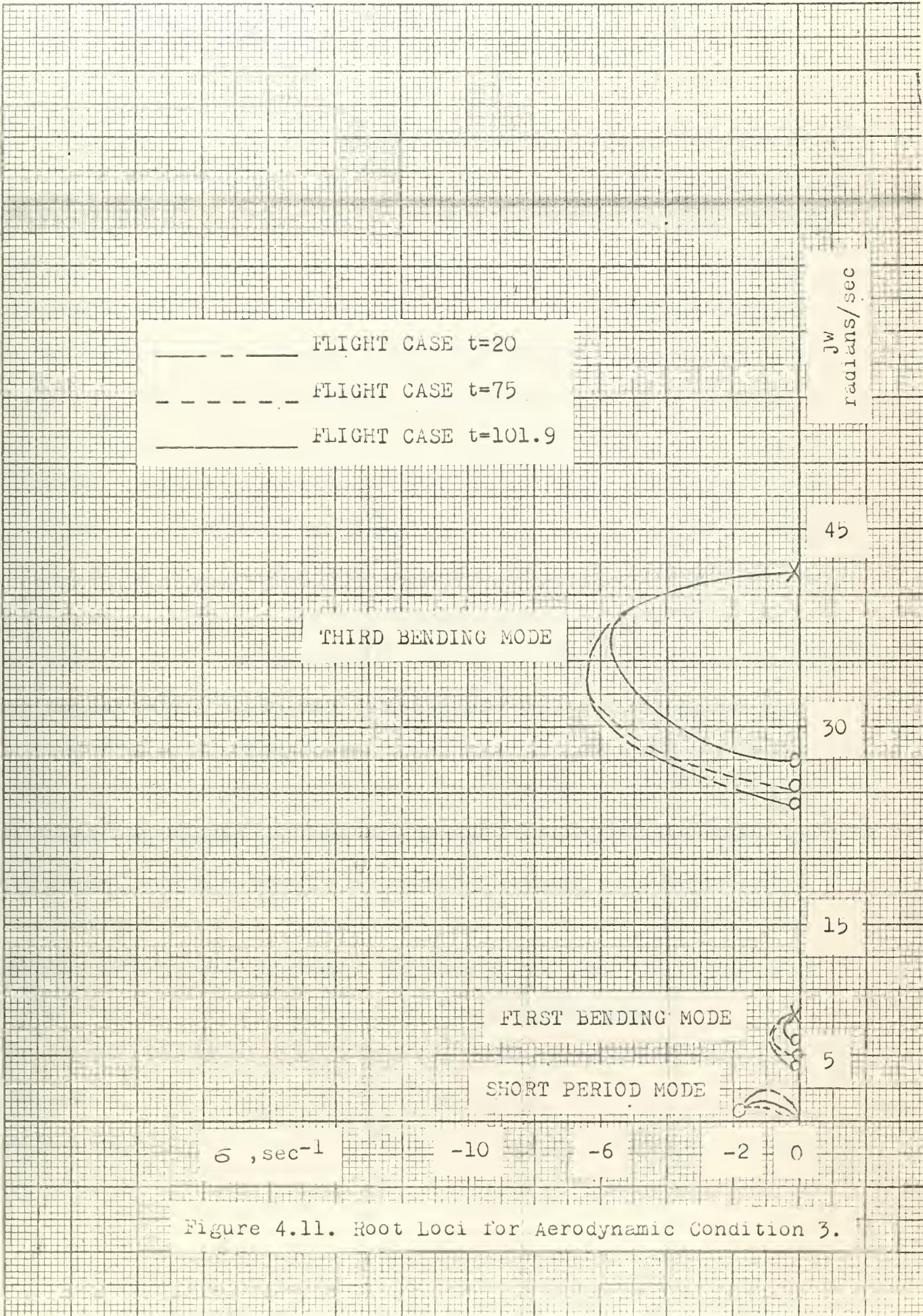
Figure 4.11. Root Loci for Aerodynamic Condition 3.

imaginary part, which is the earliest flight case considered after launch, results in a short period characteristic which has a larger adapative gain at a particular damping ratio than any of the other cases. The open loop poles and zeros associated with the short period approximation also vary during the flight, but it is assumed that the variations are negligible compared to the variations of the bending zeros. The values of adaptive gain at a particular damping ratio decreases as the imaginary part of the bending zero increases. The adaptive gains for a particular damping ratio are, therefore, inversely proportional to the time in flight. The dither system maintains the amplitude of the closed loop response constant during a flight. A constant amplitude results when the product of the adaptive gain and the dynamic gain remains constant. The dynamic gain is the gain associated with the vehicle dynamic characteristics. In order to have a minimum variation in the damping ratios, the product of the dynamic gain and the adaptive gain corresponding to the desired damping ratio must be approximately constant during the flight. Since the adaptive gain varies inversely with the time in flight, the dynamic gain must vary directly with the time in flight for the product to be a constant. If the dither frequency is selected close to a bending zero of the initial flight case, the dynamic gains will vary directly with the time in flight. The bending zero must have a value with a small real part and an imaginary part in the dither range.

If the value of the bending zero has an imaginary part in the dither range but a large real part, the selection of the dither frequency for optimum damping ratio variation is independent of the position of the zero. The value of the dither frequency does not appreciably affect the dynamic

gain and approximately constant damping ratio would be expected. During

the flight the bending modes do result in variations in the adaptive gains

for the same damping ratio. Since the value of the dither frequency can

not result in dynamic gains varying inversely to the short period gains,

large variations in the damping ratio may result. The requirement of deter-

mining when the real part of the value of the bending zero is large or small

can be eliminated by always selecting the value of the dither frequency

close to the imaginary part of the bending zero of the initial flight case.

If bending zeros do not exist in the dither range, the optimum damp-

ing ratio variation is independent of the selection of the dither frequency.

The value of the dither frequency can not vary the dynamic gain to result

in adaptive gains which correspond to the values required for constant short

period damping ratios. The variations in the adaptive gains of the short

period modes for the same damping ratio increase as the number of bending

modes increase; and therefore, the magnitude of the damping ratio variation

would be expected to increase as the number of bending modes increase.

Slosh modes may have an important effect on the dynamic performance

of the system for some airframes. Slosh modes would have a negligible

effect during the initial and final phases of the flight because the fuel

tanks are then approximately full or empty. The slosh modes would affect

the middle phase of the flight. If the slosh mode frequencies are close

to the short period frequencies, the shape of the short period characteristic

could be appreciably varied for the middle flight cases. The shape of the

characteristic would not be affected for the initial and final flight cases.

The largest adaptive gain for a particular damping ratio would be for the

middle flight case which is most affected by the slosh modes. The dynamic

gain would have to be reduced by the selection of a dither frequency for

this flight have to enable the dither system to select a large adaptive
gain if a small damping ratio variation is to be obtained. A dither
frequency at a value equal to the imaginary part of a bending zero of the
middle case will reduce the dynamic gain if the real part of the zero is
small. The dither frequency selected, however, should be between the values
of the imaginary parts of the bending zero of the initial case and the bend-
ing zero of the middle case to result in a small damping ratio variation
throughout the entire flight. The exact frequency in the area would have to
be determined by the procedure in Section 4.2.

In summary, the selection of the optimum dither frequency is as follows:

1. If no bending zeros exist in the dither range, the value of the
dither frequency is not restricted.

2. If there are no important slosh modes in the system but if
there are bending zeros in the dither range, the optimum frequency is close
to the imaginary part of a zero associated with the initial flight case.

3. If there are important slosh modes in the system and there are
bending zeros in the dither range, the optimum frequency area is between the
value of the imaginary part of an initial flight case zero and the imaginary
part of the zero of the middle case which is most affected by the slosh modes.

The dither frequency must not assume a value that is close to the value
of the imaginary part of a pole which is adjacent to the imaginary axis be-
cause the adaptive gain change per unit amplitude of the closed loop re-
sponse is large. A large gain to amplitude ratio requires a very accurate
setting of the Reference value.

CONCLUSIONS

The conclusions from the results of the investigation are as follows:

1. The dither adaptive loop employs a single parameter to control basically a single dynamic characteristic of the system. The parameter of the loop is the closed loop response amplitude and the characteristic controlled is the damping ratio.

2. The components of the loop are simple to mechanize, but a prior knowledge of the airframe dynamics are required to select the dither frequency, Reference value, and the shape of the gain curve for the adaptive gain pot.

3. The adaptive loop will adjust the adaptive gain to partially correct for the varying dynamic characteristics of a flexible airframe if the dither frequency has no coupling with a bending mode. The accuracy of the correction in maintaining a constant damping ratio is the inherent accuracy of the Amplitude Closed Loop Response Criterion.

4. The adaptive loop makes satisfactory corrections of the adaptive gain for disturbances. A further investigation into the gain curve shape for the adaptive gain pot and into the optimum loop gain is required to verify that an actuator signal will not cause an unsatisfactory variation in the adaptive gain.

5. The Amplitude Closed Loop Response Criterion does not result in a constant damping ratio. The variation of the damping ratios increases as the desired average damping ratio decreases, as the airframe flexibility increases, and as the variation of the center of gravity increases. If

78

frequencies in the dither range greatly affect the amplitude of the vehicle dynamic response, the variations of the damping ratios can be appreciably reduced by the proper selection of the dither frequency.

6. When the damping ratio variation varies with the dither frequency, the minimum natural frequency variation occurs at approximately the same dither frequency as the minimum damping ratio variation.

REFERENCES

1. Li, Yao Tzu, "Adaptive Control System Philosophy", WADC TR 59-49, March
   1959, p. 407-431.

2. Campbell, G., "Use of An Adaptive Servo to Obtain Optimum Airplane
   Responses," Cornell Aeronautical Laboratory, Inc., Report No. C.A.L.
   - 84, February 1957, p. 54-63.

3. Whitaker, H. P., J. Yamron, A. Kezer, "Design of Model - Reference
   Adaptive Control Systems for Aircraft," Massachusetts Institute of
   Technology, Report R-164, September 1958, p. 1-3.

4. Graham, K., and R. C. Lathrop, "The Synthesis of Optimum Transient
   Responses: Criteria and Standard Forms," AIEE Paper No. 53-249, June
   1953.

5. Anderson, G. W., and others, "A Self-Adjusting System for Optimum
   Dynamic Performance," IRE National Convention Record, Part 4, 1958,
   p. 182-190.

6. Geissler, E. D., "Problems in Attitude Stabilization of Large Guided
   Missiles", Aerospace Engineering, XIX (October 1960), p. 24.

7. Smith, G. W., "Synthesis of a Self Adaptive Autopilot for a Large
   Elastic Booster," IRE National Convention Record, Part 4, 1960, p. 73-80.

8. Smyth, R. K., "Self Adaptive System for Re-Entry Glider Control," paper
   presented at NAECON Conference, Dayton, Ohio, May 1961.

9. Dynamics of the Airframe, BuAer Report, AE-61-411 prepared by the
   Servo-mechanisms Section and Aerodynamics Section, Northrop Aircraft,
   Inc., 1952.

10. Aeroelasticity in Stability and Control, WADC Technical Report 55-173,
    prepared by J. B. Rea Company, Inc., March 1957.

The aerodynamic equations for the missile were obtained from the Autonetics Division of North American Aviation. The equations are two degree of freedom short period mode approximations with three bending modes and one fuel slosh mode included.

$$\dot{\alpha} = A_1 \alpha + B_1 \dot{\Theta} + C_1 \Theta + D_1 \dot{d}_1 + E_1 d_1 + F_1 \dot{d}_2 + G_1 d_2 + H_1 \dot{d}_3 + I_1 d_3 + J_1 \Delta_I + K_1 \Delta_{LOX} + L_1 \Delta_{LH} + M_1 \delta_T$$

$$\ddot{\Theta} = A_2 \alpha + B_2 \dot{\Theta} + C_2 \dot{d}_1 + D_2 d_1 + E_2 \dot{d}_2 + F_2 d_2 + G_2 \dot{d}_3 + H_2 d_3 + I_2 \Delta_I + J_2 \Delta_{LOX} + K_2 \Delta_{LH} + L_2 \delta_T$$

$$\ddot{d}_1 = A_3 \alpha + B_3 \dot{\Theta} + C_3 \dot{d}_1 + D_3 d_1 + E_3 \dot{d}_2 + F_3 d_2 + G_3 \dot{d}_3 + H_3 d_3 + I_3 \Delta_I + J_3 \Delta_{LOX} + K_3 \Delta_{LH} + L_3 \delta_T$$

$$\ddot{d}_2 = A_4 \alpha + B_4 \dot{\Theta} + C_4 \dot{d}_1 + D_4 d_1 + E_4 \dot{d}_2 + F_4 d_2 + G_4 \dot{d}_3 + H_4 d_3 + I_4 \Delta_I + J_4 \Delta_{LOX} + K_4 \Delta_{LH} + L_4 \delta_T$$

$$\ddot{d}_3 = A_5 \alpha + B_5 \dot{\Theta} + C_5 \dot{d}_1 + D_5 d_1 + E_5 \dot{d}_2 + F_5 d_2 + G_5 \dot{d}_3 + H_5 d_3 + I_5 \Delta_I + J_5 \Delta_{LOX} + K_5 \Delta_{LH} + L_5 \delta_T$$

$$\ddot{\Delta}_I = A_6 \alpha + B_6 \ddot{\Theta} + C_6 \Theta + D_6 \ddot{d}_1 + E_6 \dot{d}_1 + F_6 d_1 + G_6 \ddot{d}_2 + H_6 \dot{d}_2 + I_6 d_2 + J_6 \ddot{d}_3 + K_6 \dot{d}_3 + L_6 d_3 + M_6 \dot{\Delta}_I + N_6 \Delta_I + O_6 \Delta_{LOX} + P_6 \Delta_{LH} + Q_6 \delta_T$$

$$\ddot{\Delta}_{LOX} = A_7 \alpha + B_7 \ddot{\Theta} + C_7 \Theta + D_7 \ddot{d}_1 + E_7 \dot{d}_1 + F_7 d_1 + G_7 \ddot{d}_2 + H_7 \dot{d}_2 + I_7 d_2 + J_7 \ddot{d}_3 + K_7 \dot{d}_3 + L_7 d_3 + M_7 \Delta_I + N_7 \dot{\Delta}_{LOX} + O_7 \Delta_{LOX} + P_7 \Delta_{LH} + Q_7 \delta_T$$

$$\ddot{\Delta}_{LH} = A_8 \alpha + B_8 \ddot{\Theta} + C_8 \Theta + D_8 \ddot{d}_1 + E_8 \dot{d}_1 + F_8 d_1 + G_8 \ddot{d}_2 + H_8 \dot{d}_2 + I_8 d_2 + J_8 \ddot{d}_3 + K_8 \dot{d}_3 + L_8 d_3 + M_8 \Delta_I + N_8 \Delta_{LOX} + O_8 \dot{\Delta}_{LH} + P_8 \Delta_{LH} + Q_8 \delta_T$$

$$\Theta_G = \Theta + \lambda_1 d_1 + \lambda_2 d_2 + \lambda_3 d_3$$

α — angle of attack in degrees

$\ominus$ — pitch angle in degrees

d_1 — first bending mode in feet

d_2 — second bending mode in feet

d_3 — third bending mode in feet

$\ominus_G$ — pitch angle as measured by position gyro

$\triangle_I$ — first ignition fuel slosh mode in feet

$\triangle_{LOX}$ — first liquid oxygen slosh mode in feet

$\triangle_{LH}$ — first liquid hydrogen slosh mode in feet

δ_T — thrust control deflection in degrees.

	t_20	t_75	$t\_101.9$	t_200
A_1	-.064	-.0489	-.0336	-.0236
B_1	1	1	1	1
C_1	-.158	-.0226	-.0103	.0074
D_1	0	.00123	.000229	.00015
E_1	0	.0337	.031	-.061
F_1	0	-.000886	-.000167	-.00019
G_1	0	-.0461	-.0154	-.185
H_1	0	.001108	.000214	.00014
I_1	0	.0940	.0346	-.047
J_1	.0567	.0289	0	0
K_1	.058	.0298	.0422	-.039
L_1	.00497	.00255	.00362	-.0027
M_1	.222	.0565	.0378	.02
A_2	0	.0217	.0159	1.65
B_2	0	-.00156	-.000519	-.038
C_2	0	-.00204	-.000813	-.055

	$t=20$	$t=75$	$t=101.9$	$t=200$
D_2	0	-.0515	-.0386	-31.92
E_2	0	.00168	.000664	.042
F_2	0	.071	.0552	-12.73
G_2	0	-.00213	-.000792	-.024
H_2	0	-.163	-.127	-28.33
I_2	.00316	.248	0	0
J_2	-.0048	-.00716	.00193	-3.8
K_2	-.000919	-.00205	-.00482	.012
L_2	.0485	.0814	.157	2.28
A_3	0	.401	.213	.32
B_3	0	-.0294	-.00723	-.012
C_3	-.163	-.205	-.175	-.59
D_3	-66.5	-67.3	-66.9	-767.46
E_3	0	.0348	.00981	.023
F_3	0	1.39	.821	16.34
G_3	0	-.0482	-.0125	-.0013
H_3	0	-.3.24	-1.83	6.0
I_3	.137	-.0414	0	0
J_3	.131	.298	.634	3.08
K_3	-.00801	-.0182	-.0389	-.128
L_3	-1.	-1.	-1.79	-1.86
A_4	0	-.288	-.155	-.39
B_4	0	.0243	.00591	.009
C_4	0	.0348	.00981	.023
D_4	0	.708	.384	13.82
E_4	-.43	-.463	-.439	-.96
F_4	-462	-463	-463	-2169.63

	t=20	t=75	t=101.9	t=200
G_4	0	.0469	.0124	.015
H_4	0	2.85	1.53	12.66
I_4	.21	.373	0	0
J_4	-.224	-.51	-1.086	3.78
K_4	-.0112	-.0255	.0544	-.146
L_4	-1.57	-1.78	-1.79	-2.4
A_5	0	.36	.199	.28
B_5	0	-.0308	-.00704	-.0052
C_5	0	-.0482	-.0125	-.0013
D_5	0	-.518	-.43	10.24
E_5	0	.0469	.0.24	.015
F_5	0	1.27	.584	12.7
G_5	-.832	-.906	-.852	-1.49
H_5	-1730	-1734	-1732	-5351.8
I_5	-.0182	.476	.18	0
J_5	.0374	.085	.181	3.52
K_5	.0288	.0655	-.14	.018
L_5	-1.57	-1.78	-1.79	-2.18
λ_1	-2.3	-2.3	-2.3	0
λ_2	3.4	3.4	3.4	3.4
λ_3	-6.95	-6.95	-6.95	0

The magnitudes of the remaining coefficients were not available but are included in the transfer functions.

84

The justification for equations $\ddot{\Theta}$ and $\ddot{\alpha}$ will be shown. Information to permit the justification of the $\ddot{d}_1$, $\ddot{d}_2$, $\ddot{d}_3$, $\ddot{\Delta}_I$, $\ddot{\Delta}_{LOX}$, and $\ddot{\Delta}_{LH}$ equations is contained in Reference 10.

From Newton's second law of motion.

(1)
$$\Sigma F_x = a_x \frac{dm}{dt}$$
$$\Sigma F_y = a_y \frac{dm}{dt}$$
$$\Sigma F_z = a_z \frac{dm}{dt}$$

(2)
$$\Sigma L = \frac{dh_x}{dt} + i\,(\bar{w} \times \bar{h})$$
$$\Sigma M = \frac{dh_y}{dt} + j\,(\bar{w} \times \bar{h})$$
$$\Sigma N = \frac{dh_z}{dt} + k\,(\bar{w} \times \bar{h})$$

where ΣF_x, ΣF_y, ΣF_z are the forces in the x, y, z directions of a right hand system of Cartesian axes fixed in space; where ΣL, ΣM, ΣN are the moments about the x, y, and z axes; where h_x, h_y, and h_z are the moments of momentum about x_1, y_1, and z_1 axes which are fixed to the airframe; where $i\,(\bar{w} \times \bar{h})$, $j\,(\bar{w} \times \bar{h})$, and $k\,(\bar{w} \times \bar{h})$ arise from the angular velocity $\bar{w}$ of the x_1, y_1, and z_1 axes with respect to the x, y, z axes; where a_x, a_y, a_z, are the accelerations in the x, y, and z directions; and where m is the mass of the airframe.

The absolute acceleration of a body with respect to x, y, z axes is

$$\bar{a}_{abs} = \frac{d\bar{V}}{dt} + \bar{w} \times \bar{V}$$

where $\bar{V}$ is the instantaneous linear velocity and $\bar{w}$ is the angular velocity.

$$\frac{d\bar{V}}{dt} = \dot{U} + \dot{V} + \dot{W}$$

$$\bar{w} \times \bar{V} = (QW - RV)i + (RU - PW)j + (PV - QU)k$$

where P, Q, and R are the angular velocities along the x, y, and z axes respectively and U, V, and W are the linear velocities along the x, y, and z axes. The components of the acceleration are then

$$a_x = \dot{U} + QW - RV$$

85

$$a_y = \dot{V} + RU - PW$$
$$a_z = \dot{W} + PV - QU$$

Substituting the components of acceleration into Equations 1 and considering the mass as a constant the equations become

(3)
$$\Sigma F_x = m(\dot{U} + QW - RV)$$
$$\Sigma F_y = m(\dot{V} + RU - PW)$$
$$\Sigma F_z = m(\dot{W} + PV - QU)$$

The components of the moment of momentum are calculated from summing the moments of the velocity vectors about each axis and multiplying by the mass dm.

(4)
$$h_x = PI_{xx} - QI_{xy} - RI_{xz}$$
$$h_y = QI_{yy} - RI_{yz} - PI_{xy}$$
$$h_z = RI_{zz} - PI_{xz} - QI_{yz}$$

where $I_{xx} = \int (y^2 + z^2) dm$ and $I_{xy} = \int xy\, dm$.

XY and XZ are assumed planes of symmetry, and therefore $I_{xy} = I_{xz} = I_{yz} = 0$. Equations 4 become:

(5)
$$h_x = PI_{xx}$$
$$h_y = QI_{yy}$$
$$h_z = RI_{zz}$$

(6)
$$\frac{dh_x}{dt} = \dot{P} I_{xx}$$
$$\frac{dh_y}{dt} = \dot{Q} I_{yy}$$
$$\frac{dh_z}{dt} = \dot{R} I_{zz}.$$

Since

$$\bar{w} \times \bar{h} = (h_z Q - h_y R)\hat{\imath} + (h_x R - h_z P)\hat{\jmath} + (h_y P - h_x Q)\hat{k}$$

Equations 2 with Equations 5 and 6 substituted become

$$(7) \quad \begin{aligned} \Sigma L &= \dot{P} I_{xx} + QR(I_{zz} - I_{yy}) \\ \Sigma M &= \dot{Q} I_{yy} + PR(I_{xx} - I_{zz}) \\ \Sigma N &= \dot{R} I_{zz} + PQ(I_{yy} - I_{xx}) . \end{aligned}$$

The forces indicated by the left terms of Equations 3 represent the summation of aerodynamic, thrust, and gravity forces. The gravity forces are shown below and their derivation can be found in Reference 9.

$$(8) \quad \begin{aligned} F_{gx} &= (-mg \sin \Theta_0) \cos \Theta \cos \Psi + (mg \cos \Theta_0 \sin \phi_0) \\ &\quad \cos \Theta \sin \Psi - (mg \cos \Theta_0 \cos \phi_0) \sin \Theta \end{aligned}$$

$$\begin{aligned} F_{gy} &= (-mg \sin \Theta_0)(\cos \Psi \sin \Theta - \sin \Psi \cos \phi) + \\ &\quad (mg \cos \Theta_0 \sin \phi_0)(\cos \Psi \cos \Theta + \sin \Psi \sin \Theta \sin \phi) + \\ &\quad (mg \cos \Theta_0 \cos \phi_0)(\cos \Theta \sin \phi) \end{aligned}$$

$$\begin{aligned} F_{gz} &= (-mg \sin \Theta_0)(\cos \Psi \sin \Theta \cos \phi + \sin \Psi \sin \phi) + \\ &\quad (mg \cos \Theta_0 \sin \phi_0)(\sin \Psi \sin \Theta \cos \phi - \cos \Psi \sin \phi) + \\ &\quad (mg \cos \Theta_0 \cos \phi_0)(\cos \Theta \cos \phi) . \end{aligned}$$

where m is the mass of the body; g is the acceleration of gravity; Θ, ϕ, and Ψ are the Eulerian Angles for a ZYX system and Θ_0, ϕ_0, and Ψ_0 are the steady flight values.

Defining $\Sigma F_x'$, $\Sigma F_y'$, and $\Sigma F_z'$ as the sum of the aerodynamic and thrust forces, Equations 3 can be written as

$$(9) \quad \begin{aligned} \Sigma F_x' &= m(\dot{U} + QW - RV) - F_{gx} \\ \Sigma F_y' &= m(\dot{V} + RU - PW) - F_{gy} \\ \Sigma F_z' &= m(\dot{W} + PV - QU) - F_{gz} \end{aligned}$$

87

Each of the instantaneous velocity components can be written as the sum of a steady state value and a change in velocity.

$$U = U_0 + u$$
$$V = V_0 + v$$
$$W = W_0 + w$$
$$P = P_0 + p$$
$$Q = Q_0 + q$$
$$R = R_0 + r$$
$$\frac{dU_0}{dt} = 0 \text{ etc.}$$

In order to linearize the force and moment equations it is assumed that

1) the velocity changes are small and that the products and squares of the velocity changes are negligible compared to the velocity changes themselves

2) the disturbance angles are small and the sine of the angles can be set equal to the angles and the cosine of the angles set equal to one. The product of the angles is zero.

Equations 7 and 9 can now be written as:

$$(10)$$

$$\Sigma F_x' = m[\dot{u} + Q_0 W_0 + W_0 q + Q_0 w - R_0 V_0 - R_0 v - V_0 r + g(\sin\Theta_0) - g(\cos\Theta_0 \sin\phi_0)\Psi + g(\cos\Theta_0 \cos\phi_0)\Theta]$$

$$\Sigma F_y' = m[\dot{v} + U_0 R_0 + U_0 r + R_0 u - P_0 W_0 - P_0 w - W_0 p - g(\sin\Theta_0)\Psi - g(\cos\Theta_0 \sin\phi_0) - g(\cos\Theta_0 \cos\phi_0)\phi]$$

$$\Sigma F_z' = m[\dot{w} + P_0 V_0 + P_0 v + V_0 p - Q_0 U_0 - Q_0 u - U_0 q + g(\sin\Theta_0)\Theta + g(\cos\Theta_0 \sin\phi_0)\phi - g(\cos\Theta_0 \cos\phi_0)]$$

$$(11) \quad \Sigma L = \dot{p} I_{xx} + (Q_0 R_0 + Q_0 r + R_0 q)[I_{zz} - I_{yy}]$$

88

$$\sum M = \dot{q} I_{yy} + (P_0 R_0 + P_0 r + R_0 p)[I_{xx} - I_{zz}]$$

$$\sum N = \dot{r} I_{zz} + (P_0 Q_0 + P_0 q + Q_0 p)[I_{yy} - I_{xx}].$$

The equations which relate angular velocities about the x, y, z axes
to the Eulerian Angles Θ, ϕ, ψ are

$$P = \dot{\phi} - \dot{\psi} \sin \Theta$$
$$Q = \dot{\Theta} \cos \phi + \dot{\psi} \sin \phi \cos \Theta$$
$$R = \dot{\psi} \cos \phi \cos \Theta - \dot{\Theta} \sin \phi.$$

When linearized the equations become

(12)
$$P = \dot{\phi}$$
$$Q = \dot{\Theta}$$
$$R = \dot{\psi}$$

The steady flight condition is defined as all velocity components equal
to zero except U_0 and W_0. Using this definition and Equations 12, Equa-
tions 10 and 11 become

(13)
$$\sum F_x' = m[\dot{u} + W_0 q + g \sin \Theta_0 + g(\cos \Theta_0) \Theta]$$
$$\sum F_y' = m[\dot{v} + U_0 r - W_0 p - g(\sin \Theta_0)\psi - g(\cos \Theta_0)\phi]$$
$$\sum F_z' = m[\dot{u} r - U_0 q + g(\sin \Theta_0)\Theta - g \cos \Theta_0]$$

(14)
$$\sum L = \ddot{\phi} I_{xx}$$
$$\sum M = \ddot{\Theta} I_{yy}$$
$$\sum N = \ddot{\psi} I_{zz}$$

The aerodynamic forces and moments can be represented by a Taylor
series expansion. Because of the planes of symmetry and the steady flight
conditions $\sum F_x$, $\sum F_z$, and M are functions of only q, u, and w of the
velocity components and $\sum F_y$, L, and N are functions of only p, v, and r.

This is proved in reference 9. The other variables affecting the forces and moments are the angle of thrust deflection, the airframe flexibility, and the changing mass of the body. Since the changes are assumed small the second derivative and above for the velocity and bending terms are considered negligible and the first derivative and above is considered negligible for the change in mass. The resulting equations are of the form

$$
(15) \quad \Sigma F_x = F_{x_0} + \left(\frac{dF}{du}\right)u + \left(\frac{dF}{d\dot{u}}\right)\dot{u} + \left(\frac{dF}{dq}\right)q + \left(\frac{dF}{d\dot{q}}\right)\dot{q}
$$
$$
+ \left(\frac{dF}{dw}\right)w + \left(\frac{dF}{d\dot{w}}\right)\dot{w} + \left(\frac{dF}{d\delta_T}\right)\delta_T + \left(\frac{dF}{d\dot{\delta}_T}\right)\dot{\delta}_T + \left(\frac{dF}{dd_1}\right)d_1
$$
$$
+ \left(\frac{dF}{d\dot{d}_1}\right)\dot{d}_1 + \left(\frac{dF}{dd_2}\right)d_2 + \left(\frac{dF}{d\dot{d}_2}\right)\dot{d}_2 + \left(\frac{dF}{dd_3}\right)d_3 + \left(\frac{dF}{d\dot{d}_3}\right)\dot{d}_3
$$
$$
+ \left(\frac{dF}{d\Delta_I}\right)\Delta_I + \left(\frac{dF}{d\Delta_{LOX}}\right)\Delta_{LOX} + \left(\frac{dF}{d\Delta_{LH}}\right)\Delta_{LH}
$$

where d_1, d_2, and d_3 are the first, second, and third bending modes; δ_T is the angle of thrust deflection; and Δ_I, Δ_{LOX}, and Δ_{LH} are the changes due to the change in the mass of the fuels.

The thrust axis is assumed to pass through the center of gravity and hence does not contribute to the moment equations. The thrust force equations are

$$
\Sigma_T F_x = T \cos \mathcal{E}
$$
$$
\Sigma_T F_z = -T \sin \mathcal{E}
$$

where $\mathcal{E}$ is the angle between the X axis and thrust line.

$$
T = T_0 + \Delta T
$$
and
$$
\Delta T = \frac{dT}{du} u.
$$

Therefore

$$
(16) \quad \Sigma_T F_x = T_0 \cos \mathcal{E} + \cos \mathcal{E} \frac{dT}{du} u
$$
$$
\Sigma_T F_z = -T_0 \sin \mathcal{E} - \sin \mathcal{E} \frac{dT}{du} u.
$$

90

To determine the equations of steady flight substitute Equations 16 and 15 into Equations 13 and 14, substitute the values of the steady flight condition, and set the velocity changes equal to zero. The resulting equations are:

(17)

$$F_{x_0} + T_0 \cos \varepsilon - mg \sin \Theta_0 = 0$$

$$F_{y_0} = 0$$

$$F_{z_0} - T_0 \sin \varepsilon + mg \cos \Theta_0 = 0$$

$$L_0 = 0$$

$$M_0 = 0$$

$$N_0 = 0 .$$

When stability axes are used as the reference system and quasi-steady flow conditions are assumed, all terms containing W_0 disappear and all aerodynamic partial derivatives with respect to rates of change of velocities and with respect to rate of change of angle of thrust deflection are eliminated. For the Two Degree of Freedom Short Period Mode Approximation u is set equal to zero and only the equations $\Sigma F'_z$ and ΣM are involved. Substituting Equations 16 and 15 into Equations 13 and 14 and subtracting Equations 17 gives the following equations of motion for the disturbed body:

$$\dot{w} - U_0 q + g (\sin \Theta_0)\Theta = F_{\frac{w}{q}} q + F_w w + F_{\delta_T} \delta_T + F_{d_1} d_1 +$$
$$F_{\dot{d}_1} \dot{d}_1 + F_{d_2} d_2 + F_{\dot{d}_2} \dot{d}_2 + F_{d_3} d_3 +$$
$$F_{\dot{d}_3} \dot{d}_3 + F_{\Delta I} \Delta I + F_{\Delta LOX} \Delta LOX + F_{\Delta LH} \Delta LH$$

(18)

$$\ddot{\Theta} = M_{\frac{w}{q}} q + M_w w + M_{\delta_T} \delta_T + M_{d_1} d_1 + M_{\dot{d}_1} \dot{d}_1 + M_{d_2} d_2 +$$
$$M_{\dot{d}_2} \dot{d}_2 + M_{d_3} d_3 + M_{\dot{d}_3} \dot{d}_3 + M_{\Delta I} \Delta I + M_{\Delta LOX} \Delta LOX +$$
$$M_{\Delta LH} \Delta LH$$

where $F_q = \frac{1}{m} \frac{dF}{dq}$ and $M_q = \frac{1}{I_{yy}} \frac{dM}{dq}$.

the angle of attack, α, is defined as the angle between the wing chord line and the relative wind.

$$\Delta \alpha = \frac{w}{U} = \frac{w}{U_o + u} = \frac{w}{U_o} \quad \text{SINCE } u = 0$$

(19) Therefore $\quad w \cong U_o \alpha.$

Equations 18 with equations 12 and 19 substituted become:

$$\dot{\alpha} = F_w \alpha + \left(\frac{Eg + U_o}{U_o}\right)\dot{\theta} + \left(\frac{-g\sin\theta_o}{U_o}\right)\theta + \left(\frac{F\dot{l}_1}{U_o}\right)\dot{l}_1 +$$

(20)
$$\left(\frac{Fl_1}{U_o}\right)l_1 + \left(\frac{F\dot{l}_2}{U_o}\right)\dot{l}_2 + \left(\frac{Fl_2}{U_o}\right)l_2 + \left(\frac{F\dot{l}_3}{U_o}\right)\dot{l}_3 + \left(\frac{Fl_3}{U_o}\right)l_3 +$$

$$\left(\frac{F\Delta I}{U_o}\right)\Delta I + \left(\frac{F\Delta LOX}{U_o}\right)\Delta LOX + \left(\frac{F\Delta LH}{U_o}\right)\Delta LH + \left(\frac{F\delta T}{U_o}\right)\delta T$$

$$\ddot{\theta} = (M_w - U_o)\alpha + (M_g)\dot{\theta} + (M\dot{l}_1)\dot{l}_1 + (Ml_1)l_1 + (M\dot{l}_2)\dot{l}_2$$

$$+ (Ml_2)l_2 + (M\dot{l}_3)\dot{l}_3 + (Ml_3)l_3 + (M\Delta I)\Delta I$$

$$+ (M\Delta LOX)\Delta LOX + (M\Delta LH)\Delta LH.$$

The coefficients for any instant are constants. Equations 20 agree in form with the given equations for $\dot{\alpha}$ and $\ddot{\theta}$.

The Transfer Functions which were obtained from the Aerodynamic Equations are as follows:

1.   Aerodynamic Condition 1:

$t = 20$ $\qquad \frac{\theta_P}{\delta_T} = \frac{1.565(s + .064)}{s^2(s + .064)}$

$t = 75$ $\qquad \frac{\theta_P}{\delta_T} = \frac{2.625(s + .064)}{s(s - .1198)(s + .0204)}$

$t = 101.9$ $\qquad \frac{\theta_P}{\delta_T} = \frac{5.06(s + .0374)}{(s - .0104)(s - .686)(s + .746)}$

$t = 200$ $\qquad \frac{\theta_P}{\delta_T} = \frac{2.28(s + .038)}{(s - .0074)(s - 1.25)(s + 1.32)}$

92

2. Aerodynamic condition 2:

$$t = 20 \qquad \frac{\theta_P}{\delta_T} = \frac{5.18(s+.064)(s+.0244 \pm j\,4.483)}{s^2(s+.064)(s+.082 \pm j\,8.16)}$$

$$t = 75 \qquad \frac{\theta_P}{\delta_T} = \frac{6.75(s+.065)(s.068 \pm j\,5.1)}{(s-.023)(s-.77)(s+.89)(s+.103 \pm j\,8.2)}$$

$$t = 101.9 \qquad \frac{\theta_P}{\delta_T} = \frac{9.2(s+.038)(s+.057 \pm j\,6.06)}{(s-.01)(s-.68)(s+.74)(s+.087 \pm j\,8.17)}$$

$$t = 200 \qquad \frac{\theta_P}{\delta_T} = \frac{2.28(s+.038)(s+.318 \pm j\,28.2)}{(s-.007)(s-1.24)(s+1.31)(s+.295 \pm j\,27.7)}$$

3. Aerodynamic Condition 3:

$$t = 20 \qquad \frac{\theta_P}{\delta_T} = \frac{16.05(s+.064)(s+.175 \pm j\,24.31)(s+.022 \pm j\,4.35)}{s^2(s+.064)(s+.417 \pm j\,41.6)(s+.081 \pm j\,8.14)}$$

$$t = 75 \qquad \frac{\theta_P}{\delta_T} = \frac{19.1(s+.066)(s+.067 \pm j\,4.98)(s+.19 \pm j\,25.2)}{(s-.023)(s-.77)(s+.89)(s+.103 \pm j\,8.19)(s+.453 \pm j\,41.6)}$$

$$t = 101.9 \qquad \frac{\theta_P}{\delta_T} = \frac{21.6(s+.038)(s+.205 \pm j\,27.46)(s+.056 \pm j\,5.97)}{(s-.01)(s-.683)(s+.743)(s+.087 \pm j\,8.18)(s+.43 \pm j\,41.63)}$$

$$t = 200 \qquad \frac{\theta_P}{\delta_T} = \frac{2.28(s+.038)(s+.319 \pm j\,28.15)(s+.46 \pm j\,46.7)(s+.75 \pm j\,73.3)}{(s-.007)(s-1.24)(s+1.3)(s+.295 \pm j\,27.7)(s+.48 \pm j\,46.7)(s+.74 \pm j\,73.1)}$$

4. Aerodynamic Condition 4:

$$t = 20 \qquad \frac{\theta_P}{\delta_T} = \frac{10.78(s+.06)(s+.015 \pm j\,1.48)(s+.019 \pm j\,1.69)(s+.026 \pm j\,2.63)}{s(s+.42 \pm j\,41.6)(s+.215 \pm j\,21.5)(s+.082 \pm j\,8.17)(s+.027 \pm j\,2.77)}$$

$$\frac{(s+.028 \pm j\,4.72)(s-11.21 \pm j\,21.89)(s+11.56 \pm j\,21.6)}{(s+.018 \pm j\,1.96)(s+.015 \pm j\,1.51)(s+.029 \pm j\,.164)}$$

$$t = 75 \qquad \frac{\theta_P}{\delta_T} = \frac{13.1(s+.07)(s+.007 \pm j\,1.96)(s+.022 \pm j\,2.29)(s+.027 \pm j\,2.61)}{(s+.48)(s-.01)(s-.42)(s+.45 \pm j\,41.65)(s+.23 \pm j\,21.5)}$$

$$\frac{(s+.094 \pm j\,9.37)(s-10.2 \pm j\,22.75)(s+10.6 \pm j\,22.45)}{(s+.06 \pm j\,10)(s+.103 \pm j\,8.22)(s+.028 \pm j\,2.61)(s+.023 \pm j\,2.2)}$$

$$t = 101.9 \quad \frac{\theta_P}{\delta_T} = \frac{15.55(s+.04)(s-9.3 \pm j\,24.45)(s+9.72 \pm j\,24.2)}{(s-.011)(s-.636)(s+.693)(s+.427 \pm j\,41.6)(s+.22 \pm j\,21.55)}$$

$$\frac{(s+.036 \pm j\,11.23)(s+.06 \pm j\,6.18)(s+.032 \pm j\,3.23)}{(s+.036 \pm j\,11.24)(s+.087 \pm j\,8.15)(s+.034 \pm j\,3.42)}$$

$$t = 200 \quad \frac{\theta_P}{\delta_T} = \frac{2.28(s+.036)(s+.27 \pm j\,2.68)(s+.274 \pm j\,2.8)(s+.32 \pm j\,28.2)}{(s-.004)(s-.155 \pm j\,1.72)(s+.41 \pm j\,2.37)(s+.28 \pm j\,2.77)}$$

$$\frac{(s+.458 \pm j\,46.72)(s+.756 \pm j\,73.3)}{(s+.247 \pm j\,27.8)(s+.48 \pm j\,46.7)(s+.745 \pm j\,73.2)}$$

APPENDIX B
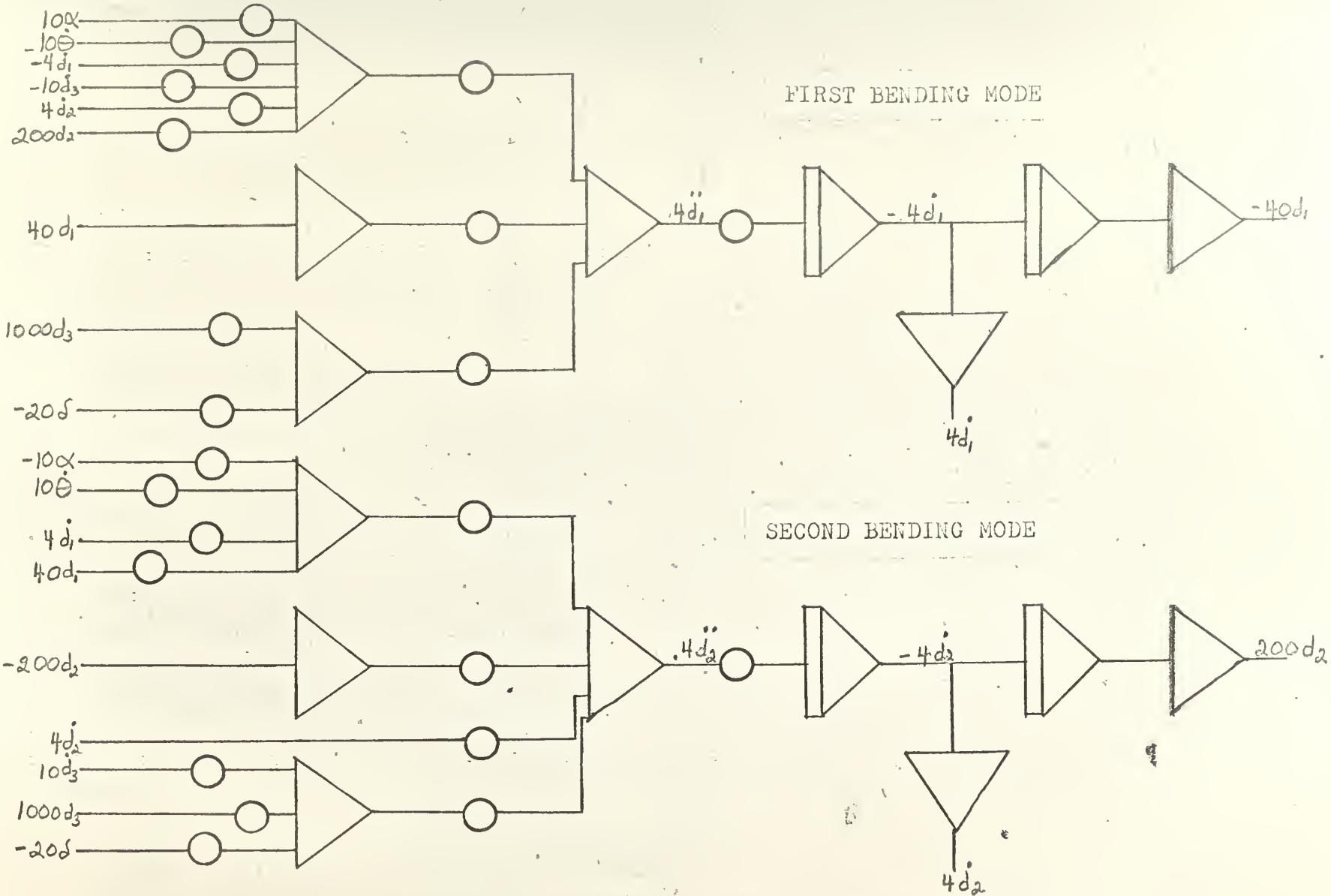
Figure B.1. Computer Simulation Diagram.

THIRD BENDING MODE

CONVERSION TO PLATFORM VALUES

Figure B.1. Continued.

97

Figure B.1. Continued.

ATTACK ANGLE

PITCH ANGLE
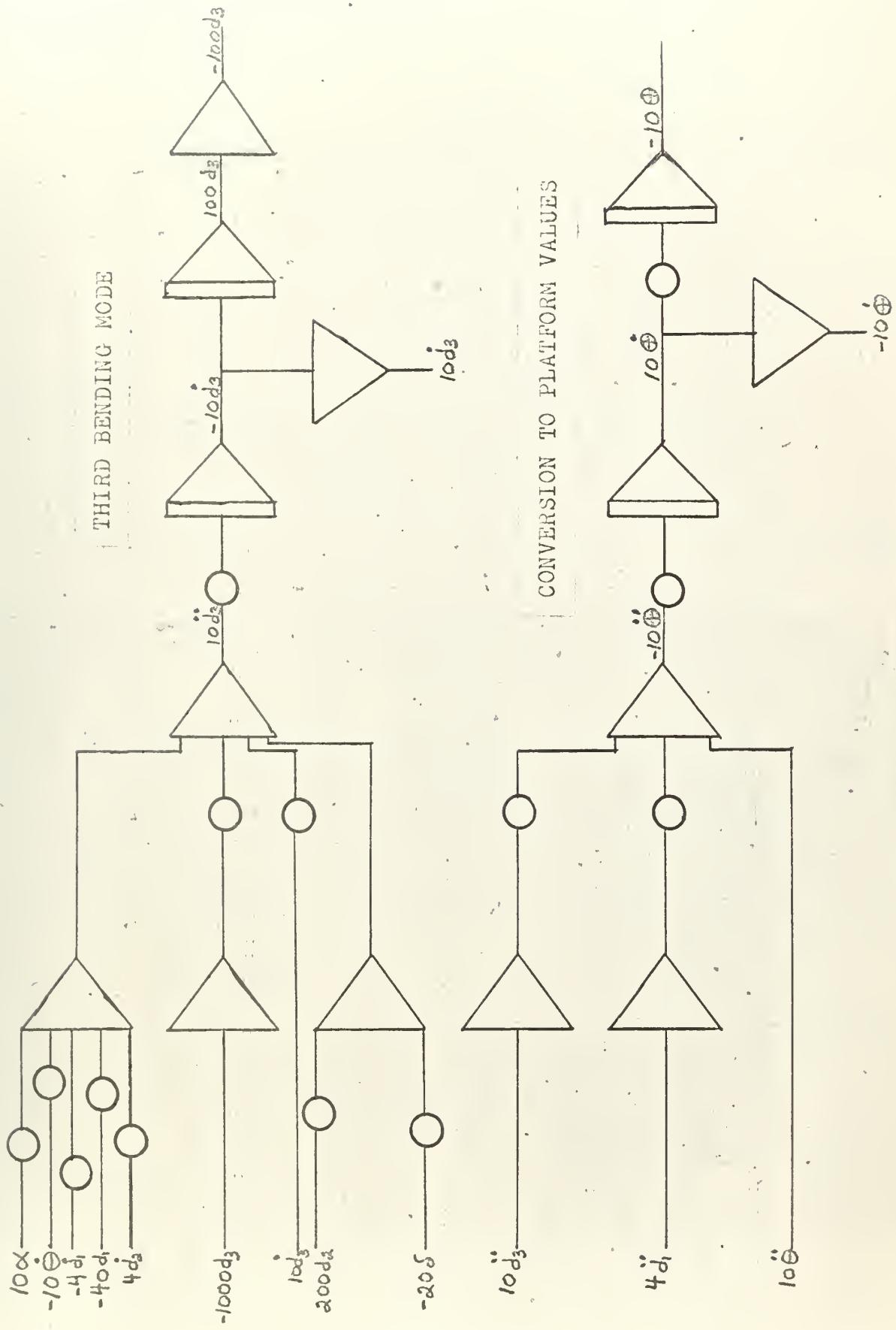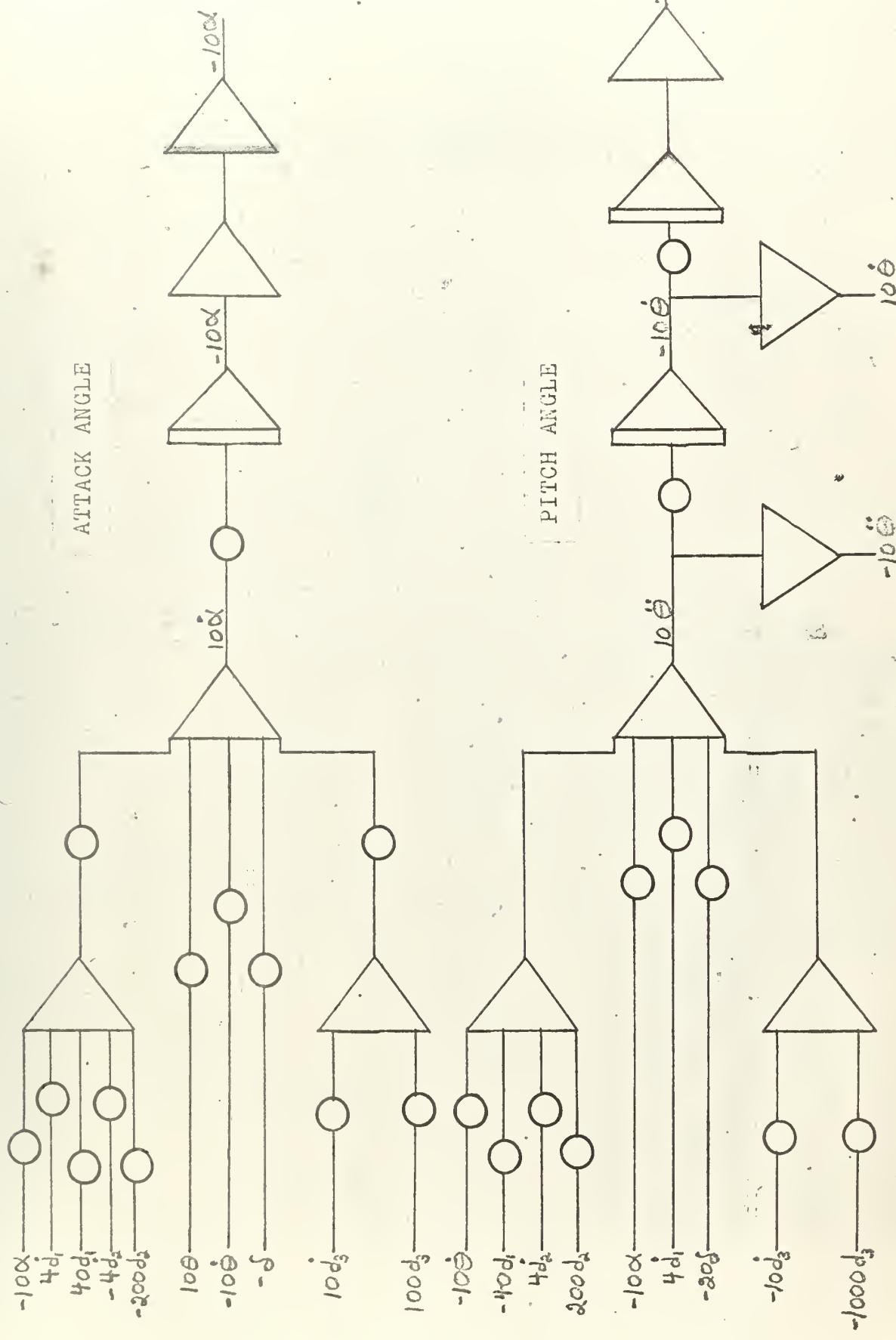
Figure B.1. Continued.
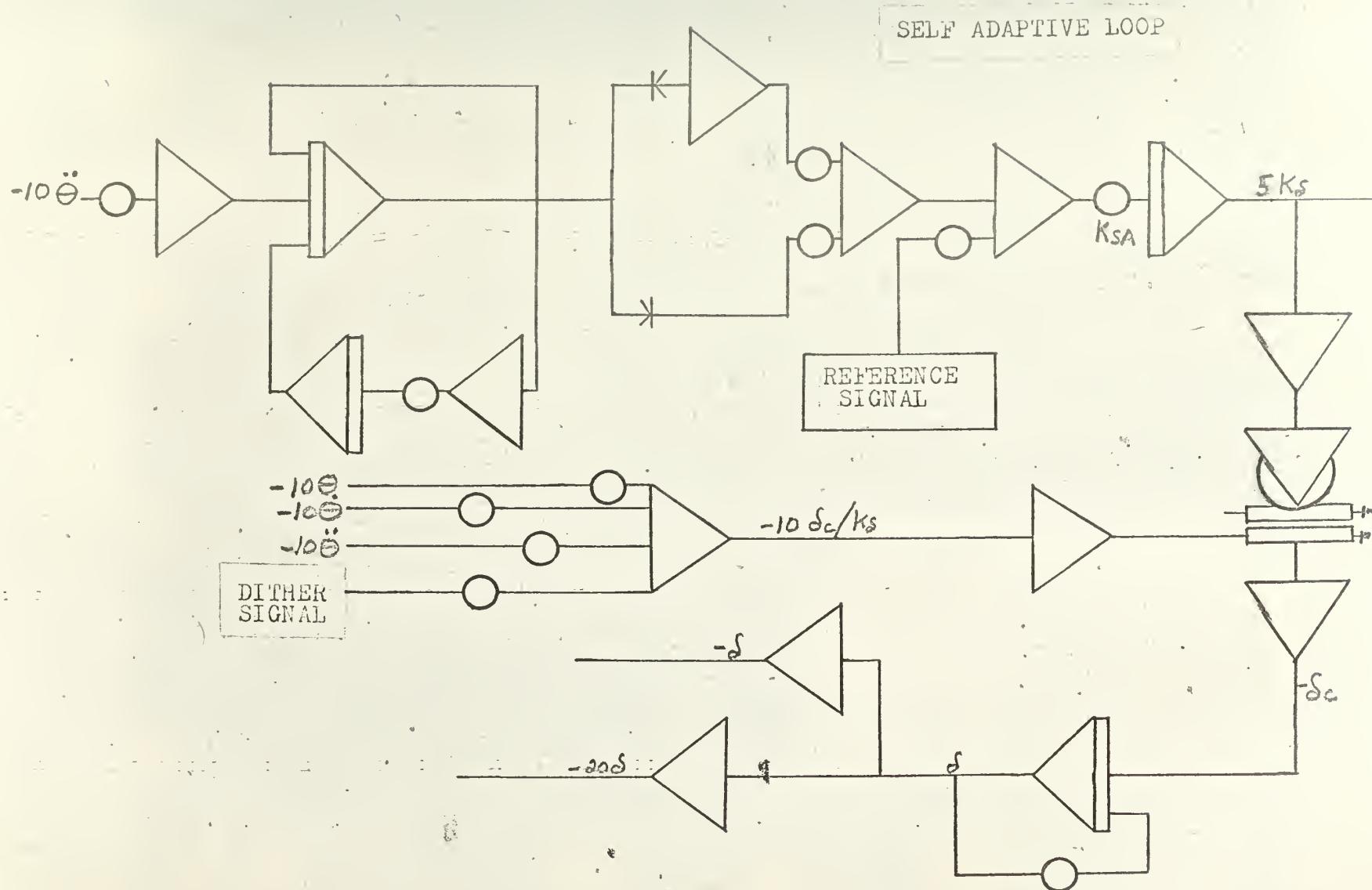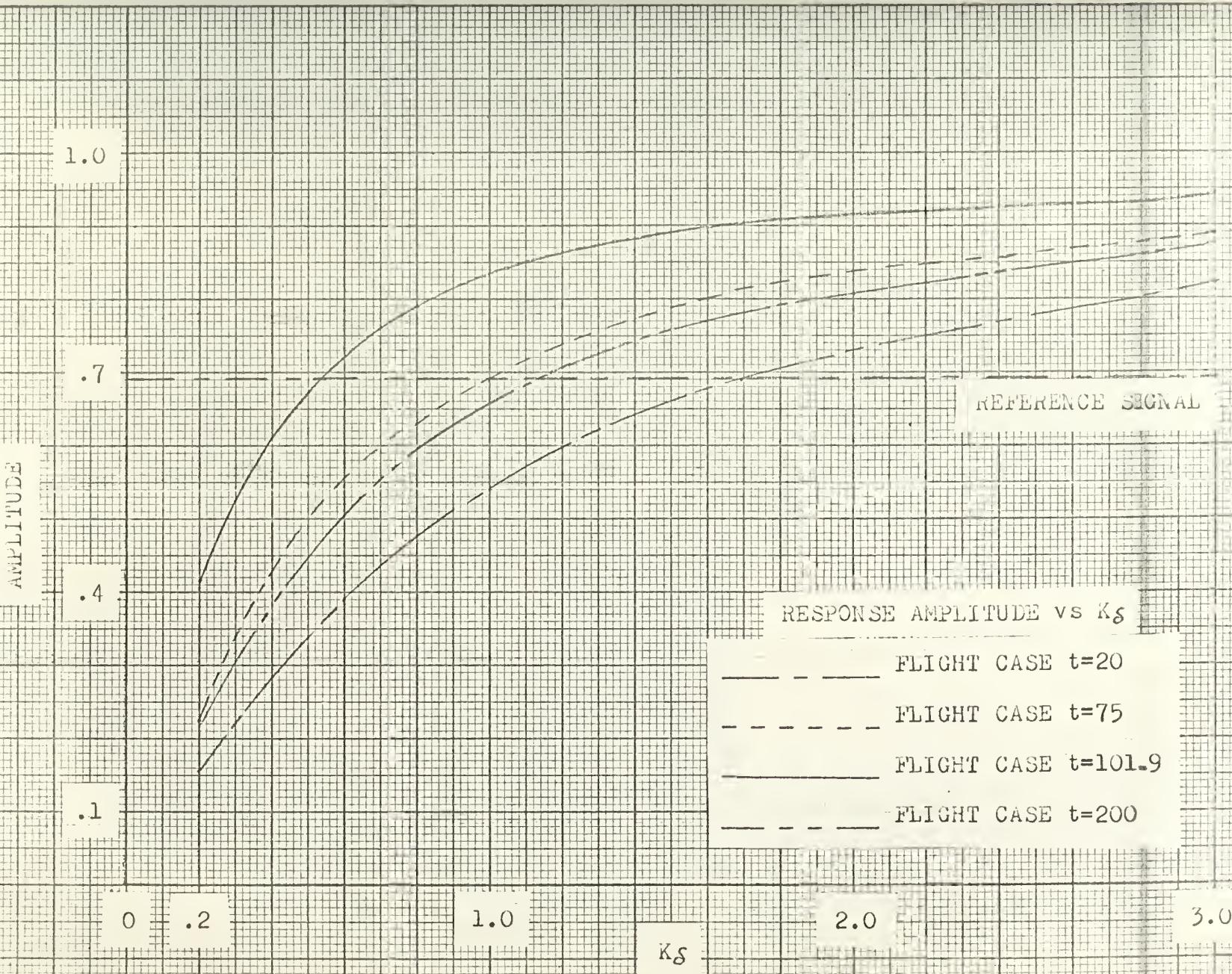
Figure B.2(a). Frequency Response Amplitude vs K_δ for Dither Frequency of 30 and Aerodynamic Condition 1.
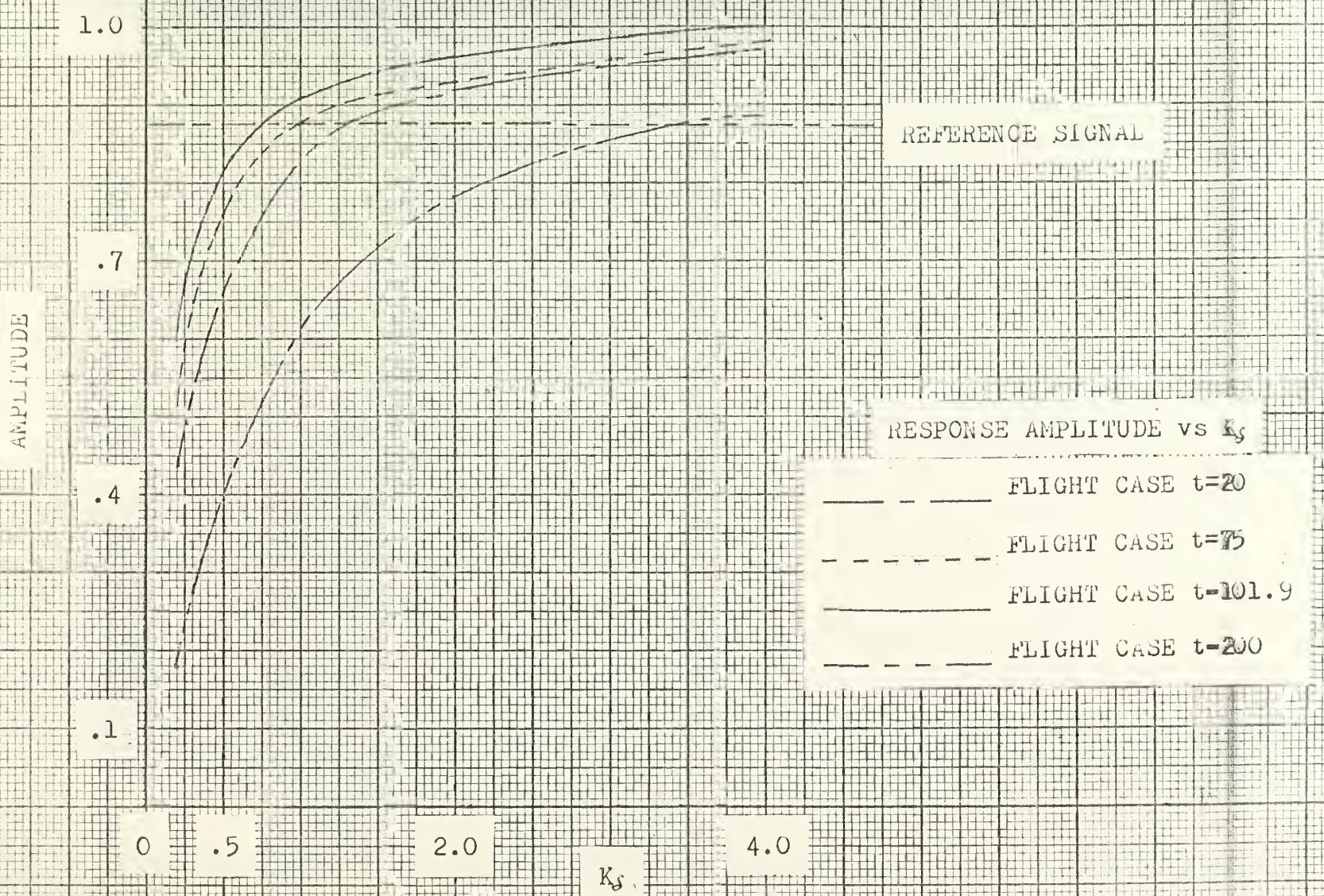
Figure B.2(b). Frequency Response Amplitude vs K_δ for Dither Frequency of 30 and Aerodynamic Condition 2.
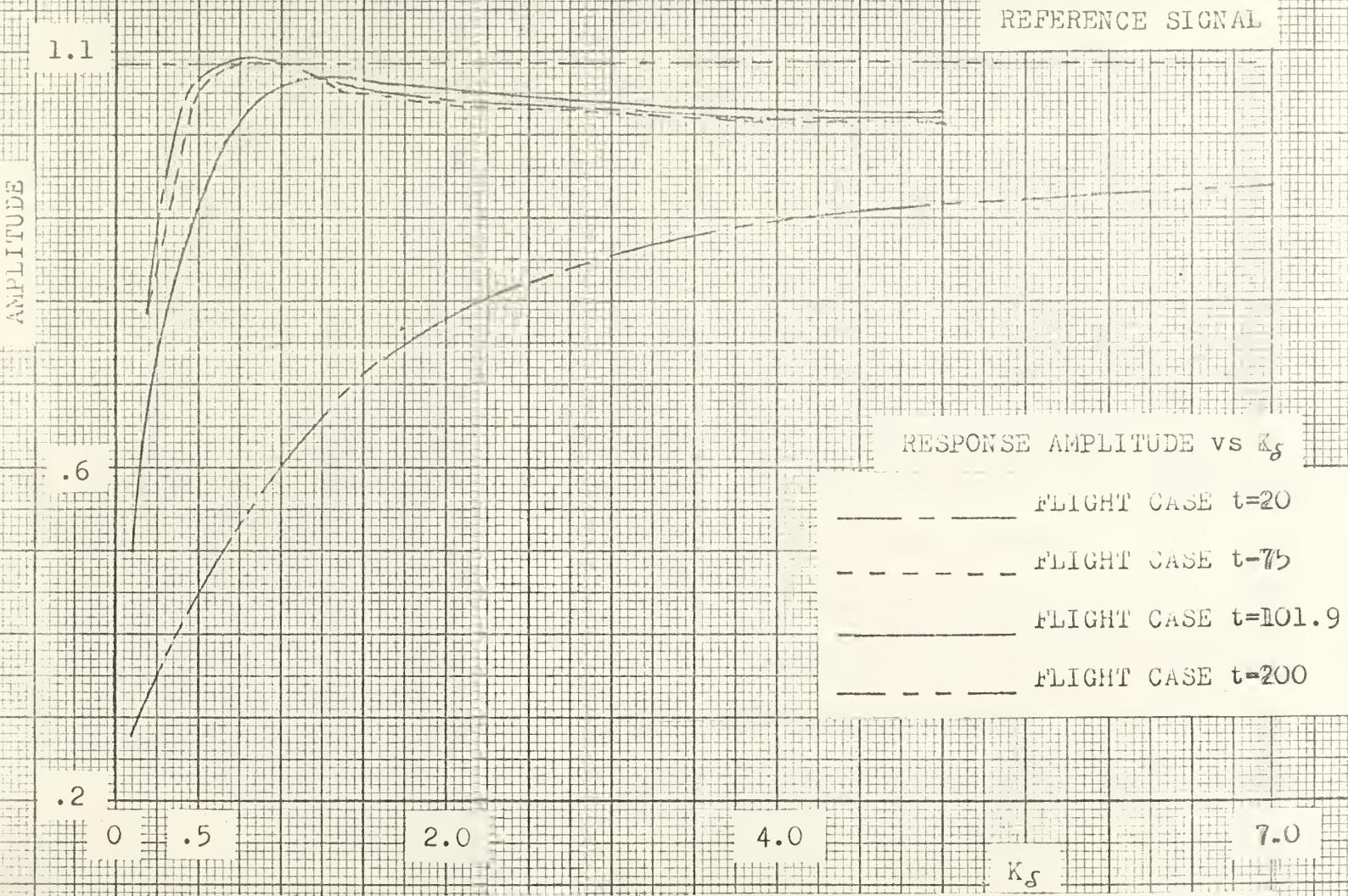
Figure B.2(c). Frequency Response Amplitude vs K_δ for Dither Frequency of 30 and Aerodynamic Condition 3.

REFERENCE SIGNAL

RESPONSE AMPLITUDE vs K_δ

_____ _ FLIGHT CASE t=20 DITHER FREQUENCY 28.5

_ _ _ _ _ FLIGHT CASE t=75 DITHER FREQUENCY 28.5

_____ FLIGHT CASE t=101.9 DITHER FREQUENCY 30

_ _ _ _ FLIGHT CASE t=200 DITHER FREQUENCY 28.17
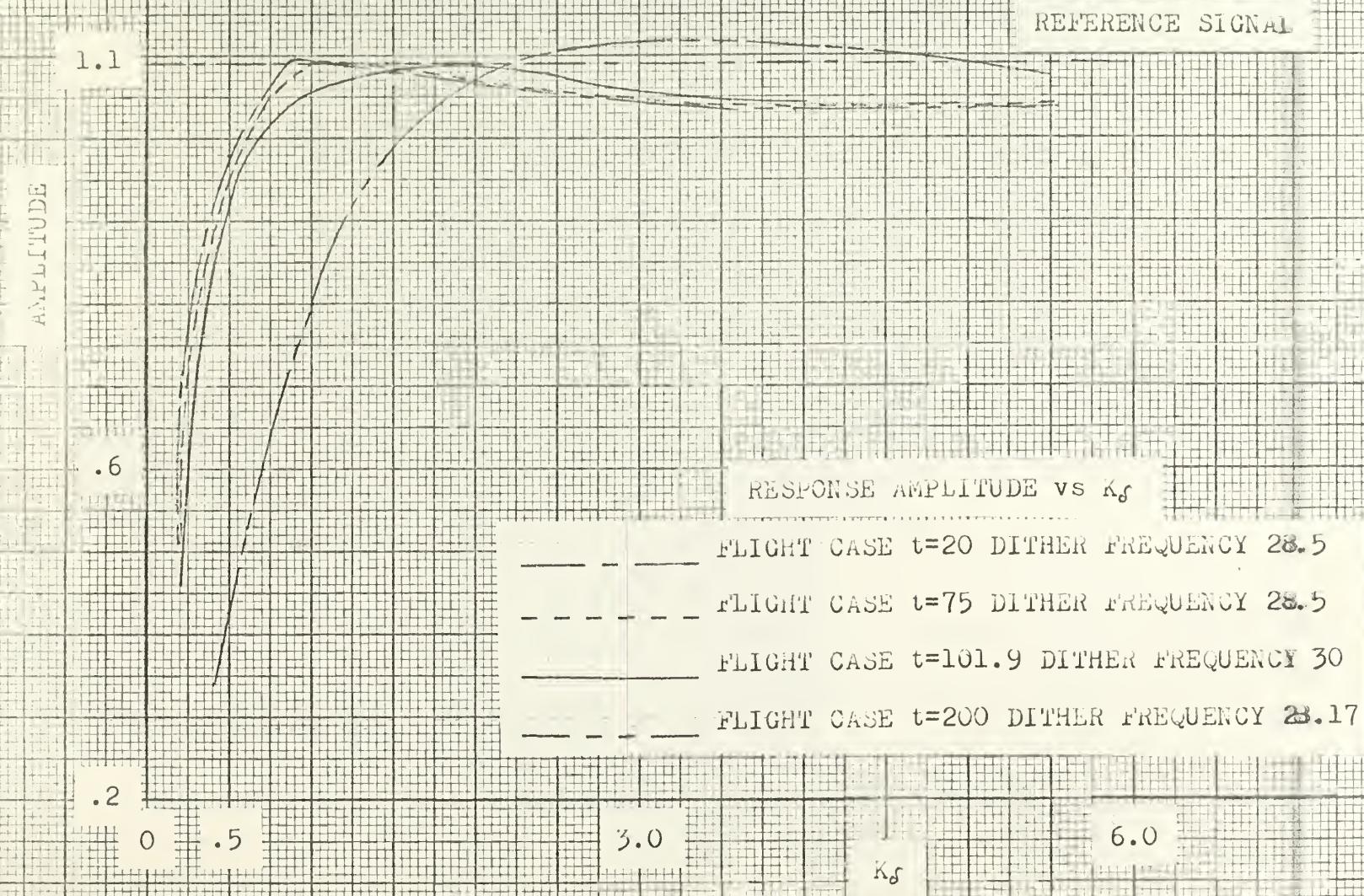
Figure B.2(d). Frequency Response Amplitude vs K_δ for Various Dither
Frequencies and Aerodynamic Condition 3.
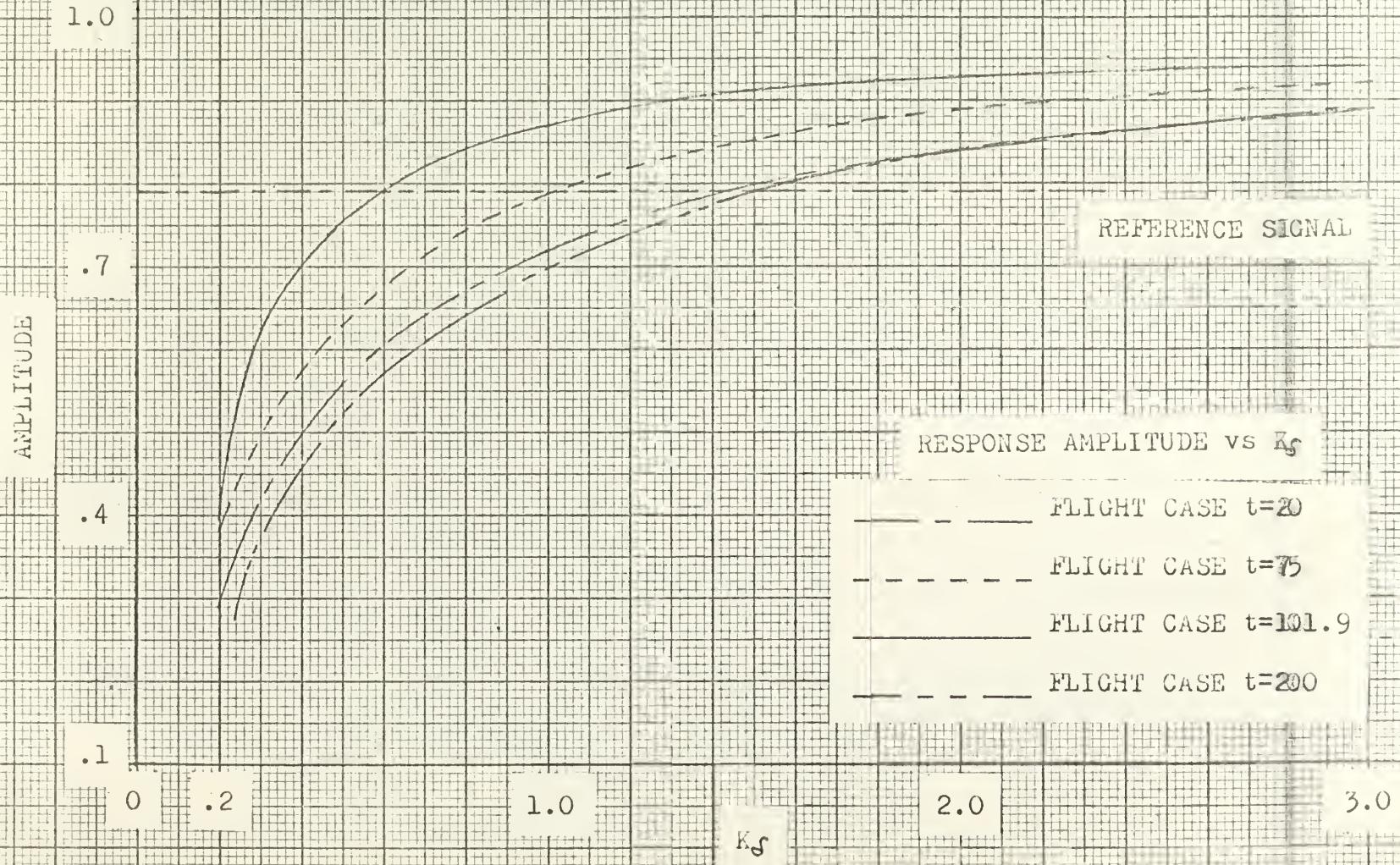
Figure B.2(e). Frequency Response Amplitude vs K_δ for Dither Frequency of 20 and Aerodynamic Condition 3.

104
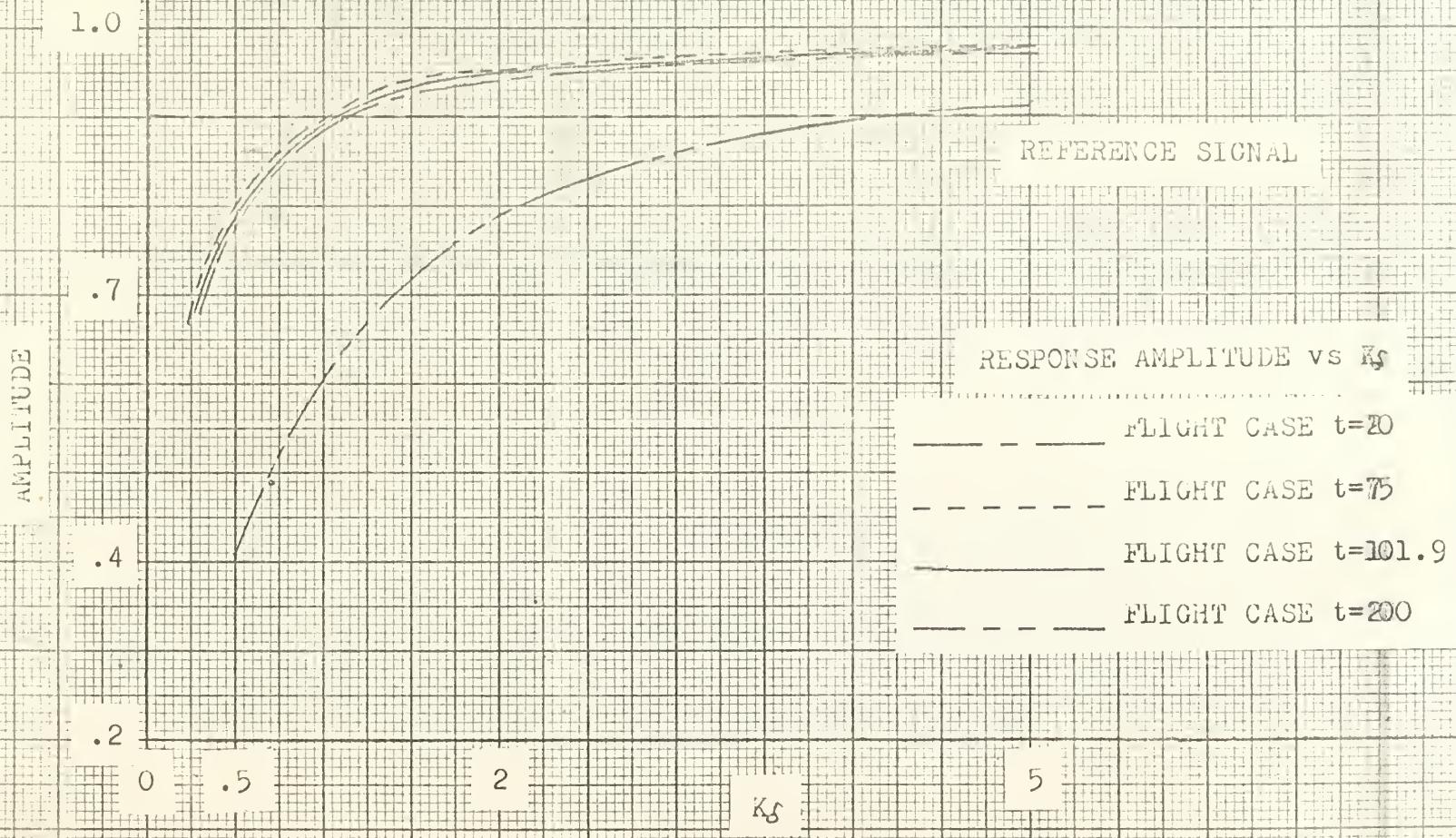
Figure B.2(f). Frequency Response Amplitude vs K_δ for Dither Frequency of 30 and Aerodynamic Condition 4.
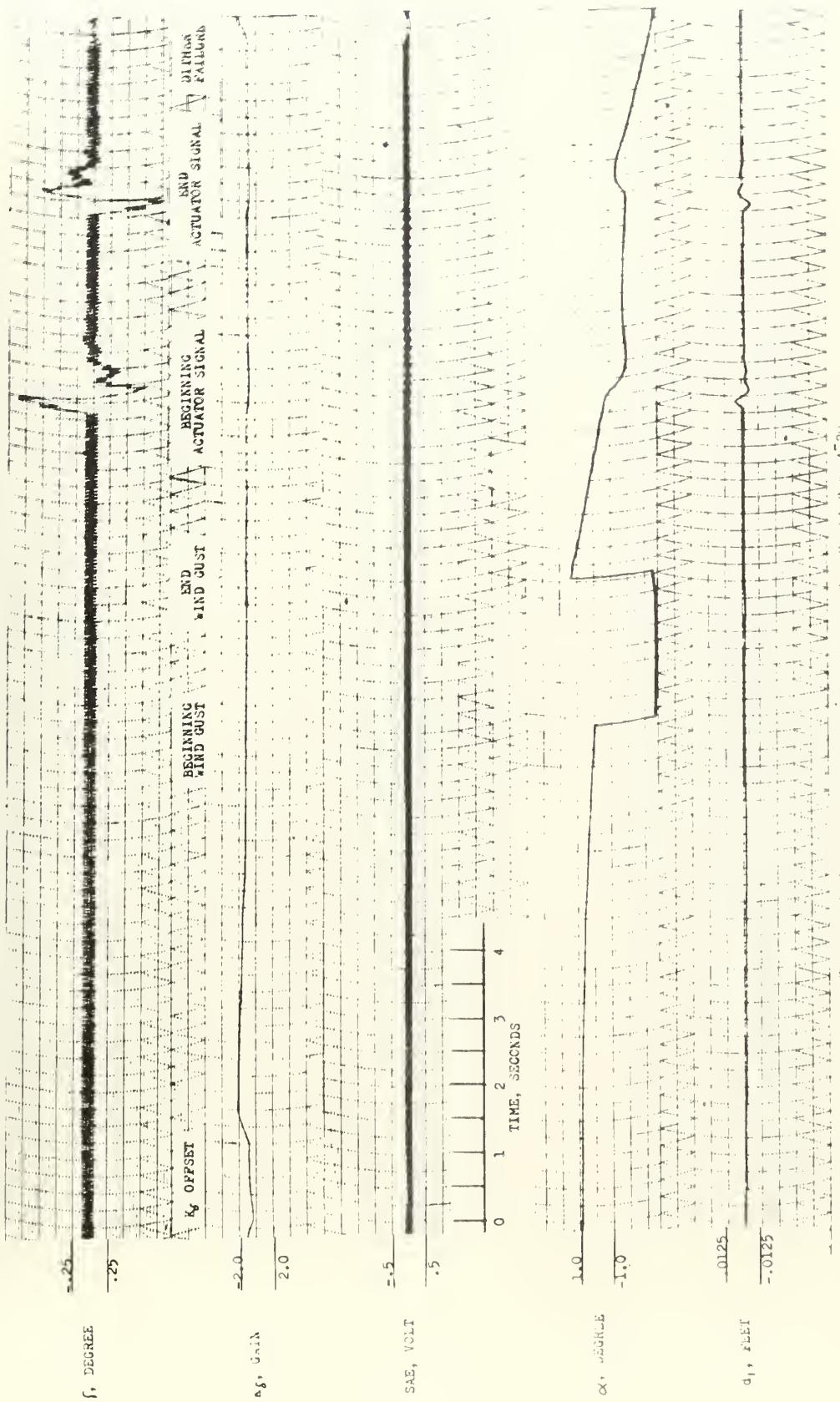
Figure B.5(w). Disturbance Reaction of System for Flight Case t=20
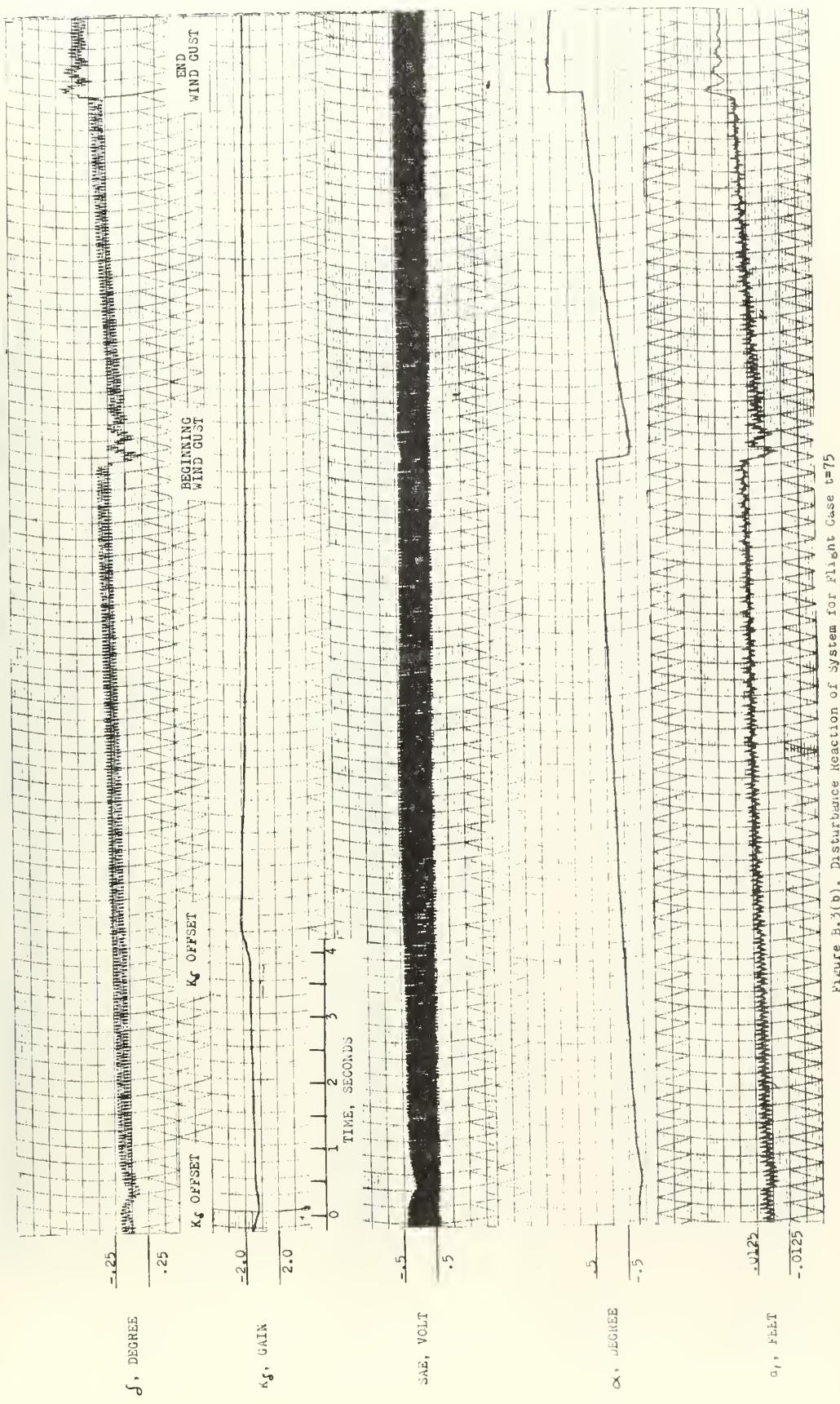
Figure B.3(b). Disturbance Reaction of System for Flight Case t=75

Figure B.5(b). Continued

Figure B.3(c). Disturbance Reaction of System for Flight Case t=101.9
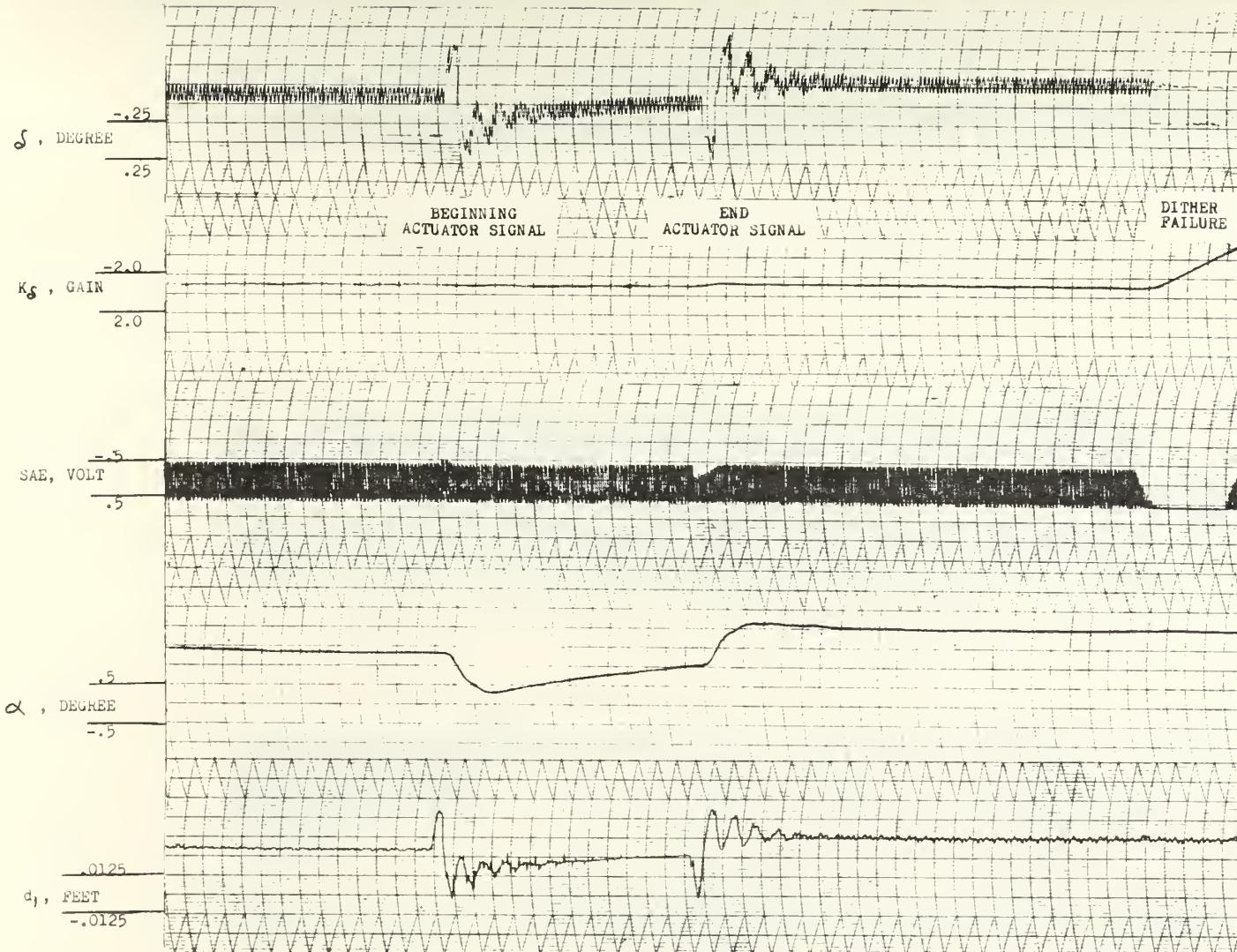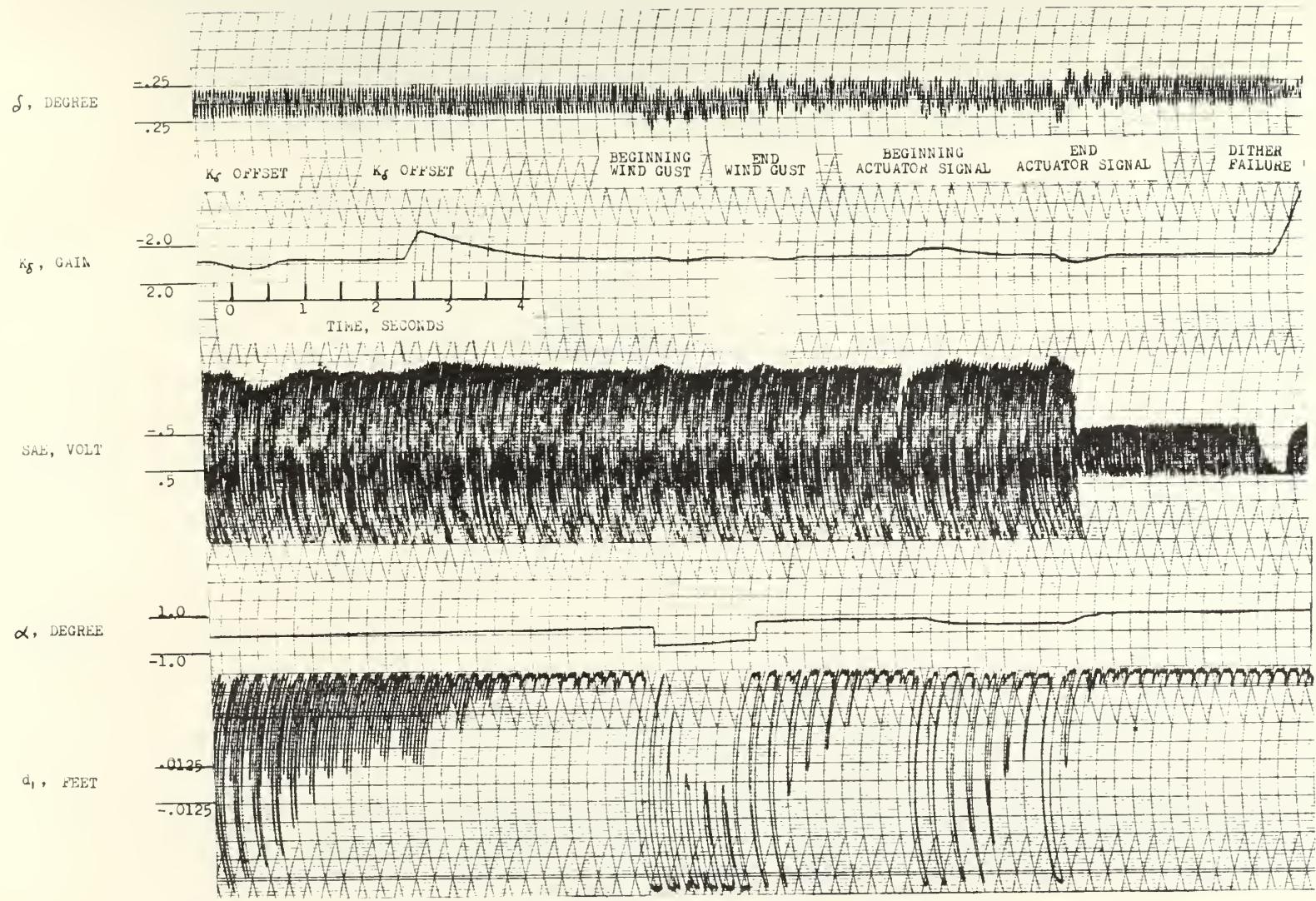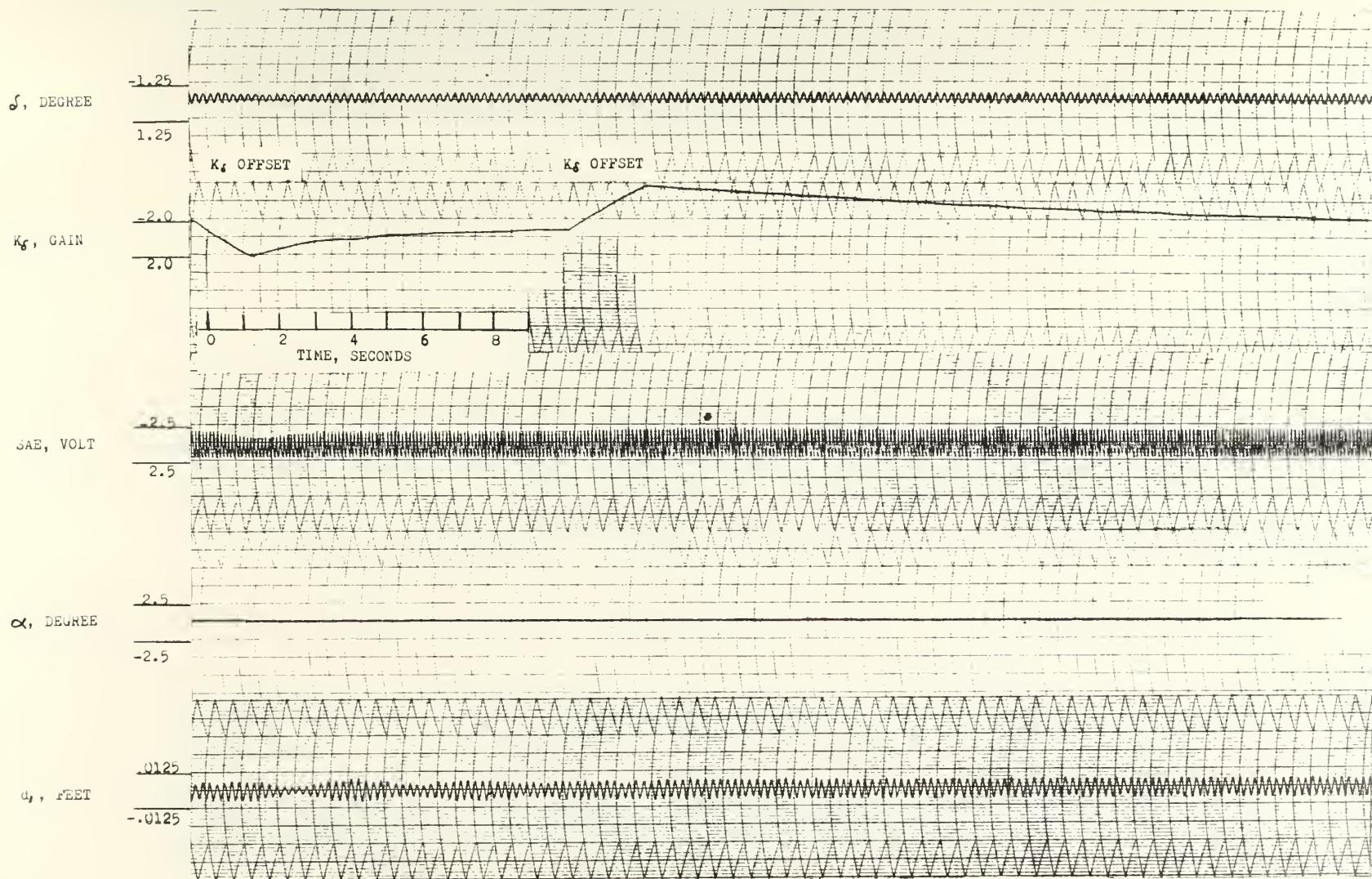
Figure B.3(d). Disturbance Reaction of System for Flight Case t=200
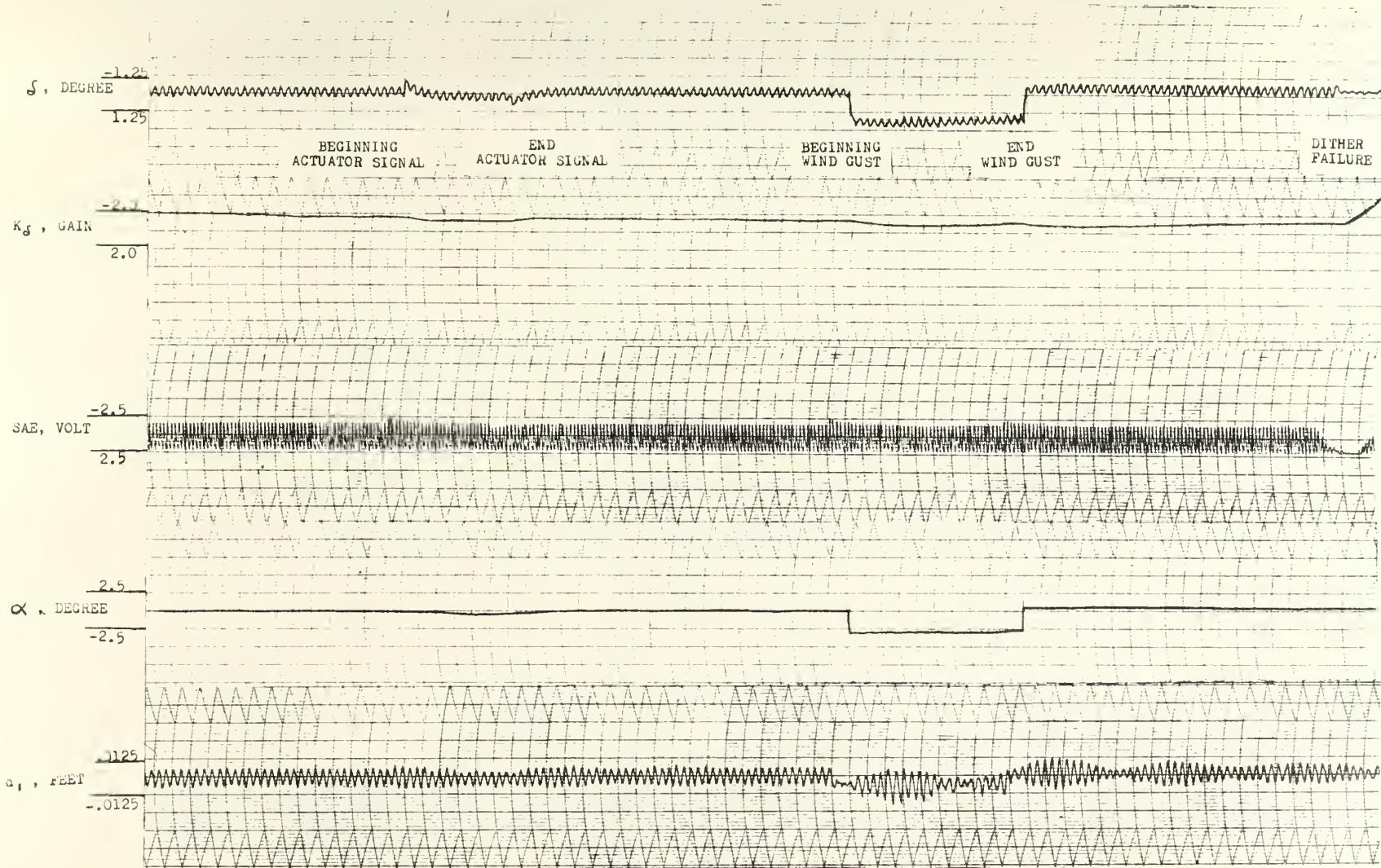
Figure B.3(d). Continued

ANALYTICAL VERIFICATION OF THE EMPIRICAL RESULTS

The results of the variation of damping ratios with dither frequency obtained by empirical methods in Chapter 4 will be analyzed by analytical methods in this Appendix.

For the analysis the root loci for the flight cases of a particular aerodynamic condition will be assumed to have the same shape and system gain values. The transfer functions of the vehicle dynamics for a particular aerodynamic condition do not vary to the extent that the use of the assumption to determine general trends would be prevented. A particular system gain, K, on the root loci for the three flight cases of a condition would determine the same damping ratio, δ. The system gain is the product of the dynamic gain, M_δ, and the adaptive gain, K_δ. The dynamic gain is the gain associated with the vehicle transfer function. Using condition 3 as an example, the dynamic gains for the flight cases are approximately equal to the following values:

$$\text{Case } t = 20 \qquad M_\delta = 16.05$$
$$\text{Case } t = 75 \qquad M_\delta = 19.1$$
$$\text{Case } t = 101.9 \quad M_\delta = 21.6$$

Since a particular damping ratio has the same value of K for the three cases, the values of K_δ for the cases are:

$$K_\delta \, t = 20 \qquad = \frac{K}{16.05}$$
$$K_\delta \, t = 75 \qquad = \frac{K}{19.1}$$
$$K_\delta \, t = 101.9 \qquad = \frac{K}{21.6}$$

and $K_\delta \, t = 20 > K_\delta \, t = 75 > K_\delta \, t = 101.9$ for a particular δ. A plot of δ versus K_δ is of the following form.

112
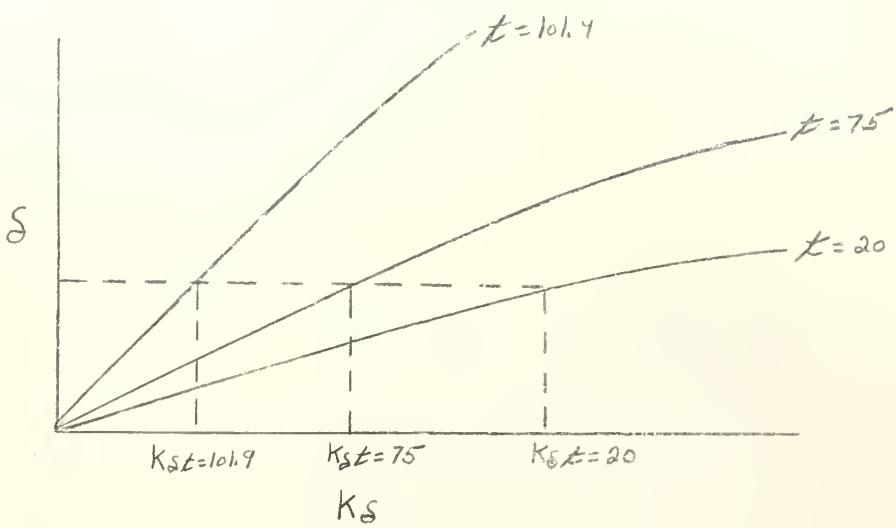
The trends shown in the δ versus K_δ plot are valid for any of the four aerodynamic conditions.

The closed loop transfer function for the system is

$$\frac{\ddot{\Theta}}{COMMAND\ SIGNAL} = \frac{K_\delta s^2 \frac{\Theta_E}{\delta_T}}{1 + K_\delta (s^2 + 3.6 s + 3.6) \frac{\Theta_E}{\delta_T}}$$

when $\frac{\Theta_E}{\delta_T}$ is the vehicle dynamic transfer function. When the dither frequency is large compared to the poles and zeros of the vehicle dynamic transfer function, the transfer function is approximated by $\frac{\Theta_E}{\delta_T} \cong \frac{M_\delta}{s^2}$.

This approximation is justified for the dither range, 10 to 40 radians per second, for conditions 1 and 2. The closed loop transfer function becomes

$$\frac{\ddot{\Theta}}{COMMAND\ SIGNAL} \cong \frac{K_\delta M_\delta}{1 + K_\delta M_\delta} .$$

Since the dither system maintains the amplitude of the closed loop response constant,

$$\left. \frac{K_{\delta 1} M_{\delta 1}}{1 + K_{\delta 1} M_{\delta 1}} \right|_{t=20} \approx \left. \frac{K_{\delta 2} M_{\delta 2}}{1 + K_{\delta 2} M_{\delta 2}} \right|_{t=75} = \left. \frac{K_{\delta 3} M_{\delta 3}}{1 + K_{\delta 3} M_{\delta 3}} \right|_{t=101.9}$$

and for Aerodynamic condition 1

113

$$\frac{K_{\delta_1} 1.565}{1 + K_{\delta_1} 1.565} = \frac{K_{\delta_2} 2.625}{1 + K_{\delta_2} 2.625} = \frac{K_{\delta_3} 5.06}{1 + K_{\delta_3} 5.06}$$

and for Aerodynamic Condition 2

$$\frac{K_{\delta_1} 5.18}{1 + K_{\delta_1} 5.18} = \frac{K_{\delta_2} 6.75}{1 + K_{\delta_2} 6.75} = \frac{K_{\delta_3} 9.2}{1 + K_{\delta_3} 9.2}$$

The relationships are independent of the dither frequency, and constant

damping ratio variation would be expected in the dither range. This agrees

with the empirical results for conditions 1 and 2 as are shown in Figure

4.4. If K_δ is assigned the value 1 for both condition 1 and 2, then for

condition 1

$$K_{\delta_1} = 1.67 \qquad\qquad K_{\delta_3} = 0.516$$

and for condition 2

$$K_{\delta_1} = 1.3 \qquad\qquad K_{\delta_3} = 0.725$$

For both conditions, $K_{\delta_1} > K_{\delta_2} > K_{\delta_3}$ which is the trend necessary

for small damping ratio variation as determined from the δ versus K_δ plot.

For condition 3 the dither frequency can be close to poles and zeros

of the vehicle dynamic transfer function. If the dither frequency is close

to a pole of the transfer function, then $\frac{\Theta_F}{\delta_T}$ is very large and

$$K_\delta (s^2 + 3.6 s + 3.6) \frac{\Theta_F}{\delta_T} \gg 1$$

and

$$\frac{\ddot{\Theta}}{\text{COMMAND SIGNAL}} \cong \frac{s^2}{s^2 + 3.6 s + 3.6} \quad.$$

The amplitude of the closed loop response is independent of the adaptive

gain; and therefore, K_δ could assume an infinite number of values with

an infinite number of damping ratio variations.

If the dither frequency is close to a zero of Case $t = 20$, then

$$\frac{\Theta_F}{\delta_T}_{t=20} < \frac{\Theta_F}{\delta_T}_{t=75} < \frac{\Theta_F}{\delta_T}_{t=101.9} \quad.$$

114

In order to have the same amplitude of the closed loop response, K_δ t = 20

$> K_\delta$ t = 75 $> K_\delta$ t = 101.9 which is the trend for a small damping ratio

variation. If the dither frequency is close to a zero of Case t = 101.9,

then

$$\frac{\Theta_F}{\delta_T t = 20} > \frac{\Theta_F}{\delta_T t = 75} > \frac{\Theta_F}{\delta_T t = 101.9} \; .$$

In order to have the same amplitude of the closed loop response K_δ t = 20 $<$

K_δ t = 75 $< K_\delta$ t = 101.9 which is the trend which would result in a

large damping ratio variation. If the dither frequency is close to a zero

of Case t = 75, the magnitude of the damping ratio variation would vary

between the magnitudes when the frequency is close to a zero of Case t = 20

and when the frequency is close to a zero of Case t = 101.9.

The damping ratio variation curve for condition 3 should, therefore,

have an undetermined damping ratio variation at the pole at approximately

40 radians, have a small value for the variation at the zero of case t = 20

at approximately 24 radians; and have a large value for the variation at

the zero of case t = 101.9 at approximately 27 radians. This agrees with

the condition 3 curve shown in Figure 4.4.

In order to determine the dither frequency that the minimum variation

in damping ratio occurs, the ideal expression for no variation which is

of the form

$$\frac{A s^2 \frac{\Theta_F'}{\delta_T}}{1 + A(s^2 + 3.6s + 3.6)\frac{\Theta_F'}{\delta_T}} = \frac{B s^2 \frac{\Theta_F''}{\delta_T}}{1 + B(s^2 + 3.6s + 3.6)\frac{\Theta_F''}{\delta_T}} = \frac{C s^2 \frac{\Theta_F'''}{\delta_T}}{1 + C(s^2 + 3.6s + 3.6)\frac{\Theta_F'''}{\delta_T}}$$

$$\frac{1}{\frac{1}{A s^2 \frac{\Theta_F'}{\delta_T}} + \frac{s^2 + 3.6s + 3.6}{s^2}} = \frac{1}{\frac{1}{B s^2 \frac{\Theta_F''}{\delta_T}} + \frac{s^2 + 3.6s + 3.6}{s^2}} = \frac{1}{\frac{1}{C s^2 \frac{\Theta_F'''}{\delta_T}} + \frac{s^2 + 3.6s + 3.6}{s^2}}$$

$$K_\delta t = 20 \; \frac{\Theta_F'}{\delta_T} = K_\delta t = 75 \; \frac{\Theta_F''}{\delta_T} = K_\delta t = 101.9 \; \frac{\Theta_F'''}{\delta_T}$$

115

where $A = K_\delta t = 20 \dfrac{20}{s+20}$

$B = K_\delta t = 75 \dfrac{20}{s+20}$

$C = K_\delta t = 101.9 \dfrac{20}{s+20}$

and for a damping ratio of 0.7

$K_\delta t = 20 = 0.86$

$K_\delta t = 75 = 0.26$

$K_\delta t = 101.9 = 0.175$

is evaluated for various dither frequencies close to the frequency of the zero for case $t = 20$, and the smallest amplitude variation between the three cases should indicate the optimum frequency. A dither frequency of 23 radians per second resulted in the smallest variation in the amplitude.

For aerodynamic condition 4 there are no zeros or poles of the vehicle dynamic transfer function which are close to the imaginary axis in the dither range. Varying the dither frequency does not result in wide variations in the values of the vehicle transfer functions, and the closed loop transfer function can be approximated by

$$\frac{\ddot{\Theta}}{\text{COMMAND SIGNAL}} \cong \frac{K_\delta M_\delta}{1 + K_\delta M_\delta}$$

A constant damping ratio variation would be expected and agrees with the curve for condition 4 in Figure 4.4. Since the values of the vehicle transfer functions can not be varied appreciably, the variation in the adaptive gain required for a constant damping ratio can not be realized and a large variation in the damping ratio results.

116